POLITECNICO DI TORINO

Corso di Laurea Magistrale in Ingegneria Civile

Tesi di Laurea Magistrale

FINITE ELEMENT NUMERICAL ANALYSIS OF THE THERMO-MECHANICAL BEHAVIOUR OF AN ENERGY DIAPHRAGM WALL

Relatore
Prof. Marco Barla
Politecnico di Torino

Candidato
Roberta Graceffa

Relatore esterno
Dr. Alice Di Donna
Universitè Grenoble Alpes

Aprile, 2019

Table of content

List of figures

List of Tables

1. Introduction

Over the last century the burning of fossil fuels like coal and oil has increased the concentration of atmospheric carbon dioxide (CO_2) (https://climate.nasa.gov/causes/). This happens because the coal or oil burning process combines carbon with oxygen in the air to make CO_2. To a lesser extent, the clearing of land for agriculture, industry, and other human activities has increased concentrations of greenhouse gases. The consequences of changing the natural atmospheric greenhouse are difficult to predict, but certain effects seem likely: on average, Earth will become warmer and some regions may welcome warmer temperatures, but others may not; warmer conditions will probably lead to more evaporation and precipitation overall, but individual regions will vary, some becoming wetter and others dryer; a stronger greenhouse effect will warm the oceans and partially melt glaciers and other ice, increasing sea level; ocean water also will expand if it warms, contributing further to sea level rise; on the other hand, some crops and other plants may respond favourably to increased atmospheric CO_2, growing more vigorously and using water more efficiently. At the same time, higher temperatures and shifting climate patterns may change the areas where crops grow best and affect the makeup of natural plant communities. However, the negative aspects are much more dangerous for our ecosystem which can be totally unbalanced and the effects are likely to become irreversible. Indeed, the industrial activities that our modern civilization depends upon, have raised atmospheric carbon dioxide levels from 280 parts per million to 400 parts per million in the last 150 years. The panel also concluded there's a better than 95 percent probability that human-produced greenhouse gases such as carbon dioxide, methane and nitrous oxide have caused much of the observed increase in Earth's temperatures over the past 50 years (https://climate.nasa.gov/causes/).

This phenomenon has been taken into consideration only since 1950 and some measures have begun to come true after the Kyoto Protocol (1997). As a matter of fact, in the last century, becoming aware of this risk, it was thought to push on clean energy provided by earth and employ it for human purpose under the prospective of sustainability. According to the United Nations (the UN’s Brundtland Commission popularized the term in 1987), sustainability is defined as “meeting the needs of the present without compromising the ability of future generations to meet their own needs.” True sustainability is when everyone, everywhere can meet their basic needs forever. Sustainable energy is energy that we will never use up or deplete, because it is inexhaustible. In particular, it is possible to classify different type of energy on the base of the natural element they take advantage of: water, sun, wind, earth’s soil and organic matter are some considerable examples. Knowing the possible form of energy presented on Earth, allows us to create structures capable to use it and make it available to humans. As engineers we have skills and tools to solve or, at least, to reduce this huge problem; as human we have a moral obligation to stop it.

This thesis has the goal to study the behaviour of one of these particulars structures: the energy diaphragm walls (EDW), based on the shallow geothermal.

The energy diaphragm walls are able to match two different tasks: the structural one, i.e. retain the soil, and thermal one, i.e. exchange heat with the surrounding soil. The latter skill is ensured by the shallow geothermal energy. Indeed, geothermal energy is thermal energy generated and stored in the Earth’s crust. It can be found from shallow ground to several miles below the surface, and even farther down to the extremely hot molten rock, i.e. magma. Indeed, it is possible to classify the geothermal energy resource on the base of the enthalpy which is proportional to temperature distinguishing between high-enthalpy and low-enthalpy systems. The first one has the purpose of producing electricity through deep boreholes and steam turbines, which reach a depth more than 500 m; on the other hand, low enthalpy, exploiting the presence of a heat pump, allows to produce thermal energy from lower values of temperature, generally less than 30°C, taken in the shallow geosphere (no more than 200 m), e.g. for the air conditioning of buildings.

Our study is focused on low-enthalpy resources, i.e. shallow geothermal energy used to couple the structural role of geostructures with the energy supply. The system used is as simple as effective: polyethylene pipes are embedded into the concrete structures, and a heat-carrying fluid circulates through them and exchanges heat with the ground. The pipes are then connected to a heat pump system, which circulates the fluid in the heating–cooling plant of the building. This system allows the heat to be extracted from the ground during winter to satisfy the heating needs of the buildings and injected into the ground during summer, to meet air conditioning requirements. The advantage of this technology is that it incorporates the geothermal equipment inside geostructures that are already in place for the stability of the construction, reducing the initial costs of installation with respect to other geothermal systems.

However, from the design point of view, it is necessary to take into account the effects that heat exchange have on the reinforced concrete in terms of stress and strain. It is well known that a gradient of temperature causes thermal strains or induced stresses in the material, that need to be added to the operational state of stress in a design stage, but there is still limited evidence on the impact of the thermal cycles on the serviceability and safety performance of the geostructures. Moreover, to justify higher initial costs of the installation, it is necessary to make a preliminary assessment of the effective energy advantages in the operational phase, in terms of energy efficiency of the structure.

A lot of studies have already been made. Starting from Brandl (1998 and 2006), experimental and numerical assessment have been carried out (Gao et al., 2008), to disclose for example the influences on the thermal efficiency of energy piles (Cecinato and Loveridge, 2015), and the geotechnical behaviour of energy piles for different design solutions (Knellwolf et al., 2011, Batini et al., 2015). In the tunnelling field, application of energy equipment in the lining have been tested (Markiewicz and Adam (2006), Franzius and Pralle (2011), Barla et al. (2016), Zhang et al. (2013)), as well as the influence of underground conditions on the heat exchange capacity of energy tunnels (Di Donna and Barla, 2015). Little work has been carried out for energy walls. Concerning retaining walls, thermal and mechanical aspects of their response as shallow geothermal heat exchanger has been investigated by Bourne-Webb et al. (2015 and 2016), as well as the energy performance of diaphragm walls and their influences by Di Donna et al. (2016), Barla et al. (2017).

Aim and objectives

The core of this thesis is the thermo-mechanical analysis of a real diaphragm wall, part of the car park Ventimiglia (Torino, Italy), under the prospective of installing pipes for geothermal use. For this purpose, the following objectives have been set:

- Develop a model for a thermo-mechanical problem.
- Quantify the stresses along an energy diaphragm wall.
- Identify the displacements due to thermal exchanges.

Structure of the dissertation

The path followed by the thesis is divided into 5 chapters thus defined:

Chapter 2 starts with an introduction on renewable energy to end up with geothermal energy, especially focusing on low enthalpy geothermal and the geothermal heat pump.

Chapter 3 is focused on energy geostructures. The functionality of these particular structures is explained, in particular three types of geostructures are analyzed, tunnels, piles and walls, through papers of real cases.

Chapter 4 develops the coupled thermos-hydro-mechanical analysis, describing the equations that govern the problem. Furthermore, the software LAGAMINE is introduced and the preliminary analyses carried out for an oedometric test are described for three different simulations: mechanical, hydro-mechanical, and thermo-hydro-mechanical.

Chapter 5 is the core of this work thus a general framework in terms of location, geotechnical condition and geometry of the case study is made. Afterward the model realized in LAGAMINE, the geometry and the boundary conditions are described as material properties and thermos-mechanical analysis. The model is run and comparison with thesis of the colleague A.Santi (Barla et al., 2018).

Chapter 6 is the last chapter where all the necessary observations and the final results of the thesis are underlined with critical opinion. Moreover, some tips for future analysis are suggested.

2. From renewable energy to low enthalpy geothermal systems

2.1 Renewable energy

Achieving solutions to environmental problems that we face today requires long-term potential actions for sustainable development. In this regard, renewable energy resources appear to be the one of the most efficient and effective solutions. That is why there is an intimate connection between renewable energy and sustainable development.

About 90% of global energy consumption is supplied by non-renewable sources. This is extremely problematic because these resources will soon be exhausted, and most of them are also major greenhouse gas emitters. On the other hand, renewable energy sources (including biomass, biofuels, hydropower, geothermal, solar, and wind) accounted for only 11% of the global energy consumption in 2010, and are projected to account for only 15% by 2040 (from U.S. Energy Information Administration, International Energy Outlook 2013). Of these, solar, wind, geothermal, and hydropower are the cleanest energy sources as they do not require combustion and therefore have no direct greenhouse gas or air pollutant emissions.

Sure, the sources of energy most commonly used may meet our current needs, but at the rate we are using our current sources, like coal and natural gas, we will burn through them, leaving none behind for future generations, who will then be forced to do what we could already be doing: finding new ways to generate energy.

Just because something works does not automatically means it cannot be improved. Why should energy be any different? Why should we stand around and wait until a change is the only option? We can make changes today that make lives better for our current generation, creating new jobs while providing clean energy, and also improving the lives of future generations.

Sustainable energy sources are the best sources of energy for our homes and businesses, because they are not only renewable but are also frequently developed closer to the end-user than are traditional power plants.

Here are some examples of clean energy, which are already developed in some countries more than others; however, they are spreading for their efficiency and long term economic benefit.

Solar power

Photovoltaic (PV) Solar power is harnessing the suns energy to produce electricity. One of the fastest growing energy sources, new technologies are developing at a rapid pace. Solar cells are becoming more efficient, transportable and even flexible, allowing for easy installation. PV has mainly been used to power small and medium-sized applications, from the calculator powered by a single solar cell to off-grid homes powered by a photovoltaic array. The 1973 oil crisis stimulated a rapid rise in the production of PV during the 1970s and early 1980s. Steadily falling oil prices during the early 1980s, however, led to a reduction in funding for photovoltaic research and development (R&D) and a discontinuation of the tax credits associated with the Energy Tax Act of 1978. These factors moderated growth to approximately 15% per year from 1984 through 1996 (www.listverse.com). Solar installations in recent years have also largely begun to expand into residential areas, with governments offering incentive programs to make “green” energy a more economically viable option.

Wind power

Wind power is the conversion of wind energy by wind turbines into a useful form, such as electricity or mechanical energy. Large-scale wind farms are typically connected to the local power transmission network with small turbines used to provide electricity to isolated areas. Residential units are entering production and are capable of powering large appliances to entire houses depending on the size. Wind farms installed on agricultural land or grazing areas, have one of the lowest environmental impacts of all energy sources. Although wind produces only about 1.5% of worldwide electricity use, it is growing rapidly, having doubled in the three years between 2005 and 2008. In several countries it has achieved relatively high levels of penetration, accounting for approximately 19% of electricity production in Denmark, 11% in Spain and Portugal, and 7% in Germany and the Republic of Ireland in 2008 (www.listverse.com). Wind energy has historically been used directly to propel sailing ships or converted into mechanical energy for pumping water or grinding grain, but the principal application of wind power today is the generation of electricity.

Hydroelectricity

Hydroelectricity is electricity generated by hydropower, i.e. the production of power through use of the gravitational force of falling or flowing water. It is the most widely used form of renewable energy. Once a hydroelectric complex is constructed, the project produces no direct waste. Small scale hydro or micro-hydro power has been an increasingly popular alternative energy source, especially in remote areas where other power sources are not viable. Small scale hydro power systems can be installed in small rivers or streams with little or no discernible environmental effect or disruption to fish migration. Most small scale hydro power systems make no use of a dam or major water diversion, but rather use water wheels to generate energy. This was approximately 19% of the world's electricity (up from 16% in 2003), and accounted for over 63% of electricity from renewable sources. While many hydroelectric projects supply public electricity networks, some are created to serve specific industrial enterprises.

Tidal power

Tidal energy can be generated in two ways, tidal stream generators or by barrage generation. The power created though tidal generators is generally more environmentally friendly and causes less impact on established ecosystems. Similar to a wind turbine, many tidal stream generators rotate underwater and are driven by the swiftly moving dense water. Although not yet widely used, tidal power has potential for future electricity generation. Tides are more predictable than wind energy and solar power. Historically, tide mills have been used, both in Europe and on the Atlantic coast of the USA. The earliest occurrences date from the Middle Ages, or even from Roman times. Tidal power is the only form of energy which derives directly from the relative motions of the Earth–Moon system, and to a lesser extent from the Earth–Sun system. Indeed, the tidal forces produced by the Moon and Sun, in combination with Earth's rotation.

Radiant energy

This natural energy can perform the same wonders as ordinary electricity at less than 1% of the cost. It does not behave exactly like electricity, however, which has contributed to the scientific community's misunderstanding of it. The Methernitha Community in Switzerland currently has 5 or 6 working models of fuel less, self-running devices that tap this energy. Nikola Tesla's magnifying transmitter, T. Henry Moray's radiant energy device, Edwin Gray's EMA motor, and Paul Baumann's Testatika machine all run on radiant energy. This natural energy form can be gathered directly from the environment or extracted from ordinary electricity by the method called fractionation.

Biomass

Biomass, as a renewable energy source, refers to living and recently dead biological material that can be used as fuel or for industrial production. In this context, biomass refers to plant matter grown to generate electricity or produce for example trash such as dead trees and branches, yard clippings and wood chips biofuel, and it also includes plant or animal matter used for production of fibres, chemicals or heat. Biomass may also include biodegradable wastes that can be burnt as fuel. Industrial biomass can be grown from numerous types of plants, including miscanthus, switch grass, hemp, corn, poplar, willow, sorghum, sugarcane, and a variety of tree species, ranging from eucalyptus to palm oil. The particular plant used is usually not important to the end products, but it does affect the processing of the raw material. Production of biomass is a growing industry as interest in sustainable fuel sources is growing.

Wave power

Wave power is the transport of energy by ocean surface waves, and the capture of that energy to do useful work, for example for electricity generation, water desalination, or the pumping of water (into reservoirs). Wave energy can be difficult to harness due to the unpredictability of the ocean and wave direction. Wave farms have been created and are in use in Europe, using floating Pelamis Wave Energy converters. Most wave power systems include the use of a floating buoyed device and generate energy through a snaking motion, or by mechanical movement from the wave's peaks and troughs. The rising and falling of the waves moves the buoy-like structure creating mechanical energy which is converted into electricity and transmitted to shore over a submerged transmission line.

Geothermal energy

Geothermal energy is a very powerful and efficient way to extract a renewable energy from earth through natural processes. This can be performed on a small scale to provide heat for a residential unit (a geothermal heat pump), or on a very large scale for energy production through a geothermal power plant. It has been used for space heating and bathing since ancient roman times, but is now better known for generating electricity. Geothermal power is cost effective, reliable, and environmentally friendly, but has previously been geographically limited to areas near tectonic plate boundaries, if we consider only the high enthalpy method. Recent technological advances have dramatically expanded the range and size of viable resources, especially for direct applications such as home heating. The largest group of geothermal power plants in the world is located at The Geysers, a geothermal field in California, United States. As of 2004, five countries (El Salvador, Kenya, the Philippines, Iceland, and Costa Rica) generate more than 15% of their electricity from geothermal sources. Geothermal power requires no fuel, and is therefore immune to fluctuations in fuel cost, but capital costs tend to be high. Drilling accounts for most of the costs of electrical plants, and exploration of deep resources entails very high financial risks. Geothermal power offers a degree of scalability: a large geothermal plant can power entire cities while smaller power plants can supply rural villages or heat individual homes. Geothermal electricity is generated in 24 countries around the world and a number of potential sites are being developed or evaluated.

The latter is more complexed than the way it is just described and, because it is the core of this thesis, it will be well developed in depth in the next chapters.

2.2 Geothermal energy

Geothermal Energy (from the ancient Greek "geo", earth, and "thermos", heat) is, in its broadest definition, the natural warmth of the Earth. The heat is produced mainly by the radioactive decay of potassium, thorium, and uranium in Earth’s crust and mantle and also by friction generated along the margins of continental plates. The subsequent annual low-grade heat flow to the surface averages between 50 and 70 mill watts (mW) per square metre worldwide. In contrast, incoming solar radiation striking Earth’s surface provides 342 watts per square metre annually. Geothermal heat energy can be recovered and exploited for human use, and it is available anywhere on Earth’s surface. The estimated energy that can be recovered and utilized on the surface is 4.5×10^6 exajoules, or about 1.4×10^6 terawattyears, which equates to roughly three times the world's annual consumption of all types of energy. The amount of heat within 10,000 meters of Earth's surface contains 50,000 times more energy than all the oil and natural gas resources in the world (www.statista.com).

The areas with the highest underground temperatures are in regions with active or geologically young volcanoes. These "hot spots" occur at tectonic plate boundaries or at places where the crust is thin enough to let the heat through. How it is shown in Figure 2.1, the Pacific Rim, often called the Ring of Fire for its many volcanoes, has many hot spots, including some in Alaska, California, and Oregon. Nevada has hundreds of hot spots, covering much of the northern part of the state.

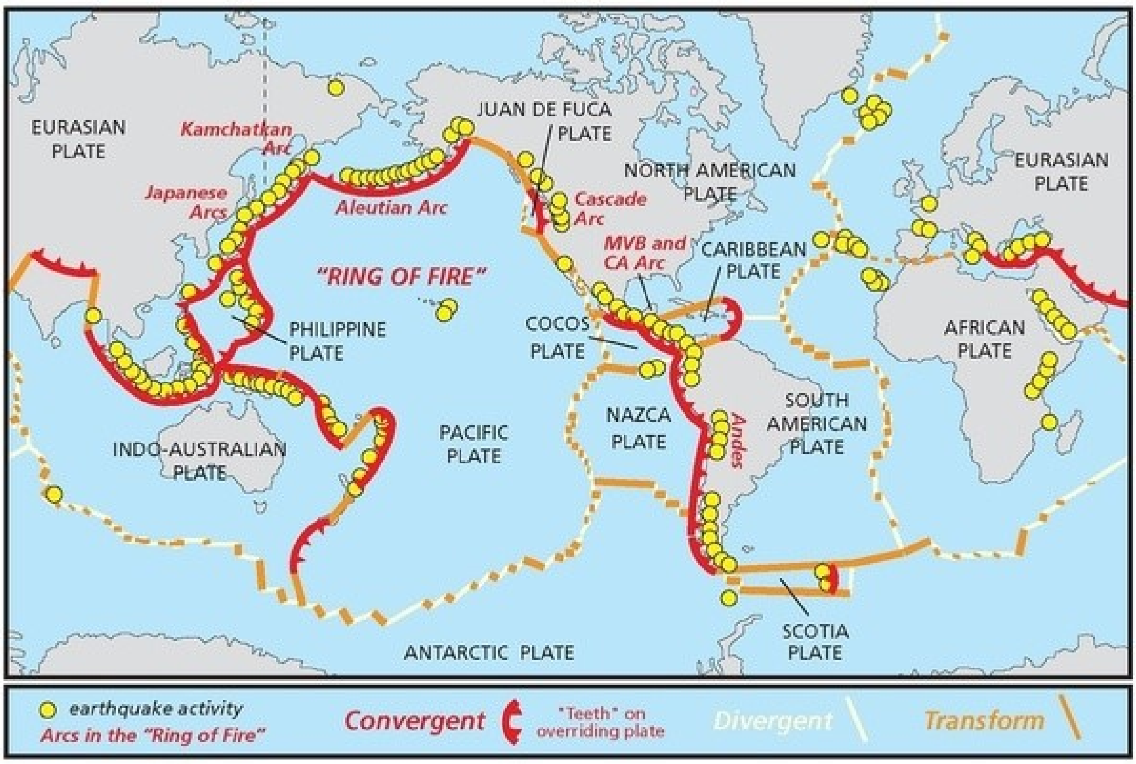

Figure 2.1 Tectonic plates boundaries (www.quora.com)

These regions are also seismically active. Earthquakes and magma movement break up the rock covering, allowing water to circulate. As the water rises to the surface, natural hot springs and geysers occur, such as Old Faithful at Yellowstone National Park. The water's temperature in these systems can be more than 200°C.

Seismically active hotspots are not the only places where geothermal energy can be found. There is a steady supply of milder heat at depths of anywhere from 10 to a few hundred feet below the surface virtually in any location on Earth. Even the ground below your own backyard or local school has enough heat to control the climate in your home or other buildings in the community. In addition, there is a vast amount of heat energy available from dry rock formations very deep below the surface (4–10 km). Using the emerging technology known as Enhanced Geothermal Systems (EGS), we may be able to capture this heat for electricity production on a much larger scale than conventional technologies currently allow. While still primarily in the development phase, the first demonstration EGS projects provided electricity to grids in the United States and Australia in 2013.

It is interesting analyse the Figure 2.2 which highlights the geothermal energy of Europe-Asia countries. How we can see, there are a lot of potential areas where this green energy can be exploited, e.g. Toscana, Italy.

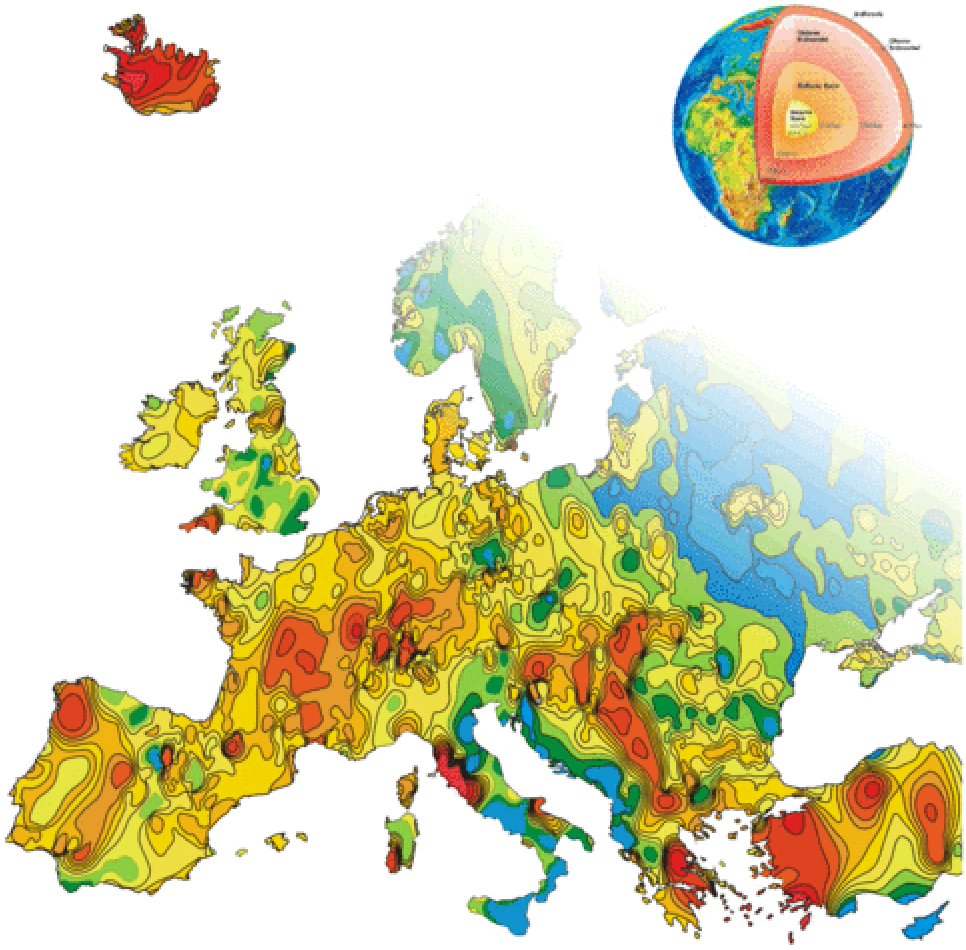

Figure 2.2 Geothermal energy in Europa-Asia (www.askjaenergy.com)

Hence, geothermal energy can be exploited in three different ways, below listed.

2.2.1 Direct use: Probably the most widely used set of applications involves the direct use of heated water from the ground without the need for any specialized equipment. This kind of applications makes use of low-temperature geothermal resources, which range between about 50 and 150 °C. Such low-temperature geothermal water and steam have been used to warm single buildings, as well as whole districts where numerous buildings are heated from a central supply source. In addition, many swimming pools, balneological facilities at spas, greenhouses, and aquaculture ponds around the world have been heated with geothermal resources. For many of those activities, hot water is often used directly in the heating system, or it may be used in conjunction with a heat exchanger, which transfers heat when there are problematic minerals and gases such as hydrogen sulphide mixed in with the fluid. Geothermal energy is best found in areas with high thermal gradients. Those gradients occur in regions affected by recent volcanism, in areas located along plate boundaries (such as along the Pacific Ring of Fire), or in areas marked by thin crust (hot spots) such as Yellowstone National Park and the Hawaiian Islands.

The total worldwide installed capacity for direct use in 2015 was about 73,290 MWt utilizing about 163,273 GW-hours per year (587,786 TG per year), producing an annual utilization factor of 28% in the heating mode.

2.2.2 Electric power generation: Depending upon the temperature and the fluid (steam) flow, geothermal energy can be used to generate electricity. Some geothermal power plants simply collect rising steam from the ground. In such “dry steam” operations, the heated water vapor is funneled directly into a turbine that drives an electrical generator. Other power plants, built around the flash steam and binary cycle designs, use a mixture of steam and heated water (“wet steam”) extracted from the ground to start the electrical generation process.

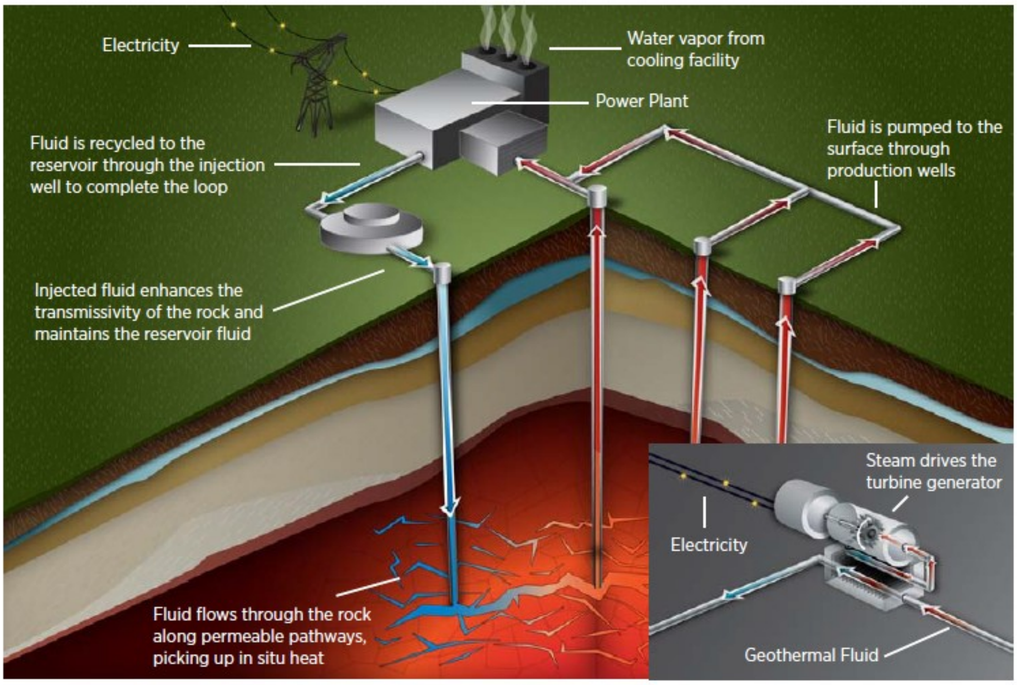

Figure 2.3 Geothermal electricity plant (www.wikimedia.com)

Electrical power usually requires water heated above 175 °C to be economical, for this reason it needs depths of 4 km and more. In geothermal plants using the Organic Rankine Cycle (ORC), a special type of binary-cycle technology that utilizes lower-temperature heat sources (such as biomass combustion and industrial waste heat), water temperatures as low as 85–90 °C may be used.

The first geothermal electric power generation took place in Larderello, with the development of an experimental plant in 1904. The first commercial use of that technology occurred there in 1913 with the construction of a plant that produced 250 kW.

2.2.3 Geothermal heat pumps (GHPs): this one takes advantage of the relatively stable moderate temperature conditions that occur within the first 300 meters of the surface to heat buildings in the winter and cool them in the summer. In that part of the lithosphere, rocks and groundwater occur at temperatures between 5 and 30 °C. At shallower depths, where most GHPs are found, such as within 6 meters of Earth's surface, the temperature of the ground maintains a near-constant temperature of 10 to 16 °C. Consequently, that heat can be used to help warm buildings during the colder months of the year when the air temperature falls below that of the ground (Figure 2.4). Similarly, during the warmer months of the year, warm air can be drawn from a building and circulated underground, where it loses much of its heat and is returned.

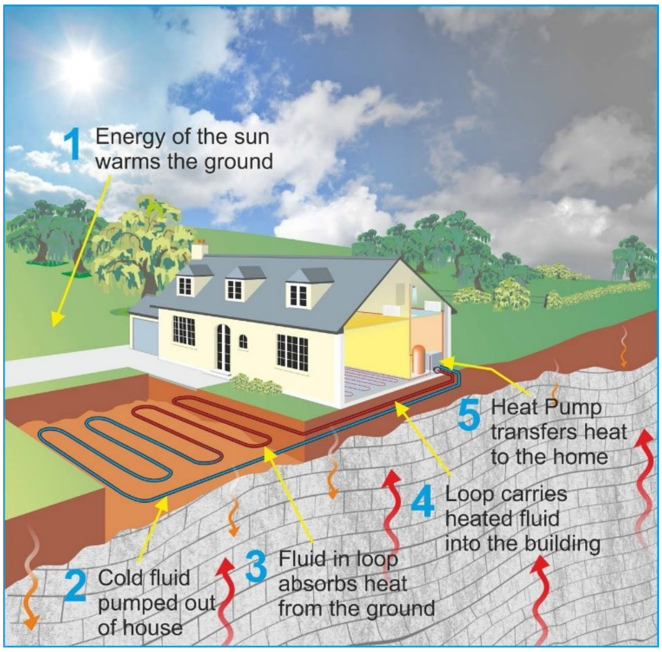

Figure 2.4 Residential heat pump operation for winter heating (www.isabelbarrosarchitects.ie)

A GHP system is made up of a heat exchanger (a loop of pipes buried in the ground) and a pump. The heat exchanger transfers heat energy between the ground and air at the surface by means of a fluid that circulates through the pipes; the fluid used is often water or a combination of water and antifreeze. During warmer months, heat from warm air is transferred to the heat exchanger and into the fluid. As it moves through the pipes, the heat is dispersed to the rocks, soil, and groundwater. The pump is reversed during the colder months. Heat energy stored in the relatively warm ground raises the temperature of the fluid. The fluid then transfers this energy to the heat pump, which warms the air inside the building.

GHPs have several advantages over more conventional heating and air-conditioning systems. They are very efficient, using 25–50 % less electricity than comparable conventional heating and cooling systems, and they produce less pollution. The reduction in energy use associated with GHPs can translate into as much as a 44% decrease in greenhouse gas emissions compared with air-source heat pumps (which transfer heat between indoor and outdoor air). In addition, when compared with electric resistance heating systems (which convert electricity to heat) coupled with standard air-conditioning systems, GHPs can produce up to 72% less greenhouse gas emissions.

Clearly there are many advantages of geothermal energy. It can be extracted without burning a fossil fuel such as coal, gas, or oil; geothermal fields produce only about one-sixth of the carbon dioxide that a relatively clean natural-gas-fueled power plant produces; binary plants release essentially no emissions; unlike solar and wind energy, geothermal energy is always available, 365 days a year. It's also relatively inexpensive; savings from direct use can be as much as 80% over fossil fuels. For these reasons, geothermal energy is starting to spread worldwide, with peaks of concentration in Europe and United State of America, as shown in Figure 2.5. Nevertheless, there are some countries that do not have any geothermal implants because of the maybe only disadvantage that geothermal energy present: initial costs. Indeed, a geothermal implant for a house can reach the initial cost of 15-20 thousand euros, which is twice the photovoltaic implant cost. Nevertheless, they can allow an annual economic saving on operating costs compared to a traditional system (natural gas boiler and split air conditioner) of about 50% and about 70-80% compared to a boiler plant fueled by LPG or diesel oil. Therefore, the cost disadvantage it can be seen as a long-term investment from which you can reap the benefits from 2 to 8 years.

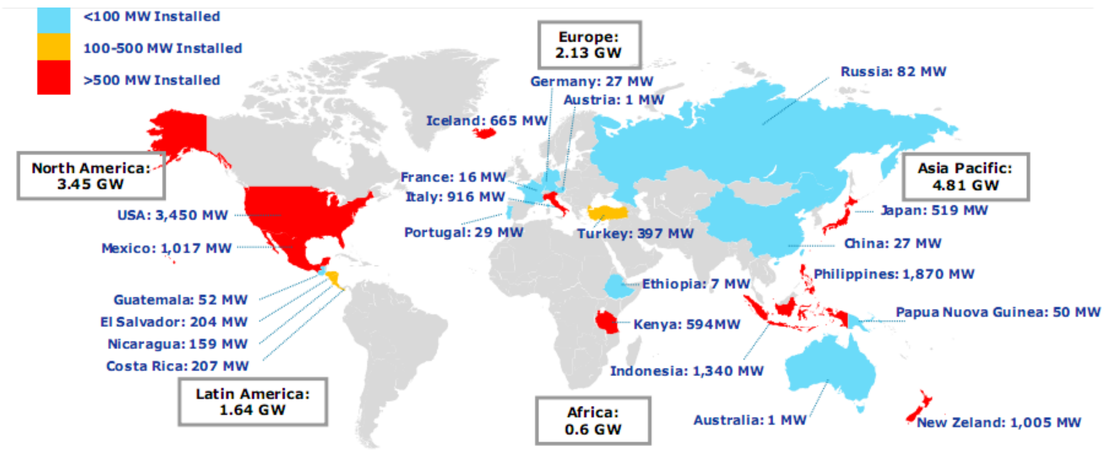

Figure 2.5 Geothermal installed capacity (MW) 2015 (www.oilprice.com)

2.3 Low enthalpy geothermal systems

Clearly, the core of the system is the geothermal heat pump (GHP) which consist of:

- a compressor that increases the pressure and temperature of the circuit fluid that enters inside the compressor in the vapor state;
- a heat exchanger (condenser) in which the steam is heated, giving heat to the building to be heated (in the heating mode) or to the outside (in the case of cooling mode), condensing and passing to the liquid state;
- an expansion valve that further cools the liquid temperature and lowers the pressure;

- a further heat exchanger (evaporator) in which the low-pressure and low-temperature liquid exiting from the expansion valve is able to absorb heat (either from a "cold" source - such as the subsoil - in the operating mode for heating, or from the building when the system operates in cooling mode) and then switch back to the steam state, from which a new work cycle resumes.

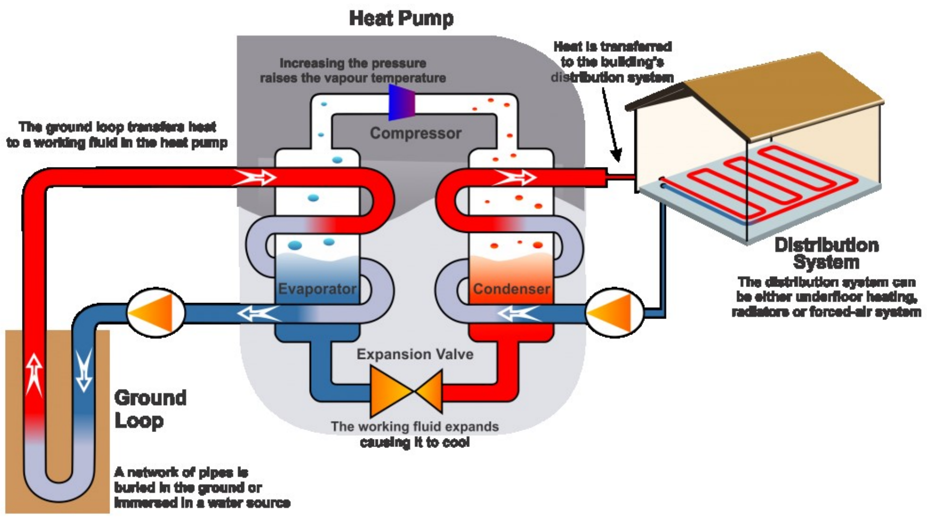

Figure 2.6 Scheme of a Geothermal Heat Pump (www.tidewatermechanical.com)

Geothermal systems are efficient, environmentally-sensitive, comfortable, and economical. Operating savings often provide paybacks of considerably less than five years, sometimes less than two years. However, this type of plants can work only if the temperature is lower than 50°C, hence, in heating mode, they must necessarily be coupled with low temperature systems such as radiant panels (wall or floor) or fan.

2.3.1 Types of Geothermal Heat Pump system

There are four basic types of ground loop systems. Three of these (horizontal, vertical, and pond/lake) are closed-loop systems. The fourth type of system is the open-loop option. Which one of these is best depends on the climate, soil conditions, available land, and local installation costs at the site. All of these approaches can be used for residential and commercial building applications.

The ground-coupled heat pump system consists of a reversible vapour compression cycle that is coupled with a heat exchanger in the form of bore holes in the ground. These types of systems can use both a water-to-air heat pump or a direct-expansion heat pump.

Ground-coupled heat pump system: Also referred to as a closed-loop heat pump, the water-to-air configuration circulates water or a water and antifreeze solution through a liquid-to-refrigerant heat exchanger and a series of buried thermoplastic piping. In comparison, the direct-expansion heat pump circulates a refrigerant through a series of buried copper pipes. Both vertical and horizontal heat exchanger configurations are used in these applications.

- *Vertical* wells generally consist of two small (1.2 m to 30 cm) diameter high-density polyethylene tubes in a vertical borehole filled with a solid medium, commonly referred to as grout. Boreholes typically range from 15 m to 200 m, depending on the local site conditions, including soil thermal conductivity and availability of equipment. Because of this configuration, vertical wells require relatively small areas of land compared to horizontal trenches.
- *Horizontal* wells generally require the greatest amount of ground area and it can be further divided into three subgroups: single-pipe, multiple pipes, and spiral-slinky. Single-pipe horizontal ground-coupled heat pumps are typically installed in a single trench to a depth of 1.2 m to 2 m and require the most ground area of the three.

While the required ground area required for multiple pipes, consisting of two to six pipes placed in a single trench, can be reduced, the total pipe length must be increased to overcome the interference from adjacent pipes. Recommended trench lengths for the spiral pipe configuration can be 20% to 30% of single pipe trench lengths, but may be increased to achieve greater thermal performance.

Figure 2.7 Closed loop system: vertical (www.firstgeothermalenergy.com)

Figure 2.8 Closed loop system: horizontal (www.firstgeothermalenergy.com)

While the vertical well configuration can yield the most efficient ground-coupled heat pump performance, due to reduced variability in soil temperature and thermal properties along with reduced piping and associated pump energy, costs associated with vertical wells are typically more. The expense of equipment required to drill the boreholes along with the limited availability of skilled contractors also contributes to the higher costs. Because of the reduced installation costs, horizontal trenches are widely used in residential applications. However, these systems generally operate at a reduced efficiency due to the impact of seasonal soil property fluctuations and higher pumping energy requirements. Vertical systems are typically installed in large buildings with limited land area.

Groundwater Heat Pump Systems: Preceding the development of ground-coupled heat pump systems, groundwater heat pump one were the most widely used type of geothermal heat pump system. This type of process uses well or surface body water as the heat exchange fluid that circulates directly through the heat pump system. Once it has circulated through the system, the water returns to the ground through the well, a recharge well, or surface discharge.

A typical groundwater heat pump system design consists of a central water-to-water heat exchanger between the groundwater and a closed water loop that is connected to water-to-air heat pumps located in the building. An alternate strategy is to circulate the ground water through a heat recovery chiller that is isolated with a heat exchanger and used to heat and cool the building through a distributed hydronic loop.

Under the right conditions, groundwater heat pump systems can cost less than ground-coupled heat pump one. For this reason, along with the compact space requirements for the water well and availability of water well contractors, this technology has become popular in large commercial applications and has been used for decades.

Nevertheless, potential corrosion issues may require the installation of an intermediate plate-type heat exchanger to protect the heat pump unit; but the hitch is site-specific and should be evaluated where the technology is to be installed.

Last but not least, an open loop system can be used only where there is an adequate supply of relatively clean water and all local codes and regulations regarding groundwater discharge are met.

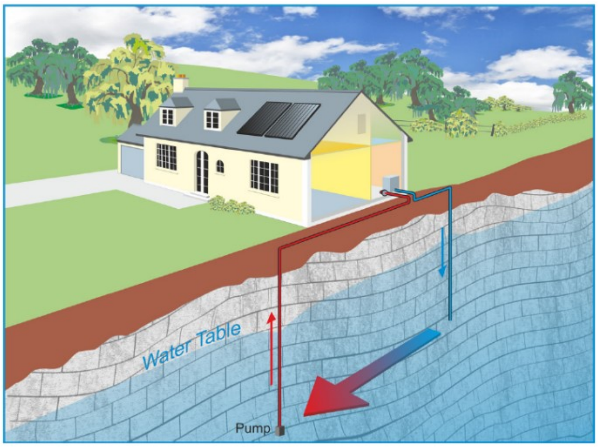

Figure 2.9 Open loop system (www.gsi.ie)

Surface water heat pump system: While the thermal properties of surface water bodies are quite different than other geothermal heat pump technologies, the applications and strategies are similar. Surface water heat pump systems can be either closed-loop systems, similar to ground-coupled heat pumps or open-loop systems, similar to groundwater heat pumps.

Closed-loop surface water heat pumps consist of water-to-air or water-to-water heat pumps connected to piping loops placed directly in a lake, river, or other open body of water. A pump circulates water or a water and antifreeze solution through the heat pump water-to-refrigerant heat exchanger and the submerged piping loop which transfers heat to or from the body of water.

Open-loop surface water heat pumps can use surface water bodies in a similar way that cooling towers are used, but without the fan energy and required maintenance. Lake water can be pumped directly to water-to-air or water-to-water heat pumps.

Because of reduced excavation costs, closed-loop surface water heat pumps can cost less than typical ground-coupled heat pump systems. While these systems have reduced pumping energy and operating costs along with low maintenance requirements, there is the possibility of coil damage in public lakes and variable performance in small and shallow bodies of water resulting from the wide fluctuation of water temperature.

Figure 2.10 Pond loop system (www.waterfurnace.com)

2.3.2 Efficiency of a GHP

Regardless of the application, the best way to measure the efficiency of a heat pump itself is to report the amount of energy that is pumped relative to the amount that must be added to do the pumping. This ratio is called the Coefficient of Performance:

$$COP = \frac{\text{quantity of heat delivered [kW]}}{\text{energy required by pump [kW]}}$$

In spite of the first law of thermodynamics, which tells us that energy can neither be created nor destroyed, a GSHP in a good installation can yield up to four units of heat for each unit of electricity consumed. The heat pump is not creating this energy, but merely separating a medium temperature from the ground into warmth (which can be used for heating) and cold (which can be returned to the ground). A COP=4 it is not always achievable, indeed, a typical efficient air conditioner has a COP of about 3.5: this means it can remove heat at a rate of about 3.5 kW while consuming about 1 kW of electrical energy.

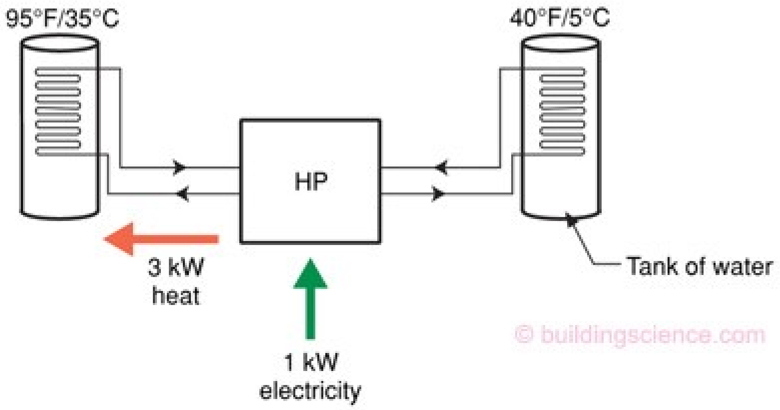

Figure 2.11 Efficiency of a GHP: COP (www.buildingscience.com)

The COP will vary with each installation, but the lower the output temperature to the heat distribution system is, the higher the COP will be. If an output temperature of 60°C is needed to heat radiators the COP is likely to fall to level of only 2.5. If the heat distribution is to a well-designed underfloor heating system that works well at an output temperature of 40°C, then the COP can rise to a level of 4.

The input temperature is also critical to the COP of the heat pump. The higher the input temperature from the ground, the lower the amount of work needed from the heat pump, the higher the COP will be. In fact, the critical factor is the "uplift" between the source temperature and the output temperature.

GSHP are unique in that their reported COP efficiency may not include the energy of the fluid or water pump required to move the fluid through the tubes in the ground. This electrical energy can be significant, particularly if the loop is long, the pipes are small, or the flow resistance within the heat pump unit is large. The largest factor in pump energy use is design: if the designer and installer of the loop and the pump are not careful, a major amount of energy can be consumed. Heat also needs to be removed by a fan or a pump and distributed to the home. To improve heat pump COP, the hot temperature of the liquid produced is often much lower than for a boiler or furnace, i.e. the lift is less. Hence, fan energy can be increased over that of a furnace. This effect is very small in systems that use low temperature radiant heating systems (circulation pumps consume relatively little electrical energy).

This leads to a more accurate definition of efficiency for a GSHP system (System Coefficient of Performance):

$$SCOP = \frac{\text{useful heat delivered}}{(\text{loop pump energy} + \text{heat pump energy} + \text{distribution fan or pump energy})}$$

In heating mode in a cold climate, the system COP of a heat pump rated at COP=4+ can easily drop to COP=3. In our experience, a system COP of 3 for a heat pump in heating mode would be considered good in cold climates (cold soil) even with very efficient heat pump equipment and well-designed and installed pumps. Field heating mode COP values of as high as 4 are possible in warmer climates (warmer soil) and with the best design and best equipment.

In cooling mode in mixed and cool climates, summer time system COP values tend to be higher because the ground temperature in summer are close to the desired air conditioning coil temperature, whereas during winter, the heating coil temperature is far from the winter ground temp. That said, the electrical energy to run the pumps, fans and compressor of the whole system is useful heat in the winter (the inefficiency in the motors results in heating, which is the whole purpose) and increases the cooling load in summer (all of the inefficiency results in heat, which then has to be removed by the heat pump).

3. Energy geostructures

3.1 Introduction to energy geostructures

The geostructures are structures designed from the point of view of geotechnics, i.e. they are structures designed to transfer loads to the soil and some of them, like tunnels, are used to integrate engineering with nature. Some practical examples of geostructures are: retaining wall, tunnels, foundation piles and diaphragm walls.

In the last century, it was thought to fuse together the need for ever-increasing renewable energy and geotechnical engineering. Hence, energy geostructures were designed.

Energy geostructures can link the geostructural role to the energy supply, using the principle of a ground source heat pump system. Indeed, energy geostructures present pipes directly installed in the reinforced concrete structural element, usually fastened to the steel bars to guarantee continuity and reinforce the structure (Amis et al., 2010). Moreover, the only use of elements conventionally designed and realized to perform a structural function, assure success in term of cost.

Brandl (2006) explains, in a simple way, how a thermo-active system works. Basically there are two circuits: the primary circuit contains closed pipework in earth-contact concrete elements (piles, diaphragm walls, columns, etc.) through which a heat carrier fluid is pumped that exchanges energy from the building with the ground. The fluid is a heat transfer medium of either water, water with antifreeze (glycol) or a saline solution. It is shown that glycol–water mixtures are the best option, especially because containing also additives to prevent corrosion in the header block, of valves, of the heat pump, etc.

The secondary pipework is a closed fluid-based circuit embedded in the floors and walls of buildings or bridge decks, road structures, etc. A heat pump connects the two closed circuits, in which heat exchange occurs, as it is shown in the figure below. The main charge of the pump is to increase the temperature level from 10-15°C to 25-35°C. Hence, a low electrical energy is required to raise the originally non-usable heat resources to a higher, usable temperature.

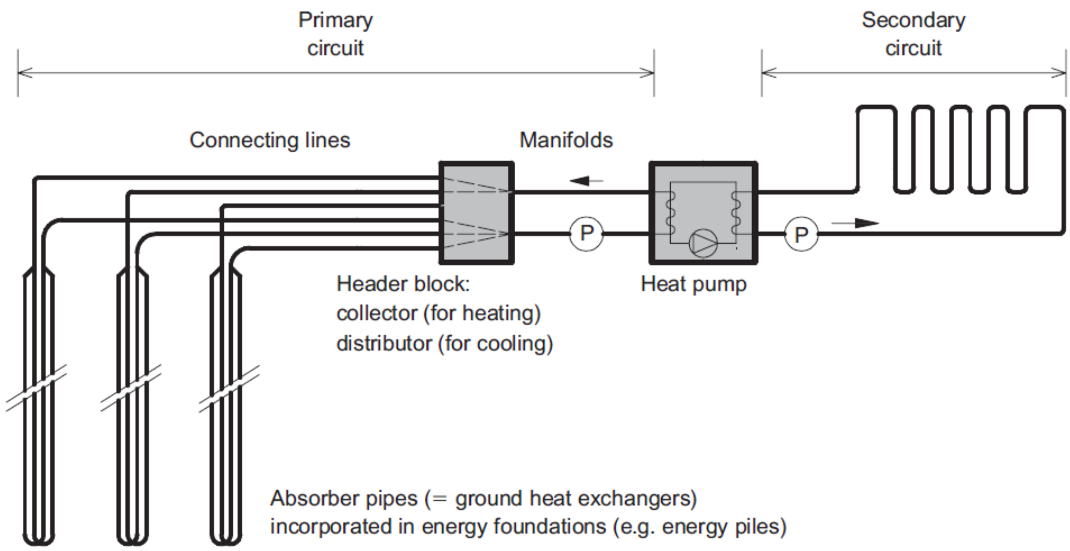

Figure 3.1 Thermo-active system of energy geostructures (Brandl, 2006)

The use of civil engineering structures that are in contact with the ground to replace the more conventional heat-exchange methods is creating great interest in many countries. Bearing piles have been used for this purpose since the mid-1980s and since the mid-1990s, retaining walls also (Brandl, 2006). Energy geostructures are now common in Austria, Germany and the UK. However, the lack of technical evidence regarding the impact of the thermal cycles on the serviceability and safety performance of the geostructures is one of the major obstacles that are preventing the complete acceptance of the system by the countries.

For this reason, many authors have conducted studies related to energy geostructures to strengthen their efficiency. Brandl (2006) described the use of energy walls at a rehabilitation centre in Austria and Section LT24 of the Lainzer tunnel near Vienna, both of which involved the use of piled retaining walls, and underground stations on the Vienna Metro U2 line that used diaphragm walls. Suckling and Smith (2002) describe the first use of energy walls in the United Kingdom where an installation at Keble College, Oxford included a thermally-activated, bored pile retaining wall in addition to thermally-activated bearing piles. A bored pile type wall was also used in a shallow geothermal energy system installed in the Palais Quartier development in Frankfurt, Germany (Katzenbach et al., 2013). Amis et al. (2010) describe the UKs first thermally-activated diaphragm wall system that was constructed for the new Bulgari Hotel in Knights bridge, London. Diaphragm walls and bearing piles formed as part of the construction for the new Shanghai Museum of Natural History have been thermally-activated to provide heating and cooling to the museum (Xia C. et al., 2012).

As just said, some articles were published to highlight strength and weakness of geothermal system, however, being a relatively new field, there is still much to analyze. To do this, first it is necessary to report specific examples of each geostructures, in particular: tunnels, piles and diaphragm walls.

3.2 Energy Piles

Figure 3.2 gives a partial view of the absorber pipes fitted to the reinforcement cage of a large-diameter bored energy pile.

Figure 3.2 Energy Pile (Brandl, 2006)

The percentage of (large-diameter) bored piles has been steadily increasing since the year 2000. The piles consist of 5 m long standard elements that can easily be assembled to longer sections during the driving procedure. The tubes are filled under pressure with concrete and shaft grouting to increase friction is also possible.

Austria is the main promoter of this type of energy geostructures, indeed, since 1985 more than 1 million metres of cast iron piles have been installed. At present, about 130000 m are driven every year, with an increasing proportion of energy piles. As known, the heat exchangers are inserted into the fresh concrete, and have to be secured against uplift until the concrete has sufficiently hardened (Brandl, 2006). The standard diameter of such driven piles is d 42.5 mm, but this can be increased significantly by shaft grouting. Nevertheless, the geothermal effectiveness of such thin energy piles is smaller than that of driven precast concrete piles or large-diameter bored piles, despite the high thermal conductivity of cast iron. The small diameter enables the installation of only one pipe loop and no coiled piping. Moreover, the contact area with the ground is relatively small. In soft soils, buckling of the piles also has to be considered.

Di Donna and Laloui (2014) investigated, numerically, the behaviour of energy piles foundations during heating-cooling cycles, through combined effects of mechanical and thermal loading on both single pile and raft deep foundations. What it is take into account in this section, are the displacements due to thermal cycles of a raft deep foundation, as figure 3.3 shows.

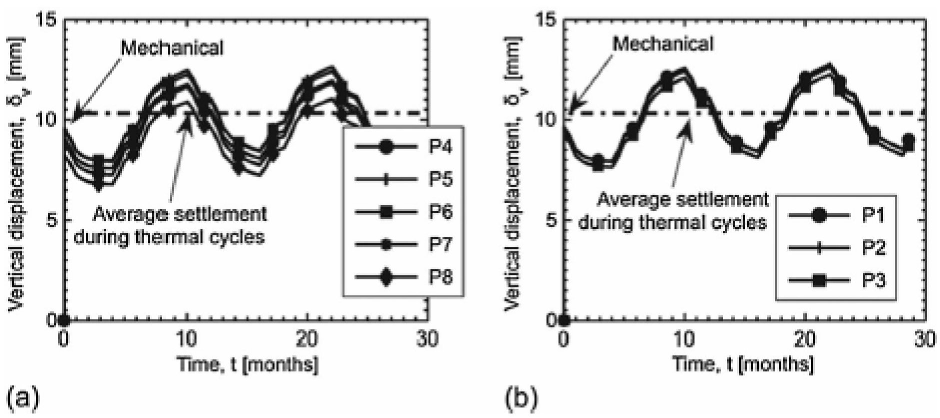

Figure 3.3 Evolution of vertical displacements during thermal cycles at the piles head for (a) central piles and (b) external piles (Di Donna and Laloui, 2014)

The central piles (P1, P2 and P3) start from the same mechanical-induced settlement of roughly 1 cm, and their response during heating and cooling is definitely similar. The effect of the thermoplastic response of the soil corresponds to 1 mm additional irreversible settlement, but it is negligible with respect to the mechanical one.

The vertical reversible displacement due to the thermos-elastic deformation of the pile (upwards during heating and downwards during cooling) has total amplitude of 4 mm. The external piles (P4, P5, P6, P7 and P8) have a differential displacement, although small, between them and with respect to the central ones. However, the thermal loading does not enhance it, and for these piles, the same conclusions drawn for the central ones can be made. The same observation has made for a single pile.

In the design practice, is important to analyse this aspect, i.e. displacement, hence stresses. When subjected to a temperature variation, a pile deforms thermally but a portion of its free thermal deformation is prevented and generates additional stresses in the pile that are compressive during heating and tensile during cooling.
Moreover, the interface shear stress, which is mobilized upwards during axial compressive mechanical loading, is mobilized both upwards and downwards during thermal loading depending on the pile deformation and position of the null point. Whereas the heating-induced compressive stress, is admissible with respect to the concrete strength and the cooling-induced reduction of compressive stress inside the central pile is observed. The admissibility of the maximum compressive stress during heating with respect to the concrete strength, as well as the development of tensile stress during cooling, depends also on the entity of the mechanical induced stress.
The last observation reported, is the important difference between a single pile and a group of them. For a single pile it is valid the theory according to which the higher the thermal-induced observed deformation and the lowest the thermal-induced stress, but for a group of energy piles is not the same. This is attributed to the presence of the slab and to the consequent redistribution of stresses from the external piles to the central ones that

result to be consequently more charged. The response is likely to be sensitive to the slab stiffness: the more rigid the slab, the more the response will be governed by it and the less rigid the slab, the more the response will be governed by the single pile behaviour. Nevertheless, the simulations show that the problem of the eventual development of tensile stress inside the piles after the cooling phase might be enhanced by the presence of a rigid slab with respect to the case of an energy pile considered alone.

3.3 Energy tunnels

During the last years, considerations were made how the technology can be extended to tunnels. In comparison with building foundations, substantially larger ground volumes can be activated for geothermal heat use. In high overburden tunnels, significantly higher temperatures can also be utilized. In addition, shallow tunnels, like those for metros, can be used profitably for geothermal heat production. The first application of this kind can be found in the Lainzer tunnel in Austria (Adam & Markiewicz, 2009). For the installation of absorbers in tunnels, cut-and-cover and mined tunnels have to be differentiated. For cut-and-cover tunnels, the well proven methods already used in deep foundations are tapped. For mined tunnel construction, new developments are necessary (Unterberge et al., 2005). Moreover, with existing methods, the equipment of the invert of tunnel tubes can be realized and research activities for the development of suitable absorber systems were performed to use the inner lining.

When mechanized tunnelling is used, the tunnel segmental lining optimized for heat exchange is precast in factory and then placed on site by the tunnel boring machine (TBM) (Frazius and Pralle, 2011; Barla and Perino, 2014). The system could also allow cooling the tunnel using the heat produced internally by fast moving trains or vehicles. The heat exchanged at the tunnel level can be transferred to the surface by placing pipes into the ventilation shafts or through the portals (Barla and Di Donna, 2018). The stations of metro tunnels can also be used for this purpose.

The pipe line length can be optimized in order to reduce heat losses(Barla et al., 2016) and the system can be used to allow heat distribution at the district scale.

It is possible to do a distinguish between ‘‘cold” and ‘‘hot” tunnels in base of their thermal conditions.

In cold tunnels, all year round, the air temperature is roughly 15°C, and it is not increased by the passage of trains. Generally, the diameter of this type of tunnel is large (around 10-12 m).

The prevailing temperatures in the tunnel only have a limited effect on the temperature in the surrounding ground.

Indeed, hot tunnels, usually present high internal temperatures. Urban tunnels (diameters around 7 m), during summer, can reach an air temperature of 30°C. Rapid cycle frequency of trains leads to additional heat, therefore the air temperatures in the tunnel, which warms the ground. Moreover, deep tunnels could be heated by the ground itself, which can achieve a temperature of 50°C.

Barla et al. (2016) studied the thermal activation of the South extension of the Metro Torino line 1. The line connects Fermi station to Porta Nuova since 2006, while a second section was constructed between 2006 and 2011 to connect Porta Nuova and Lingotto stations, for a total length of 13.4 km.

The portion considered to test the energy tunnel technology, with the ENERTUN patent, is the new south extension of the line toward Piazza Bengasi (Figure 3.4), which is currently under construction.

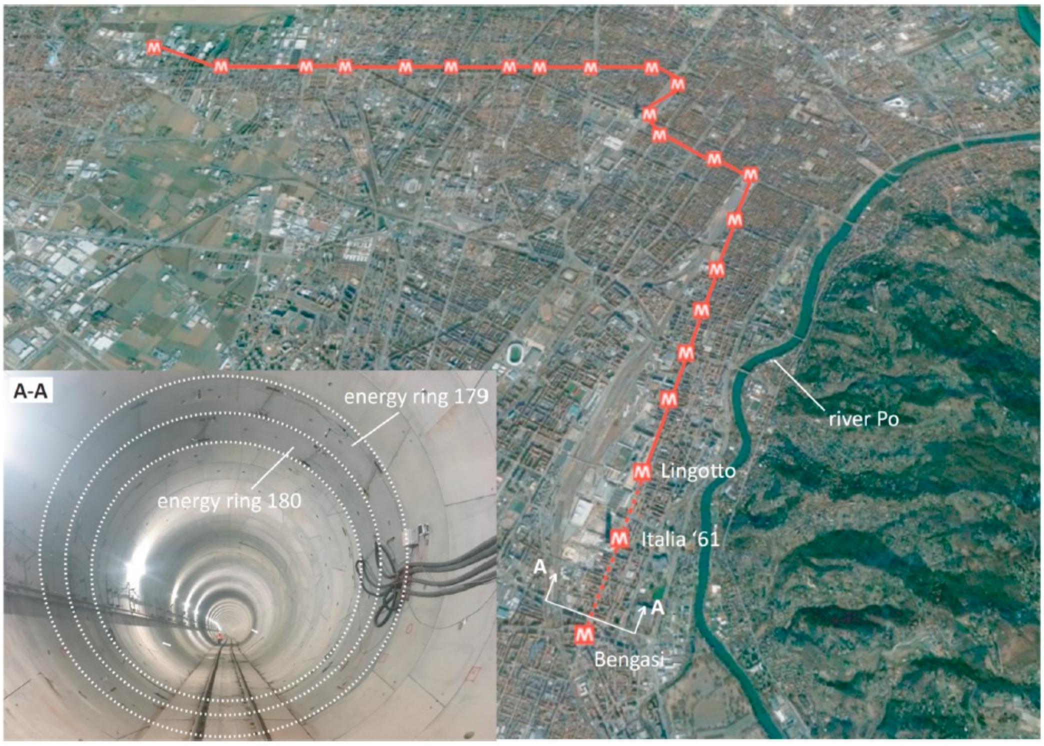

Figure 3.4 Map of Turin Metro Line 1 along with a picture of the Enertun experimental site (Barla et al., 2019)

The tunnel has approximately 8 m of diameter, excavated by shielded EPB TMB (Earth Pressure Balance Tunnel Boring Machine). The tunnel lining is made of precast concrete rings (thick-ness 30 cm), each constituted by 7 segments mounted by the TBM itself (Barla et al., 2016). Cement foam is injected to guarantee full contact with the ground and the segments are appropriately sealed in order to avoid groundwater ingress. The average cover of the tunnel is 21.5 m and excavation takes place below the water table. From the thermal point of view, the tunnel is of a cold type as ventilation is guaranteed by a number of wells that inject external air into it. All the knowledge on the Turin subsoil properties and conditions is supported by various amounts of data (Bottino and Civita, 1986; Barla and Barla, 2005, 2012; Barla andVai, 1999). In addition, in order to allow for easy inspection during the tunnel lifetime, with the metro system in service, the inflow pipe and the outflow pipe is located in the sidewalls of the tunnel, below the security pedestrian footpath. In the specific case, the described system would allow to activate a total length of tunnel of 1350 m.

Regarding the pipes are able to withstand high pressures and temperatures, resist to corrosion and guarantee high durability. Furthermore, the ENERTUN patent, leaded by Barla and Di Donna, suggest a layout of pipes perpendicular to the tunnel axis (Figure 3.5) . Thus, thanks to the groundwater flow perpendicular to the tunnel axis, imply a head losses reduction of 20-30% (Barla et al., 2016).

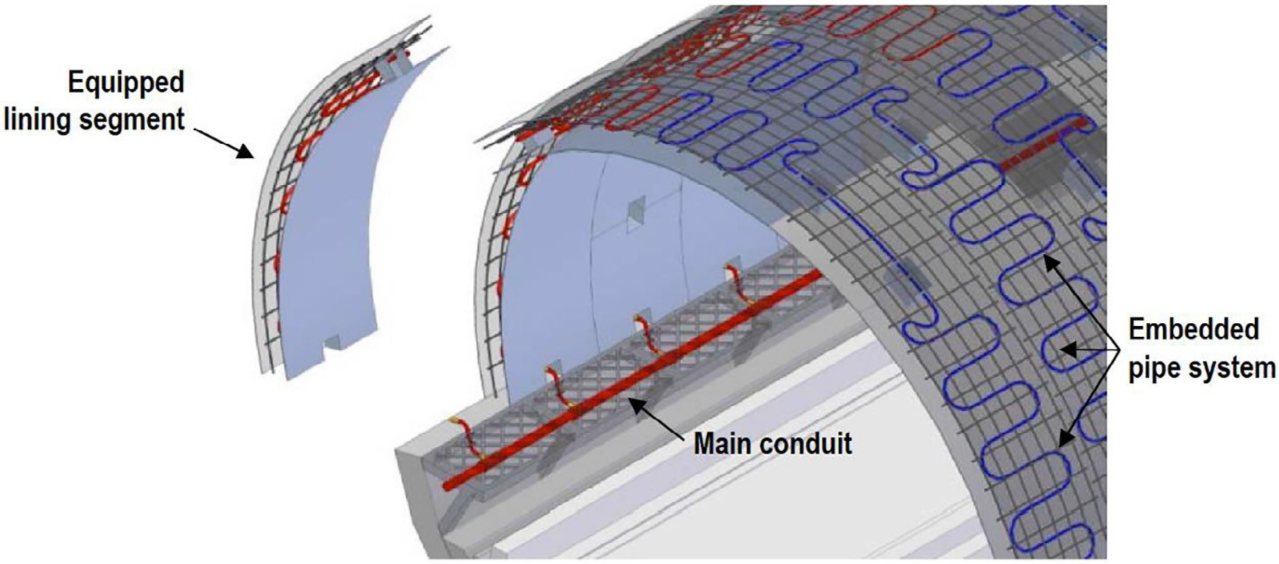

Figure 3.5 Schematic representation of a tunnel segmental lining equipped as ground heat exchanger (Barla et al., 2016)

Two rings of segmental lining were fully equipped with the ground and air net of pipes for a total of 12 ENERTUN segments. The two nets of pipes, one close to the extrados (tunnel surface in contact with the ground), and the other close to the intrados (tunnel surface in contact with the air) allowed to test alternatively three different configurations of the ENERTUN energy tunnel precast segmental lining (Barla et al., 2019). The figure below shows the main steps that characterized the preparation of the segments.

Figure 3.6 Preparation stages of energy segments: (a) moulding, (b) casting, (c) demoulding and (d) circulation test. (Barla et al., 2019)

For this case, it was used as thermo-fluid circulating into the pipes, a propylene glycol mixed with water that can work down to a temperature of −20° C. The inlet temperatures of 4° C for winter (heating mode) and 28° C for summer (cooling mode) were assumed.

One of the many studies done on the Line 1 South Extension is about the changing of soil's temperature around the tunnel due to geothermal system in a time frame of 3 years (Figure 3.5).

As shown in Figure 3.7, at 2 m distance from the tunnel contour, there is the most changeable area and to avoid the progressive heating or cooling of the ground with time, the most optimised solution is to use the system both for heating and cooling.

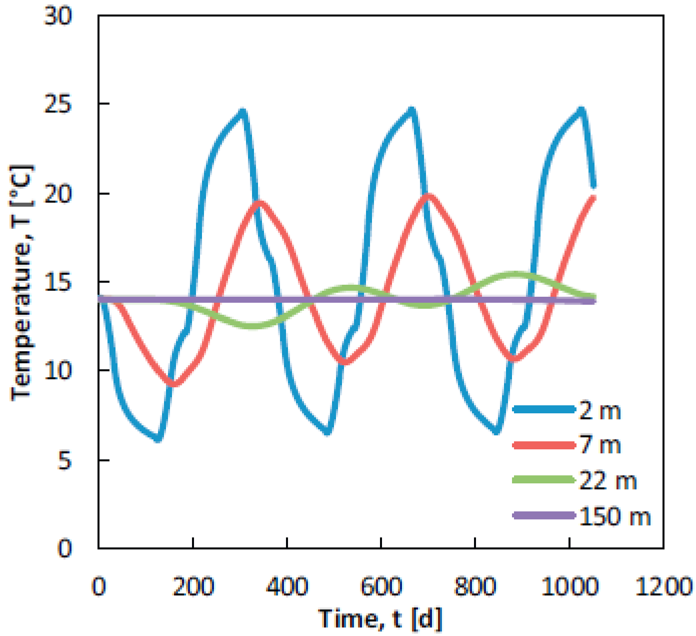

Figure 3.7 Temperatures in the soil at different distance from the tunnel during three years of cycling heating and cooling (Barla, Di Donna, & Perino, 2016)

Moreover, the energy tunnel system would allow exchanging between 53 and 74 W/m^2 of tunnel lining in winter and in summer respectively. If it is considered the total length of the tunnel, the extracted heat is 1.67 kW (heating mode) and injected 2.34 kW (cooling mode). Owing to the favourable underground water flow conditions in Torino, which allows a continuous thermal recharge of the ground, significant improvement of the heat extraction and injection efficiency is guaranteed.

In conclusion, it has been demonstrated that the additional cost required to activate the tunnel lining is less than 1% of the total cost of the project so that the thermal activation of the tunnel lining is 41% less expensive than using vertical piles with ground source heat pumps to cover the same energy requirement.

Because of the very promising results, a test site was recently installed in the tunnel under construction to validate the results found and provide quantitative information for future installations (Barla, Di Donna, & Insana, 2017). In terms of heat exchange, for example, thermally active tunnels could allow exchanging from approximately 10–20 W/m^2 when no groundwater flow is present, and up to 50–60 W/m^2 when there is significant groundwater flow.

Finally, from Di Donna et al. (2017) paper, it is possible to highlight some key aspects for energy geostructures such as tunnels. Indeed, with respect to cut-and-cover tunnels and underground tunnels in urban areas, these are more likely to be constructed in saturated soils and will be less influenced by the external air temperature variation as a result of their higher cover, this should at the same time improve their heat exchange potential. An additional aspect which must be considered specifically for tunnels, that is not necessary with energy piles, is the effect of temperature and speed of the air inside the tunnel or underground space (Nicholson et al., 2014). These energy geostructures will exchange heat not only with the ground, but also with the air inside the underground space. In the case of hot tunnels this might represent an additional source of heat during winter, but a drawback during summer. Some examples of heat exchange in real energy tunnel are plotted in the following chart, where it is evident to understand what is was said before.

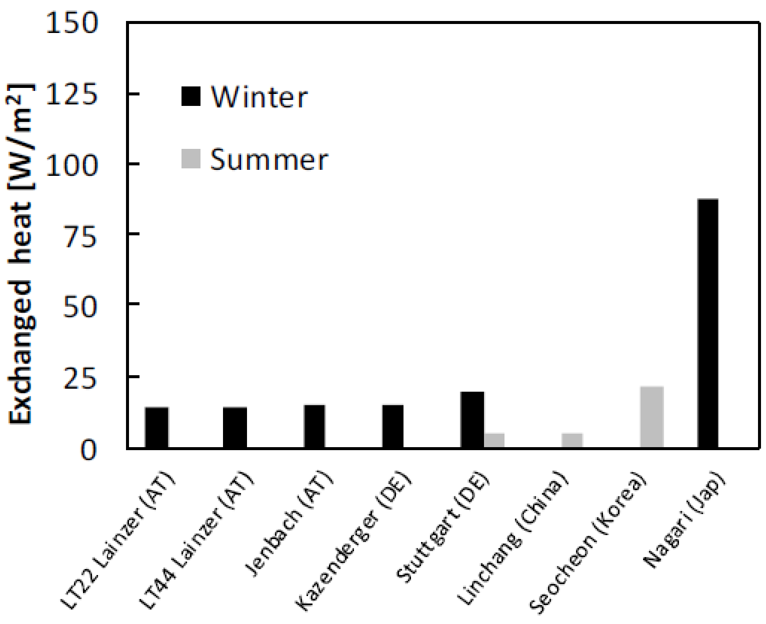

Figure 3.8 Heat exchange per square meter of wall in real energy tunnels. (Di Donna et al.,2017)

3.4 Energy diaphragm walls

A diaphragm wall is a vertical structure, partially or entirely embedded in the ground, which function is to supporting the soil.

Generally, it is a prefabricated structure or cast in place, designed to support artificial temporary or definitive excavations, preventing the slipping of the soil inside the digging.

The diaphragm walls are generally made with alternating modules of 2.5 m, with thicknesses ranging from 0.4 m to 1.5 m. Beyond the excavation, the execution of the actual diaphragms covers, common steps, consisting of the setting of the reinforcement cages and the concrete casting. The reinforcement cages, generally preassembled to transportable modules with a maximum length of 12 m, consist of longitudinal irons, brackets and diagonal bracing bars. The completion of the diaphragms occurs with the construction of a head beam that connects the walls and has the function of solidifying the various elements constituting the diaphragm and making them collaborating to share local actions.

For the realization of this type of structures, it is prefer able to use the hydromill, and the implementation phases include:

- preparation of the area;
- pre-excavation activity (2 ÷ 3 m depth using a clamshell bucket and bentonite support;
- milling of alternate panels;
- lower the armature cage;
- concrete casting with bentonite recovery;
- head beam construction.

The phases just described are shown in figure 3.9.

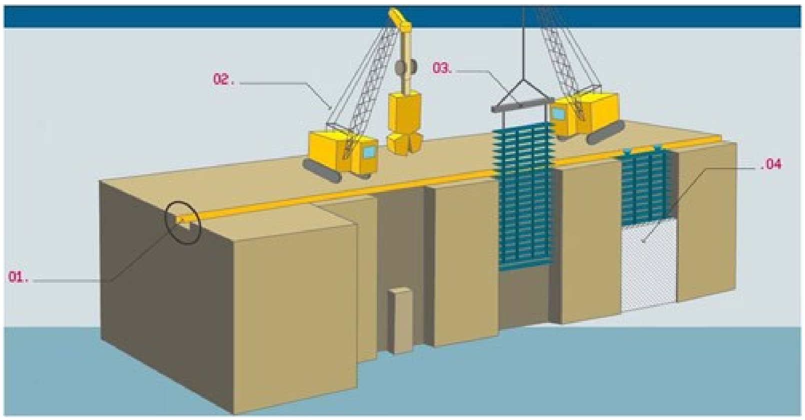

Figure 3.9 Construction phases of a diaphragm wall in reinforced concrete (www.omranista.com)

The energy diaphragm walls, unlike conventional diaphragms, have bundles of polyethylene pipes necessary for the transport of the heat transfer fluid which is responsible for the heat exchange. Where geothermal loops are also incorporated in the wall, the loops are installed onto the cage as it is being lowered into position; the loops have to be secured to ensure the pipes are not snagged during the construction of the wall. In addition, the free ends of the loop have to be protected until being exposed for connection when the head beam is constructed. The last step is to immerse the loops in the concrete to ensure good thermal contact. As a reminder, the effective area of the concrete wall is only marginally reduced by the introduction of geothermal loops and can be ignored in the capacity calculation (Amis, 2010).

The construction phases are a bit different in comparison to the ones described before, indeed they can be summed like following:

- quality control and pre-installation testing;
- lifting of the diaphragm armature cage;
- installation of the pipes;
- fixing the pipes to the cage as it is lowered;
- cutting of excess pipes and their protection;
- aptitude test of the pipes before casting concrete;
- casting (of the diaphragm) of concrete.

Figure 3.10 Inserting the geothermal pipes into the diaphragm cage (Amis et al., 2010)

Two important precautions must be kept in mind when the pipes are setting up. The first is that the pipes are not inserted inside the reinforcement cage in the prefabrication plant, as during the transport phases, they could be irreparably damaged, with difficulty of identification, evidence of damage and consequently laying of pipes malfunctioning (Amis et al.,2010).

The second provides that, once the reinforcement cage has been installed correctly (also containing the heat exchanger tubes), the pipes are subjected to pressure to verify their integrity and ensure that there has been no damage during installation; the pressurization must be applied during the concrete casting phase of the panel and kept constant for the following day (Amis et al., 2010).

Figure 3.11 Coupling of the pipes to the cage (Amis et al.,2010)

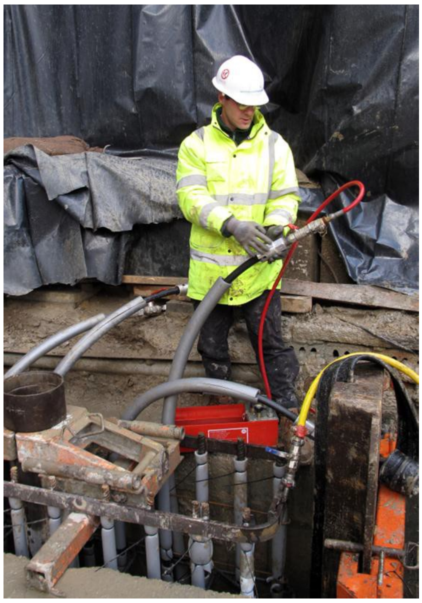

Figure 3.12 Pressure testing geothermal loops once reinforcement cage installation (Amis et al.,2010)

At the end of the construction, the arrangement of coils on the entire surface of the bulkhead is noted: several exchangers are thus arranged along the diaphragm wall in the longitudinal direction (Figure 3.13). Generally, they are placed only along the surface in contact with the ground in conditions of low damping of the diaphragm and optionally, in case of further internal coatings, the exchanger pipes can also be arranged on both sides of the diaphragm.

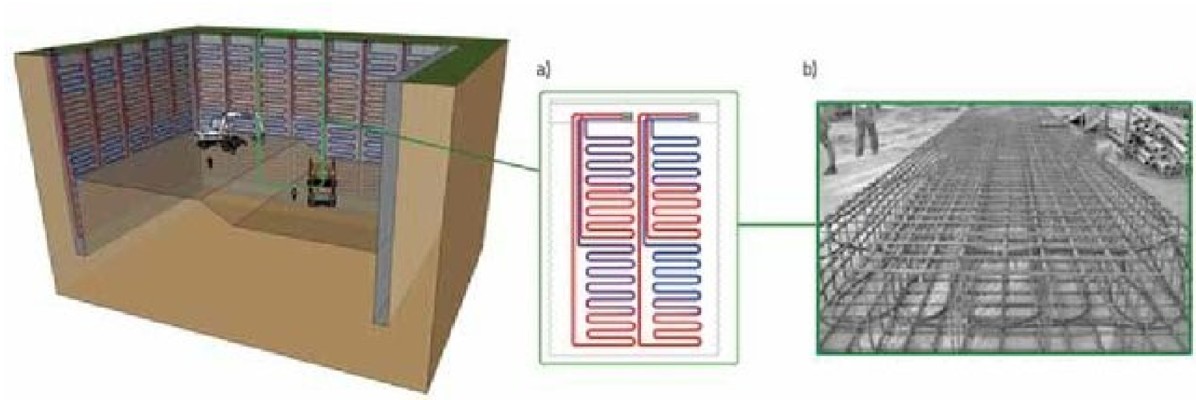

Figure 3.13 Energy DW scheme position (Kovacevic, Bačić, & Arapov, 2013)

In reference to the soil, Brandl (2006), through actualized projects in Austria, underlines the non-influence of the geothermal system to the surrounding ground in terms of shaft resistance, base pressure and bearing resistance. Moreover, the temperature induced settlement or heave is negligible.

On the other hand, the diaphragm walls, carrying out its function, is mainly subjected to lateral pressure of the ground, therefore the internal stresses to the section, from the side of the ground, are mainly traction, while they are of compression on the side of the excavation. Moreover, the flow of liquid inside the heat exchangers is always changing and in the project, the maximum and minimum temperature of the liquid must be set considering the possible evolutions. Once the heat exchanger tubes have been incorporated into the concrete, the fluid inside them transports the heat-carrying fluid with a variable temperature during the year and, due to the temperature difference between the fluid and the concrete, is thus generated a thermal stress around the tube. The temperature range induced inside the diaphragm wall is uniformly distributed around the tubes and the influence region is quite limited. Furthermore, in areas away from heat exchangers, the thermal stress in the structure is mainly caused by the temperature of the surrounding soil; the value of over voltages will therefore be small and can be neglected, since it does not have a negative impact on the structure.

Following all these considerations, would be smart to evaluate the thermal influence in the structural analysis, as the thermo-mechanical effects on the DW should be investigated during the design and verification of the geotechnical work.

The application and research of heat exchanger buried in diaphragm wall are so far relatively rare. Only in 1996, absorber tubes were first embedded in diaphragm walls as heat exchanger in Austria and Switzerland (Brandl, 2006). For the first time, in 2003, in the sections of Viennese Metro Line Extension U2, absorber tubes were applied as heat exchanger in diaphragm wall, foundation floor and linings of sector tunnel, proving the power of the type of system.

Suckling and Smith (2002) described the first embedded energy wall in the UK at Keble College, Oxford, while Amis et al. (2010) dealt with the installation of the first energy diaphragm wall for the new Bvlgari Hotel in London. Farther, the new underground railway line in London has been equipped with geothermal technology in diaphragm walls (Amis and Loveridge, 2014).

Diaphragm walls formed as part of the construction for the new Shanghai Museum of Natural His-tory have been thermally-activated to provide heating and cooling to the museum in the new Shanghai Museum of Natural History (Xia et al., 2012). In Frankfurt, Germany, a bored pile type wall was installed in the construction of the Palais Quarter development (Katzenbach et al., 2017).

The efficiency of an energy diaphragm wall depends on many factors such as: the arrangement of the loops inside the cage, the spacing between two consecutive pipes, the concrete and soil thermal conductivity, the length of the bulkhead, the presence of groundwater flow, the velocity if the inlet fluid, boundary conditions and, obviously, the temperature difference between the soil and the inlet fluid of loops in the DW. Almost all this parameters were taken into account from different authors during the last years.

For example, Xia et al. (2012) analyzed the new technology on the *Shangai Museum of Nature History* from the point of view of heat exchanger type, water velocity, inlet water temperature and operation mode.
First of all, three different types of underground heat exchangers were considered: W-shaped, improved W-shaped and single U-shaped (Figure 3.14). For each of them, three different inlet fluid temperature were coupled to the sundry loops and the heat exchange rate per meter of tube is marked. Results showed an increasing of 20-40% of the heat rate for the type (a) and (b) over (c). Moreover, the type (b) demonstred a better performance, roughly 10% more, over (a). Hence, for the W-shaped tubes in this experiment, by enlarging the distance of branch tubes near the soilward face, the heat transfer rate increased by 11%. Therefore, to enlarge the distance of branch tubes is an effective way to improve the heat transfer performance.

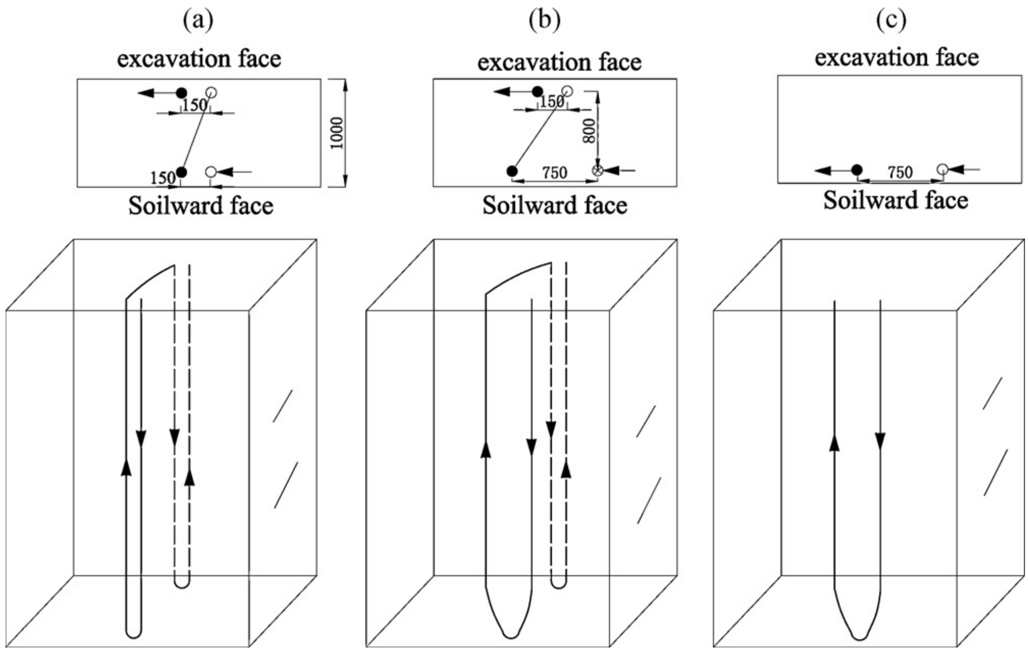

Figure 3.14 Types of underground heat exchangers: a) W-shaped type, b) improved W-shaped type, c) single U-shaped (Xia et al., 2012)

About internal water flow, the paper shows a rising of the heat exchange rate with the increasing of water velocity when it remains below 0.9 $\frac{m}{s}$ and changes slightly when it is larger than this value. In the design of heat exchanger in diaphragm wall, it is suggested to find a reasonable velocity pursue instead of an extensive high water velocity.

The last observation made by Xia et al. (2012), reported here, is about temperature: if the inlet water temperature increases 1°C, the heat transfer rate improves by 15%. This remark is valid for all different shaped pipes.

Bourne-Webb et al., (2016) demonstrated the non-conservative effect, with respect to heating capacity, of a simple constant temperature boundary condition at the wall-air void surface, although airflow in the excavation is faster than 3 to 5 $\frac{m}{s}$ as for instance in a tunnel.

The last work here mentioned, is the one of Di Donna et al. (2016) who was able to analyze the fundamental aspects that influence an energy diaphragm wall: DW width, depth of excavation, spacing between two consecutive loops, concrete cover, inlet fluid velocity, excess temperature, concrete thermal conductivity. Futhermore, all the parameters were taken into account in four time frames: 3,5,30 and 60 days after the activation of the geothermal system. The geometry considered for the model analysis is reported in the figure below, jointly with the different spacings considered.

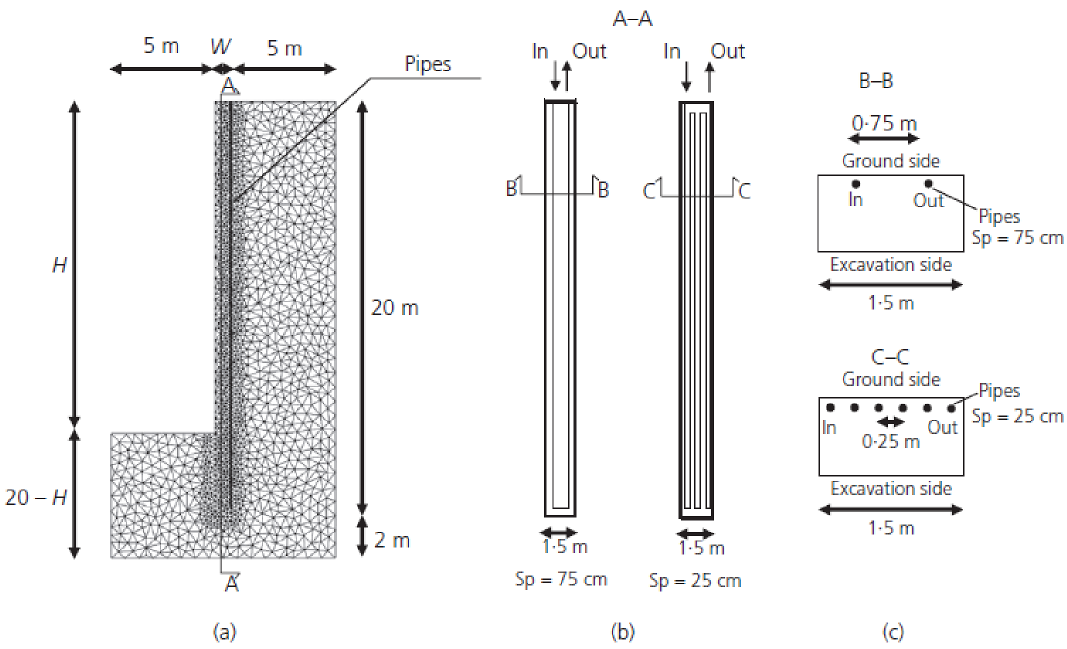

Figure 3.15 Geometry of parametric analysis: (a) vertical cut of the FE model, (b)vertical and (c) horizontal cut of the DW assuming upper and lower values of pipe spacing (Di Donna et al., 2016)

The coupled numerical simulation and statistical analysis led to state that the most important factor that improves significantly the energy efficiency is the pipe spacing reduced, i.e. increasing the number of pipes is the primary route to be considered in order to optimise the design. Nevertheless, this kind of influence goes into the background in a long-term prospective, where other factors take the lead. Indeed, the temperature excess between the wall and the excavation is the long-term parameter which governs the energy efficiency. This is consistent with the long-term steady-state analysis proposed by Bourne-Webb et al. (2016) where the interface with the inside of the excavation governs heat transfer. Of course, the thermal conductivity is crucial too, i.e. the concrete mix should be the optimal one in terms of maximum thermal conductivity.

As it is shown in Figure 3.16, spacing and temperature excess are the most important one above the other factors. For this reason, Di Donna et al. (2016), suggests to equip both sides of the DW with pipes over the wall's full depth in order to increase energy efficiency. An optimal pipe spacing of 40 to 60 cm is suggested by ICConsulten (2005) ensuring a long-term pay-back periods and a balance between heating and cooling applications.

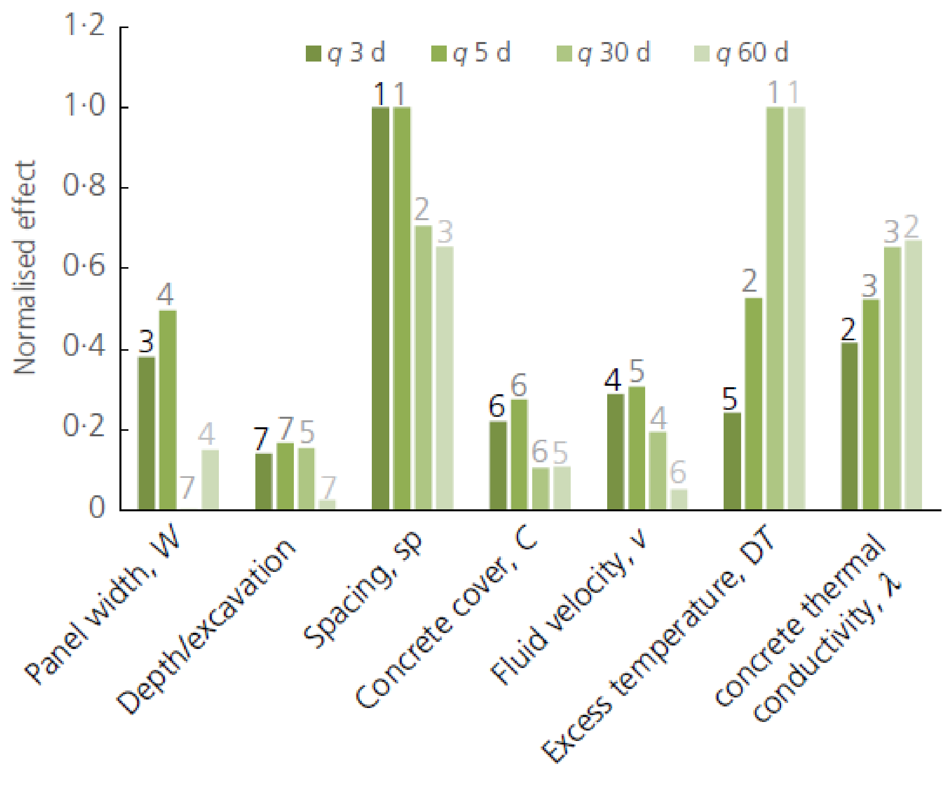

Figure 3.16 Normalised effect of each parameter in terms of heat exchanged (Di Donna et al., 2016)

The ensemble of this analysis, allows to not be too far in error assuming that the technology is mainly governed by the inlet temperature, the shape of the loops, the spacing and the excess temperature. Award of this, an efficient energy diaphragm wall can be design in order to exploit the shallow geothermal energy.

As done for tunnels, refer to real cases regarding the heat exchange is almost an obligation. In Figure 3.17 it is shown the efficiency, in term of heat exchange, of a several energy diaphragm walls present all around the world. Moreover, it can be seen that the heat exchange is generally in the range between 10 to 50 W/m^2, with some exceptions, i.e. EA Center in Austria. It is anticipated that the
differences might depend on the depth of the installation and on soil thermal and hydraulic properties and underground conditions, especially the presence of groundwater flow.

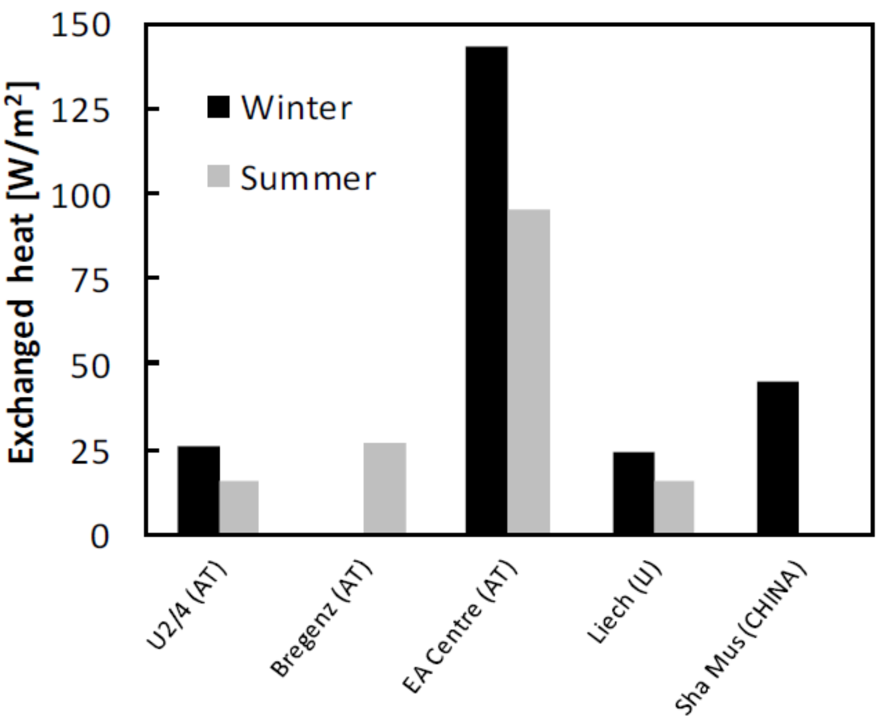

Figure 3.17 Heat exchange per square meter of wall in real energy walls. (Di Donna et al.,2017)

Moreover, it is important to make thermo-mechanical observations and not just thermal capacity considerations. Indeed, although the energy capacity of these geostructures has only advantages, it is also necessary to analyze the mechanical variations induced by thermal variations and guarantee the stability of the structure. To achieve this goal, some studies have been conducted and will be reported here.

Based on the study of the section LT24 of the Lainzer Tunnel in Austria, P.J. Bourne-Webb et al. (2015) suggests that, after the end of construction, the next major alteration in the behaviour of the wall system is the thermal equilibration to the imposed ground surface and tunnel wall boundary conditions. Operation of the absorber pipes appears to make very little difference to the wall response. Furthermore, as shown in Figure 3.18, the effect of heating (or cooling) operations on the mechanical behaviour of the wall system examined appears to be largely benign, with the major changes being attributable to climatic variations (ground and tunnel environments) that will occur anyway.

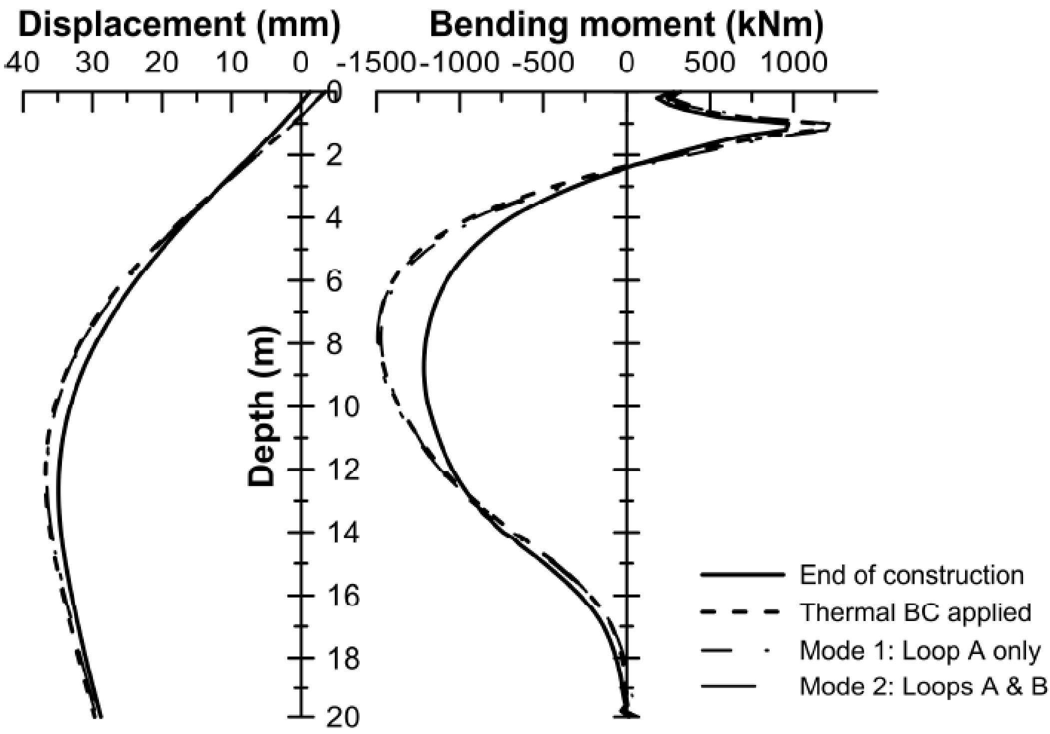

Figure 3.18 Wall response to heat injection with differing heating modes (P.J. Bourne-Webb et al., 2015)

Another interesting and complete study done concerning thermo-mechanical behaviour of an energy diaphragm wall is the one of Barla et al., (2018). Displacements and bending moment of a possible energy diaphragm wall in Turin was analysed. As Figures 3.19 and 3.20 show, thermal induced horizontal displacements are negligible, while the corresponding stress change rises up producing an increase of 17% of bending moment during winter. On the other hand, bending moment is minimum during summer, when the displacement is maximum. However, the stress variations computed in the analyses are largely below the strength limits of the structure.

Moreover, this is a clear (and rather obvious) indication that the mechanical effects of thermal loading on diaphragm wall are strictly function of the structural conditions. This implies that the proper construction sequence and structural behaviour need to be properly simulated in the numerical analysis to allow for reliable results to be obtained.

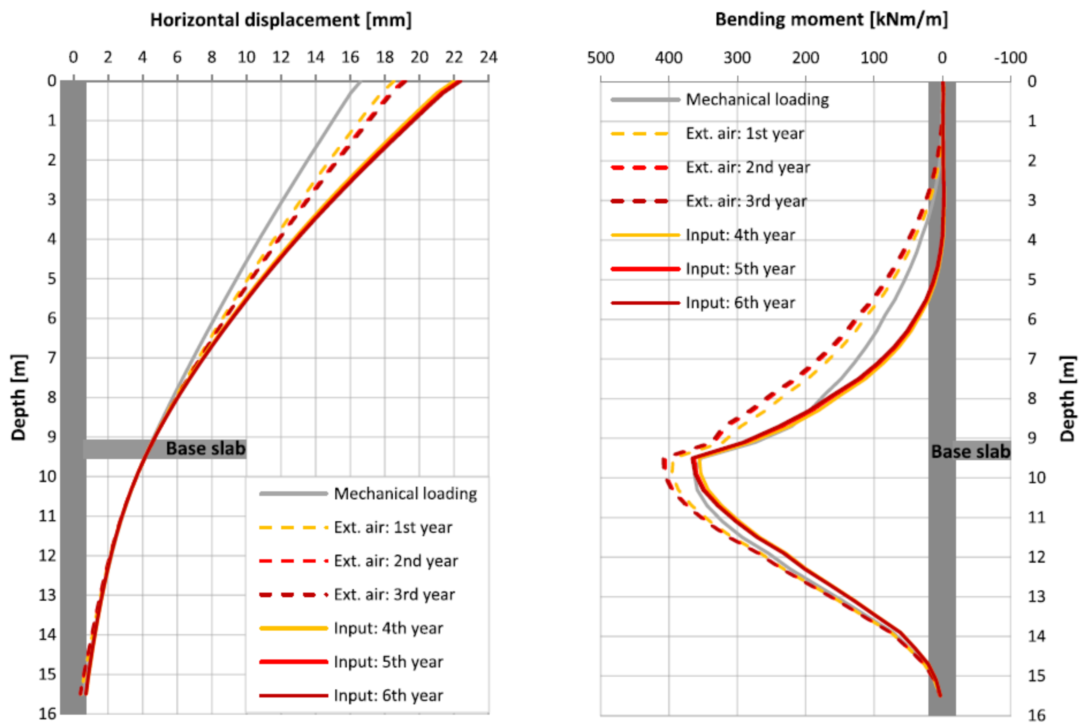

Figure 3.19 Bending moment and horizontal displacement change with: mechanical loading, external air and the activation of the geothermal system in Summer (August) (Barla et al., 2018)

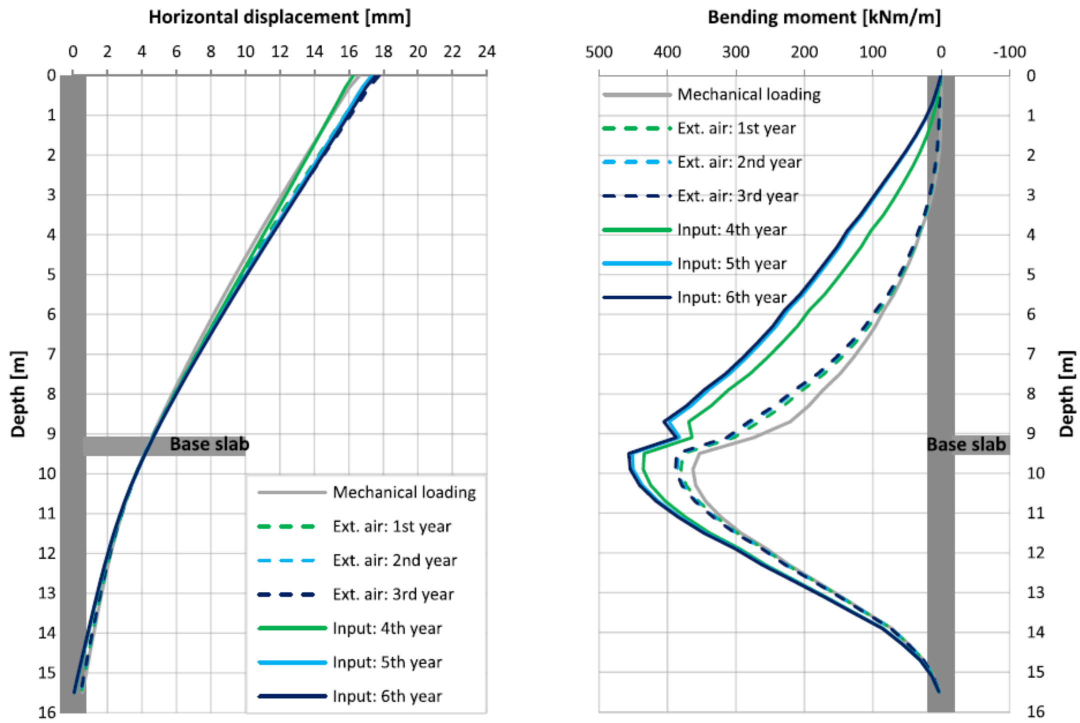

Figure 3.20 Bending moment and horizontal displacement change with: mechanical loading, external air and the activation of the geothermal system in Winter(February) (Barla et al., 2018)

3.5 How much does an energy structures cost?

One of the main problems that an engineer faces designing a structure is the amount of money needed for it. Indeed, generally speaking, the client wants to save as much as possible. For this reason, proposing an energy geostructure, at the beginning, doesn't seems convenient at all because of the additional costs of pipes and test needed. Nevertheless, the advantage of an energy geostructures is clear in a long-term view.

Barla et al. (2016) reported an interesting comparison, in terms of costs, between different kinds of heating-cooling geothermal plants used in tunnels. Specifically, it is remarked that traditional heating-cooling systems present an annual operating costs about 75-145% higher than the geothermal one. The great advantage is achieved with an additional initial cost, in this analysed case, for tunnel thermal activation of 0.78% of the total cost of the tunnel construction project total costs. In addition, the pay-back time for the additional cost is maximum 5 years. Figure 3.21 shows the cost saving if a geothermal system is favoured over other choices, e.g. gas, LPG, oil and pellet.

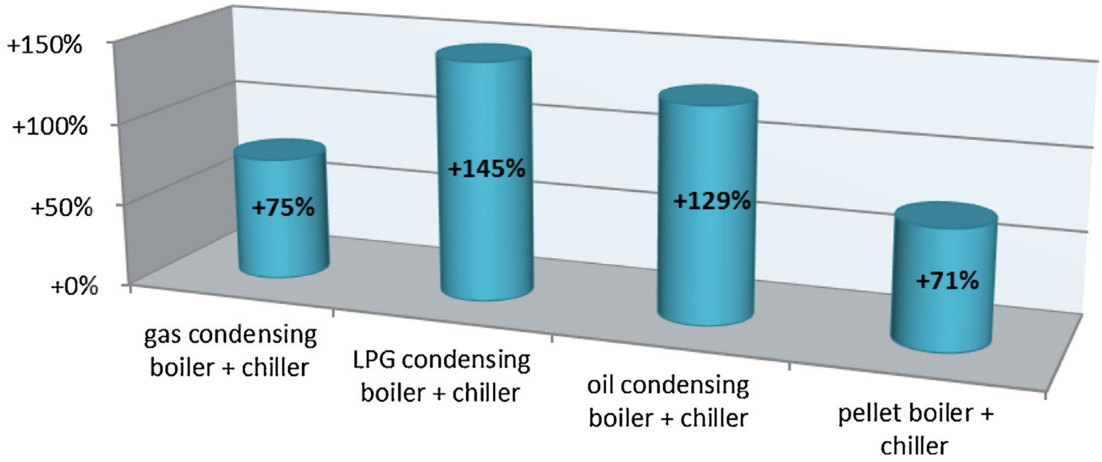

Figure 3.21 Annual operating cost savings with respect to other heating/cooling system (Barla et al., 2016)

Another observation was made by Barla et al. (2016) about open and closed loop system. Considering a borehole heat exchangers (BHE), an open loop method is more economically convenient with respect to the energy tunnel system. However the energy tunnel is a closed loop system and will avoid direct influence on the groundwater, reducing the concurrent environmental problems.

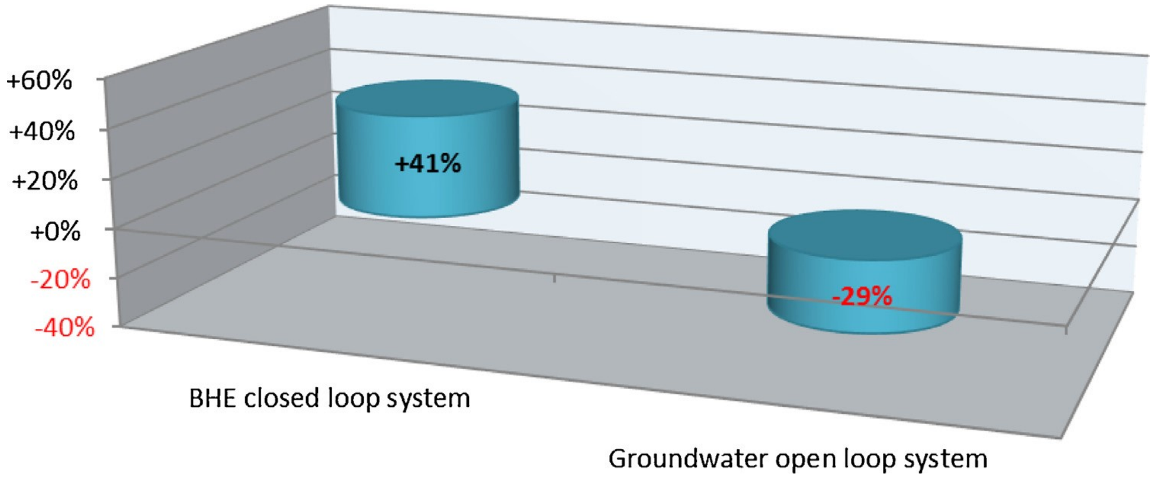

Figure 3.22 Economic convenience with respect to the other geothermal exchangers (Barla, Di Donna, & Perino, 2016)

For doing a practical example, if a tunnel about 1 km long, from the project to the final realization, may cost around 400’000/500'000 €, the addition of a geothermal system; i.e. pipes (included labour and test) will add around 1% at the sum, in this case 5'000 € more. This amount of money can seems a lot took apart, but, for a work like a tunnel, it can be considered negligible especially considering the long-term benefits which are derived from the new technology. In addition, if it is taken into account that a tunnel has a nominal life of operation of roughly 100 years, such us the polyethylene pipes used for the geothermal implant, and that a geothermal system needs 5 years to reach the expected pay-back, it points out that the proposed system guarantees success in many ways, from being environmental-friendly to be a cost-effective solution.

4. Numerical modeling for thermo-hydro-mechanical analysis

4.1 Coupled Thermo-hydro-mechanical problem

Energy geostructures need specific analysis, different from the one taken into account for standard structures, because of their complexity. Indeed, a numerical modeling of coupled thermo-hydro-mechanical analysis is required in order to predict the distribution of stresses, strains, displacements and interstitial pressure around the construction.

For an energy geostructure, the problem is presented by elements in reinforced concrete, such as bulkheads, piles, foundation slab, subjected to a mechanical component of stress given by the load and able to exchange heat with the surrounding environment. Both the soil and the concrete are considered porous materials composed mainly of a solid and fluid phase; in our study, the whole material is considered to be saturated with water. The three aspects, thermo-hydro-mechanical, are coupled since the variations of the solid volume are influenced by the presence of temperature gradient, the heat exchanged depends on the presence of water flow, the density of the water varies with the heat load and the mechanical response of the materials depends both on the interstitial pressure of the fluid (concept of effective tensions) and on the variation in temperature. Consequently, a correct formulation of the complete Thermo-Hydro-Mechanical coupling (THM) is necessary in order to analyze the problem. Thus, it is usual, based on investigations needs, to take into account only a partial analysis. Indeed, this thesis will study only the thermo-mechanical behavior of the diaphragm wall. However, in order to give a general overview of the problem, all the equations that governs a THM analysis will be introduced, bearing in mind that the knowledge of these equations offers the opportunity to do all the analysis desired.

4.1.1 Governing equations

The analysis carried out for this thesis is based on the hypothesis of an elastic behaviour, thus it is necessary introduce a set of equations and boundary conditions dictated by THM problem.

- Mechanical field:

  Equilibrium equations

  Congruence equations

  Constitutive laws
- Hydraulic field

  Mass conservation equation

  Darcy's laws
- Thermal field

  Energy conservation equation
- Boundary conditions

Equilibrium equations

Timoshenko and Goodier (1951) equations must be satisfied by the soil:

$$div(\sigma_{ij}) + \rho g_i = 0 \tag{4.1}$$

Where the *div* operator is the divergence, σ_{ij} is the tensor of the total stresses, $\vec{g_i}$ the gravity vector and ϱ the density of the material, which includes the density of the water ϱ_w and the solid particles ϱ_s. Through the porosity n, we can define:

$$\rho = np_w + (1 - n)\rho_s \tag{4.2}$$

The definition of effective stress allows to consider the hydraulic component, thus the hydro-mechanical coupling is introduced and the equation is transformed as:

$$div(\sigma'_{ij}) + \nabla p_w + \rho g_i = 0 \tag{4.3}$$

∇ is the gradient, p_w the pore water pressure and σ'_{ij} the effective stress tensor that can be written in incremental form by introducing the constitutive law.

Compatibility equations

It has been assumed the theory of small deformations and a convention of positive sign for the compression. As know, the deformations ε can be written in terms of displacements u along x axis, displacement v along y axis and displacement w along z axis:

$$\varepsilon_x = \frac{\partial u}{\partial x} \qquad \varepsilon_y = \frac{\partial v}{\partial y} \qquad \varepsilon_z = \frac{\partial w}{\partial z}$$
$$\gamma_{xy} = \frac{\partial u}{\partial y} + \frac{\partial v}{\partial x} \qquad \gamma_{yz} = \frac{\partial v}{\partial z} + \frac{\partial w}{\partial y} \qquad \gamma_{xz} = \frac{\partial w}{\partial x} + \frac{\partial u}{\partial z} \tag{4.4}$$

Since deformations are a function of only three displacements, these are not independent. Mathematically it can be demonstrated that for the existence of a compatible displacement field, all the above mentioned deformation components and their derivatives must exist and be continuous for at least the second order. The displacement field must satisfy any displacement or condition imposed on the contour.

In these equations all terms are related to the mechanical part of the coupled system THM.

Constitutive laws

In order to obtain a solution for the system, other equations must be introduced: constitutive laws relate stresses to strains. For an elastic material, they are:

$$\sigma_x = \frac{E\left[(1-\nu)\varepsilon_x + \nu\varepsilon_y + \nu\varepsilon_z\right]}{(1+\nu)(1-2\nu)}$$
$$\sigma_y = \frac{E\left[(1-\nu)\varepsilon_y + \nu\varepsilon_x + \nu\varepsilon_z\right]}{(1+\nu)(1-2\nu)}$$
$$\sigma_z = \frac{E\left[(1-\nu)\varepsilon_z + \nu\varepsilon_x + \nu\varepsilon_y\right]}{(1+\nu)(1-2\nu)} \quad (4.5)$$
$$\tau_{xy} = G\gamma_{xy} \qquad \tau_{yz} = G\gamma_{yz} \qquad \tau_{zx} = G\gamma_{zx}$$

Where, for homogeneous, linear, isotropic, elastic materials, E is Young's modulus, v is the Poisson coefficient, while G is the Lamè constant (shear modulus) which is linked to E and v through the formulation:

$$G = \frac{E}{2(1+v)} \quad (4.6)$$

In order to consider the thermal coupled effects, the vector form is introduced:

$$d\sigma'_{ij} = C_{ijkl}(d\varepsilon_{kl} + d\varepsilon^T{}_{kl}) \quad (4.7)$$

Where C_{ijkl} is the stiffness matrix composed by 36 elements, which can be written in function of only E and v in case of isotropic, linear, elastic material:

$$C_{ijkl} = \frac{E(1-\nu)}{(1+\nu)(1-2\nu)}\begin{bmatrix} 1 & \frac{\nu}{1-\nu} & \frac{\nu}{1-\nu} & 0 & 0 & 0 \\ \frac{\nu}{1-\nu} & 1 & \frac{\nu}{1-\nu} & 0 & 0 & 0 \\ \frac{\nu}{1-\nu} & \frac{\nu}{1-\nu} & 1 & 0 & 0 & 0 \\ 0 & 0 & 0 & \frac{1-2\nu}{2(1-\nu)} & 0 & 0 \\ 0 & 0 & 0 & 0 & \frac{1-2\nu}{2(1-\nu)} & 0 \\ 0 & 0 & 0 & 0 & 0 & \frac{1-2\nu}{2(1-\nu)} \end{bmatrix} \tag{4.8}$$

Thermal deformation is defined as:

$$d\varepsilon^{T}{}_{kl} = \beta_{kl} dT \tag{4.9}$$

Where β is the linear coefficient of thermal expansion [°C^{-1}] and dT is the temperature increment.

Mass conservation equation

The principle of conservation of mass postulates that the mass of fluid M does not change with the motion of an arbitrary volume V, i.e. that the material derivative of M over time is always identically equal to zero. The mass conservation equation was obtained using some theorems of fluid mechanics and using Darcy's law. The latter describes the motion of a fluid within a porous material and it is expressed as:

$$\vec{v} = -K\vec{\nabla}h \tag{4.10}$$

v is the velocity, k the permeability of the soil and $\vec{\nabla}h$ the hydraulic load.

The mass conservation equation in transitory conditions can be mathematically described by Poisson's equations:

$$K\left(\frac{\partial^2 h}{\partial x^2}+\frac{\partial^2 h}{\partial y^2}+\frac{\partial^2 h}{\partial z^2}\right)=\frac{\partial \varepsilon_v}{\partial t} \quad (4.11)$$

ε_v is the volumetric deformations.

If the conditions of stationary regime exist, the volume does not change over time and the previous equation is reduced to that of Laplace:

$$\left(\frac{\partial^2 h}{\partial x^2}+\frac{\partial^2 h}{\partial y^2}+\frac{\partial^2 h}{\partial z^2}\right)=0 \quad (4.12)$$

The latter one describes a decoupled problem, since there are no mutual influences between the mechanical problem and the hydraulic one, therefore the field of interstitial pressure can be determined independently from the solution of the mechanical problem. In vector form, the Poisson equation becomes:

$$div\left(K\vec{\nabla}h\right)=\frac{\partial {\varepsilon_v}^M}{\partial t} \quad \leftrightarrow \quad (4.13)$$

$$K\overrightarrow{\nabla^2}h=\frac{\partial {\varepsilon_v}^M}{\partial t}$$

Where the Laplacian operator $\overrightarrow{\nabla^2}$ is defined as divergence of the gradient.

Adding the thermal rate, the final equation is:

$$K\overrightarrow{\nabla^2}h=\frac{\partial {\varepsilon_v}^M}{\partial t}+\frac{\partial {\varepsilon_v}^T}{\partial t} \quad (4.14)$$

Where the thermal deformation is defined as:

$${\varepsilon_v}^T=3\beta\Delta T \quad (4.15)$$

The equation number (3.14) presents the hydraulic contribution to the first member, while the components of the mechanical and thermal field are at the second one.

Energy conservation equation

It is possible to do an energy balance between the temperature T and the heat flow q, as it was already done for the mass and the water flow.
Firstly, it is necessary to introduce some concepts about heat transmission. The latter, is guaranteed by a difference of temperature between two interactive systems, in accordance with the principle of energy conservation.
Experience has shown that the heat transmission is a complex phenomenon which involves many material properties where the transmission takes place. However, there are three different ways or better mechanisms of transmission, described in the following.

Conduction is an energy transporting way which is proper of solid or liquid phase in a porous material, no fluid's macroscopic movement is required. Fourier's law governs this mechanism where the transfer of kinetic energy takes place from high temperature zones to the adjacent low ones, and the heat transfer $[\frac{W}{m^2}]$ expressed as:

$$q_{cond} = -\lambda\vec{\nabla}T \tag{4.16}$$

Where λ is the thermal conductivity of the material $[\frac{W}{mK}]$ and $\vec{\nabla}T$ is the temperature gradient. The sign "-"is related to the way of decreasing temperatures (Bonacina et al., 1980).

Convection happens through a fluid in movement, hypothesis of saturated material was made, always with different temperature; the transfer energy with macroscopic transportation is equal to:

$$q_{conv} = c_w\rho_w\overrightarrow{v_w}\Delta T \tag{4.17}$$

Where c_w is the specific heat of water $[\frac{J}{kgK}]$ and ΔT is the difference of temperature between the two systems.

Clearly, this rate can be taken into account only if there is a fluid flow. In a soil, for example, convection gives an important contribution in incoherent soils, i.e. sand and gravel, on the other hand is negligible for cohesive soils, i.e. clays.

Radiation is the mechanism of transfer between two surfaces with different temperatures. In this context it is not relevant, indeed its contribute is minor than 1% for sand and even less for clays (Ree et al.,2000). For this reason, it will not be taken into account in our analysis.

The equation of conservation of energy under steady-state conditions in the case of only conduction is provided by the Laplace equation:

$$\overrightarrow{\nabla^2}T = 0 \tag{4.18}$$

On the other hand, in the case of transitory conditions, always only by conduction, the mass conservation equation can be described mathematically by the Poisson equation:

$$\lambda\overrightarrow{\nabla^2}T = \rho c\frac{\partial T}{\partial t} \tag{4.19}$$

The second member is the accumulation of heat and it is formed from:

$$\rho c = n\rho_w c_w + (1-n)\rho_s c_s \tag{4.19}$$

That is the specific heat of the soil in which water specific heat c_w and solid skeleton one c_s are included;

Conduction and convection can be blended together and, in the case of transitory conditions, the final equation would be:

$$\lambda\overrightarrow{\nabla^2}T + div(\rho_w c_w \overrightarrow{v_w}\,\vec{\nabla}T) - \rho c\frac{\partial T}{\partial t} = 0 \tag{4.20}$$

Boundary conditions

It is known that, to solve a problem, boundary conditions are necessary firstly to reproduce a real condition, e.g. symmetry, secondly to reduce the unknowns, i.e. to be sure to have a determinated system. A THM problem can involve a large number of variables between fields and material properties coupled between them. Thus, doing an associated analysis, requires a heavy computation but it may be unnecessary from an engineeristic point of view. For this reason, it is fundamental to understand which field, mechanical, thermal or hydraulic, is more important in our analysis in order to create an appropriate model and reduce costs.

Generally speaking, boundary conditions are referred to:

- Forces and/or displacements for the mechanical field;
- Hydraulic conditions for the hydraulic field;
- Temperature for the thermal field.

4.2 Numerical modelinig and FE method

The numerical modelling is born with the purpose to create virtual models of physical reality to approximate the behaviour and be able to perform analyses in order to predict the in situ behaviour of the system response to a specific action. This tool is very powerful, as it allows to solve increasingly complex problems from the geometric, the constitutive behaviour and the stresses point of view, succeeding in involving fields of application that are increasingly broader and more competitive. Nevertheless, it is just a tool that a good engineer must use wisely and interpret the results critically.

In the field of geotechnical engineering a problem can be studied in three different ways: continuous, equivalent-continuous or discontinuous. The latter, is used when discontinuities govern the stress-strain behaviour. Whilst, the continuous model is valid when the presence of macrostructures is negligible in order of global behaviour. On the other hand, an equivalent-continuous takes into account the global characteristics, thus it is common to scale the properties of intact rock to the rock mass using empirical formulations.

Based on the approach chosen, a numerical method is associated:

- Continuous method: finite element (FEM), finite difference (FDM), boundary element (BEM);
- Discontinuous method: distinct element (DEM);
- Equivalent-continuous method: finite discrete element (FDEM).

Boundary element method (BEM) uses a constitutive model only for elements on the contour, whereas, differential displacements between elements are allowed in *Distinct element method* (DEM). On the other hand, Finite discrete element method (FDEM) guaranties differential displacements between two elements with the discretization to finite elements inside of them.

Actually, the most common methods used are FEM and FDM. The latter, is perhaps the oldest numerical technique for the solution of boundary problems. In the FDM every derivative in the set of governing equations is replaced directly by an algebraic expression written in terms of the field variables (e.g. stress or displacement) at discrete points in space; these variables are undefined within elements. In contrast, the FEM has a central requirement that the field quantities vary throughout each element in a prescribed fashion, using specific functions controlled by parameters. Both

FDM and FEM methods produce a set of algebraic equations to solve. The FE programs often combine the element matrices into a large global stiffness matrix, whereas this is not normally done with finite differences because it is relatively efficient to regenerate the finite difference equations at each step.

The FE method used in this thesis can be easily described through 6 steps:

1. Element discretization: modelling the geometry of the problem by assemblage of finite elements;
2. Primary variable approximation: a primary variable must be selected as well as how it should vary over a FE. In geotechnical engineering it is usual to adopt displacements as the primary variable;
3. Element equations: use of an appropriate variation principle to derive element equations;
4. Global equations: combine element equations to form global equations;
5. Boundary conditions: formulate boundary conditions and modify global equations;
6. Solve the global equations: to obtain the displacements at all the nodes, from which secondary quantities such as stresses and strain are evaluated.

The fundamental step is the construction of the mesh. First of all, the geometry of the boundary value problem must be approximated as accurately as possible and the discretization process need be performed carefully. Moreover, a denser mesh, i.e. high number of elements, in relation to the type of element adopted (triangular or rectangular) should be used where higher stress gradients are expected, e.g. near holes, in corner zones. If non homogeneous zones occur, it is essential that nodes are located along the contours from one zone to the other one. Whereas, the dimensions of the mesh should be chosen big as much as to avoid influences from boundary restraints. The shape chosen for the element is important too. Indeed, if the behaviour of a structure such as a diaphragm or a pile, wants to be performed, a rectangular mesh should be selected, otherwise a triangular shape is the best choice, e.g. to model soil or a tunnel.

Contrary to the FDM, which sees the domain to be analysed as a series of points in a grid, the FEM sees dominance as the union of many subdomains of elementary form.

In the FEM, the differential equations are unchanged (relative to each finite element) while the domain comes discretized. In a continuous problem of any dimension, the field variable, such as pressure, displacement, temperature, velocity or density, it is a function of each generic point of the definition domain. As a result, the problem presents an infinite number of unknowns. The finite element discretization procedure reduces it to a problem with a finite number of unknowns, by dividing the domain into finite elements and expressing the unknown field in terms of approximate functions, defined within each element. The term finite elements was used in a 1960 Clough article where the method it was presented for the solution of a state tension plan. The term derives from the fact that the integration domain comes divided into a determined number subdomain, within which the differential equations governing the problem are solved through the approximate functions.

The latter, also called shape functions, are identified through the values that the dependent variable has in a specific points called nodes. The nodes are usually placed on the outline of the elements, in points common to two or more elements. In addition to the boundary nodes, an element can have nodes inside it. Values that vary on the of field assumed on the nodes, they unequivocally define the trend within the element. In the representation to the finite elements of a problem, the nodal values of the field variable represent the new unknowns.

As mentioned, the discretization of the domain then leads to the generation of nodes and finite elements. The nodes, in the applications of the FEM, are extremely important entities because the solution of the whole structure is referred to them: in order to extend the values of the field of unknowns on the whole body, some functions are used that with the desired approximation report the nodal values in each subdomain. It is evident that as the number of nodes increases, increases the degree of the polynomial used for interpolation of data at the nodes and, therefore, also increases the quality of the approximation. The choice of shape functions, which are generally polynomial (or at least to known behaviour) is another fundamental point that allows to obtain a solution of the FEM model more or less close to the desired reality. In order to correctly represent the value at the nodes, the shape functions must assume unit values in the considered node and null values on the rest of the nodes. The field of unknowns for a three-dimensional problem can be represented by the following general report:

$$[u(x,y,z)] = [H(x,y,z)][u]_e \tag{4.22}$$

Where [H(x,y,z)] is the element shape function which interpolates the solution between the discrete values obtained at the mesh nodes.

As said earlier, displacements are the primary variable favourite in geotechnical field. Stress and strain are treated as secondary quantities which can be derived from the displacements. Thus, the main approximation in the FEM, is to assume a particular form for the way the primary variable varies over the domain under study. Clearly, this assumed variation must satisfy the conditions of compatibility.

The solving equations con be written in explicit or implicit form. FDM often use an explicit, time marching method to solve the algebraic equations, while implicit, matrix-oriented solution schemes are more common in FEM.

The explicit approach uses a time-dependent differential equation that considers other parameter beyond that mass, displacements and applied load:

$$[m][\ddot{u}] + [c][\dot{u}] + [k][u] = [F] \tag{4.23}$$

m is the mass of the system, c is the damping, k is the stiffness and u the displacement with its temporal variables.

On the other hand, implicit form is favoured by the FE method. In this case, the displacements are not dependent by time, i.e. acceleration and velocity are equal to zero and the damping and mass matrices can be neglected. Indeed, in order to solve the equation, it is necessary to invert the global stiffness matrix [k], thus the computational burden can be really high:

$$[K][u] = [R] \tag{4.24}$$

Indeed, the main effort for the software is to assemble the entire element's stiffness matrix into the global one and then invert it, multiplied by matrix force, to obtain the displacement desired. Moreover, the global stiffness matrix is equal to:

$$[K] = \sum_e \int [B]_e^T [C]_e [B]_e \, dV_e \tag{4.25}$$

Where [B] contains only derivatives of the shape function and [C] is the elastic matrix.

Lastly, in equation (4.24), the [R] is the vector of the forces at the nodes and it is a sum of all the forces possibly present in a system.

The use of the FEM is established as one of the best tools for the investigation those complex problems, for which investigations and experiments in the laboratory would involve excessive expenses, logistical difficulties and difficulties related to the physical measurement of the various quantities. If the first automatic approaches to the solution of the differential equations that governing physical phenomena, are affirmed with finite differences, the FEM evolves the possibilities of solution by giving one possibility of application that has no equal, thanks to its incontrovertible flexibility. The generality of the method, initially developed by engineers and subsequently demonstrated also by mathematicians, it has allowed many studies and applications, paving the way for new lines of research that currently address notional issues the interest of a theoretical and practical nature.

4.3 Calculation software

In this thesis the LAGAMINE software was used to compute the Thermo-Mechanical analyses. The introduction and explanation of the FEM, allows to understand how the calculation program works. As a matter of fact, LAGAMINE is a finite element code developed by the department MSM of University of Liege since 1982 (Charlie R., 1987, Collin F., 2003). It is a solid, nonlinear, great deformations code that has been adapted to numerous finite elements and constitutive laws. The code has been developed along with innovations and science for the last forty years. The continuous work of researchers around the world, in university as well as in the industry, has maintained it at the leading edge of technology and research. More specifically, LAGAMINE is able to deal with complex nonlinear constitutive models, multiphysical coupling, strain localization and multiscale approaches for applications in the fields of environmental geotechnics, engineering geology, reservoir engineering and metal forming ("2nd International Workshop on the Finite Element Code LAGAMINE," 2018).

The program is presented as shown in the figure 4.1 and the interface is user-friendly as well as funny because of the cartoon-shaped buttons. Nevertheless, do not be fooled by the appearance because the software is able to solve really complex problems, such as a THM analysis with the option 2D or 3D without too many difficulties.

As most calculation programs, it is necessary to pay attention to what is asked and how it is done, indeed, due to the fact that the program reads text files, spaces and numbers are fundamental.

The steps to follow are exactly the same of all those necessary in a numerical model:

1. Discretizing the model with the creating of a finite element mesh;
2. Define boundary conditions;
3. Assign material properties to the elements;
4. Assign the initial stress state to the nodes;
5. Define computational stages, in order to reproduce construction sequence;
6. Compute;
7. Interpret the results.

Figure 4.1 LAGAMINE's interface

The first step required by the software is the definition of the geometry, understood as domain, segment division, type of mesh and boundaries, e.g. fixed points, foundation, structured mesh or internal contour. All these information are saved in the "*GMAIL file*".

After choosing the type of analysis, the material properties and initial stress state assignment is the next step doable through the *Lagalaw* button. Mechanical, thermal, flow and coupled laws are available, around 444 choices, on the base of the kind of elements, 66 choices, selected for the geometry. All these selections are drafted in "*DATA file*" which is the complete one, i.e. it contains the whole information of the defined model from the node's coordinates to the list of different elements chosen. The *Prepro* button let the program checks the *DATA file*, if everything is appropriate for LAGAMINE, it is possible to proceed with the "*LOADING file*". Here the type of load, the first increment, the number of steps and strategy parameters are defined. *Lagamine* runs appling the *LOADING file* to the *DATA file* and then results are proposed.

A useful capacity is to print the results in terms of tensions and deformations, for examples, of only the elements and nodes required. Moreover, it is possible to “turn of” some elements, e.g. to simulate the stage of an excavation, all this always through a text file.

4.4 Software validation

In order to understand how the program works, it was decided to run a simulation of a loading step if an oedometric test for 3 different problems: mechanical, hydro-mechanical and thermo-hydro-mechanical. Due to the fact that LAGAMINE uses text file, i.e. can be really complex to understand it at the beginning, the considered choice was made of starting from a simple analysis and then arriving at the more complex one of interest for the thesis. Thus, the following subchapters will describe the preliminary analysis made for an oedometric test of a sample of sand, high 2 cm with a radius of 3 cm and subject to a uniform vertical load of 1 MPa (Figure 4.2). Each side was divided into 10 segments so a mesh of 10x10 and 8-nodes quadrangular element was created and axysimetry problem is considered, i.e. the left side is the axis of symmetry. An elastic law was chosen to make easier the comparison between the results given by LAGAMINE and hand-made one, to validate the software; properties are reported in table 1. Clearly, to simulate the behaviour of an oedometer, rollers were set as lateral and bottom boundaries. In this way, the lateral deformation of the soil is prevented, i.e. only vertical variations are allowed.

Table 1 Mechanical-fluid-thermal properties of oedometer sample

Parameter	Symbol	Unit	Value
Young modulus	E_d	[MPa]	215
Poisson coefficient	v	[-]	0.3
Specific weight	γ	[kN/m³]	19.5
Thermal conductivity	Λ_s	$Wm^{-1}K^{-1}$	2.8
Specific heat coefficient	ρ_s	$Jkg^{-1}K^{-1}$	1053
Coefficient of linear thermal expansion	c_s	[-]	10^{-5}
Intrinsic permeability	k_p	[m²]	$3.78 \cdot 10^{-10}$
Porosity	N	[-]	0.4

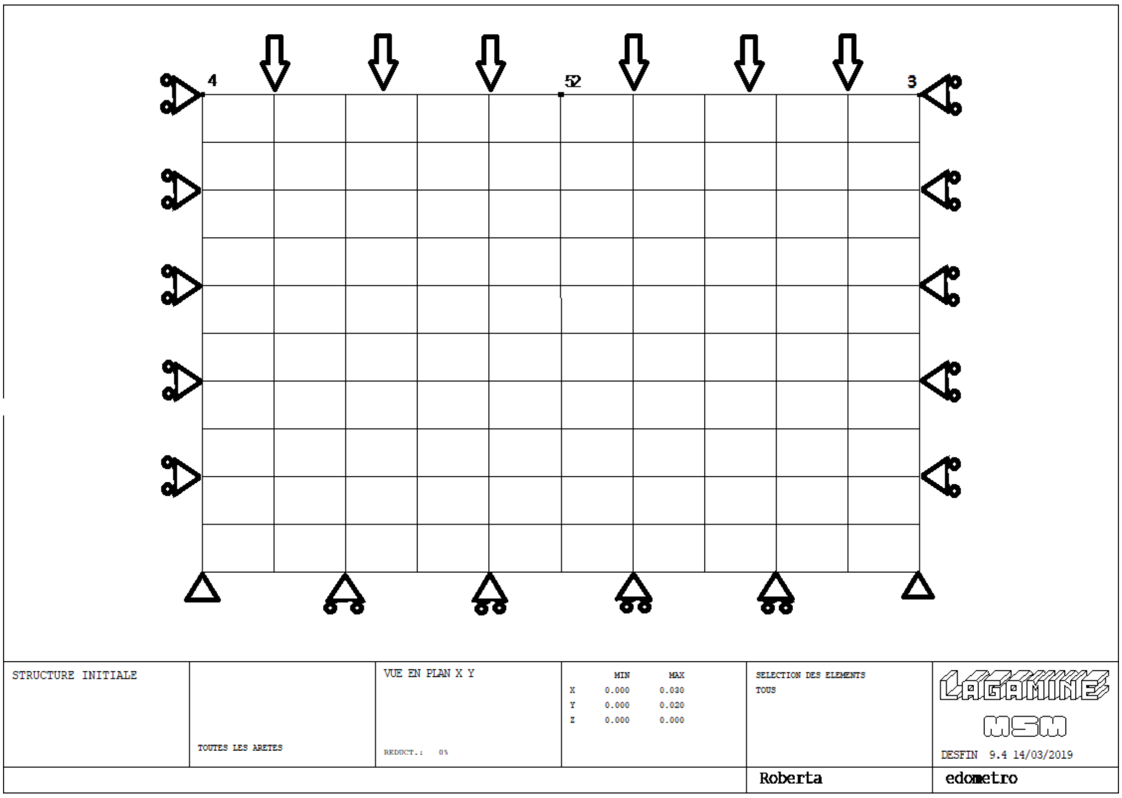

Figure 4.2 Initial structure with boundary conditions and load

4.4.1 Oedometer: mechanical problem

The first preliminary analysis is the mechanical one, means that temperature and water pressure are blocked. Thus, the load is applied through a manual strategy which divided the 1 MPa force in 10 steps each of 0.1 MPa and the loading-time is chosen equal to 100 seconds.

The figure 4.3, shows the comparison between the initial and the deformed structure. As expected, the oedometer undergoes a vertical along x lowering equal to 6.89 E^{-05} m and a fast check is made in base of the elastic relationships:

$$\varepsilon_x = \frac{1}{E}[\sigma_x - v(\sigma_y + \sigma_z)] \tag{4.26}$$

Inasmuch as an oedometer simulation is proposed, the lateral deformation must be equal to zero and the stresses in the two directions y and z must be the same. Thus, it is possible to write:

$$\sigma_z = \sigma_y = \frac{v}{1-v}\sigma_x = \frac{0.3}{1-0.3}\ 1 = 0.429\ MPa \tag{4.27}$$

Considering a material with Poisson's ratio of 0.3, Young modulus of 215 MPa and a vertical stress equal to 1MPa, the lateral stress the one represented in (4.27).

Knowing the stresses, it is possible to calculate the vertical deformation, i.e. the displacements:

$$\varepsilon_y = \frac{1}{215}[1 - 0.3 * 2 * 0.429] = 3.46\ E^{-03} \tag{4.28}$$

Multiplying the result in the (4.28) for the high of the oedometer, i.e. 2 cm, the displacement is obtained

$$u_y = 3.46\ E^{-03} * 0.02 = 6.9\ E^{-05} m \tag{4.28}$$

The vertical displacement calculated is exactly the same proposed by the software, visible at the bottom of Figure 4.3 and, as a trend in Figure 4.4.

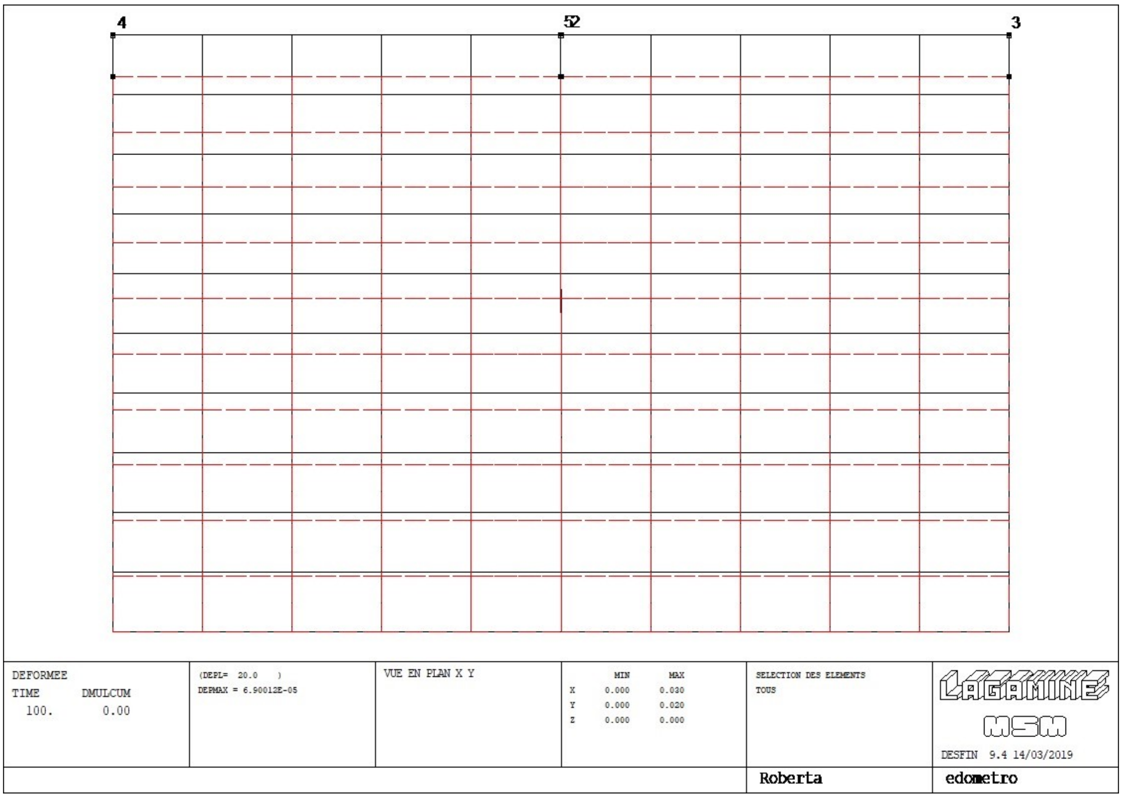

Figure 4.3 Initial structure in black, deformed structure in red

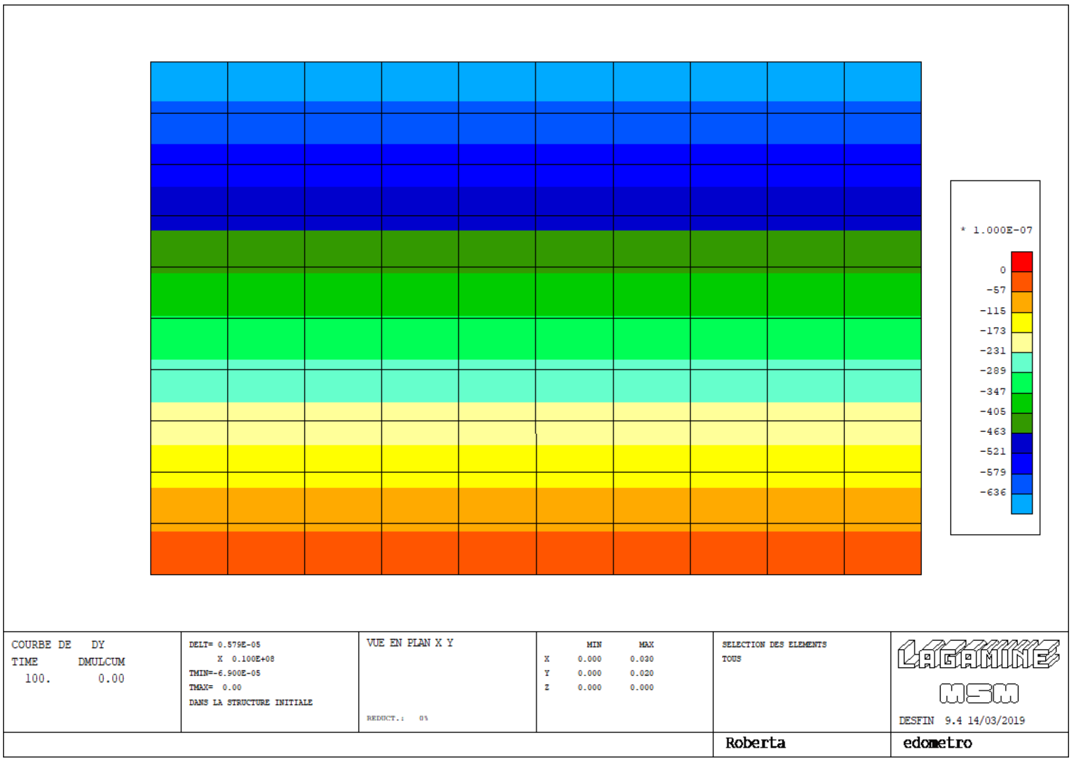

Figure 4.4 vertical displacement for mechanical problem

4.4.2 Oedometer: hydro-mechanical problem

The second simulation is a hydro-mechanical analysis. To reach the purpose, the water pressure has been blocked only at the bottom and only at the right side, because of the axisymmetric problem. Beyond the usual mechanical properties, hydraulic ones are introduced, table 1. Thus, being the sample saturated, interstitial pressures will arise within the material and their trend is highlighted in the Figure 4.6. For this analysis, the time has been increased of 20 seconds to check the behaviour after the application of the load and the chart of displacement versus time for the point 4, i.e. the node at the top of the axis of symmetry, is shown below.

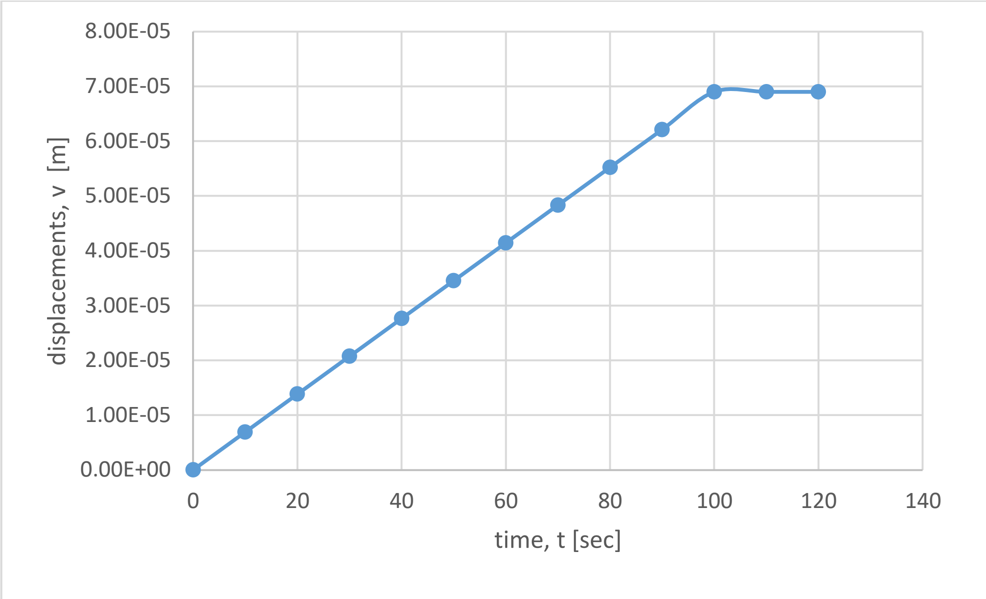

Figure 4.5 Vertical Displacements of point 4 for HM problem

As expected and as Figure 4.5 points out, the displacements increase linearly until the end of the application of the load, i.e. 100 seconds, after which, a plateau appears. The same trend is observed for the vertical stresses.

Regarding the water pressure, due to the fact that our sample is coarse sand, the material quickly dissipates overpressure, which is very low as value, and, as soon as the application of the load ends, water pressure drops to zero. This phenomenon is glaring watching the two figures below.

The figure 4.6 represents the water pressure within the sample at the first step, i.e. 10 seconds; it is possible to notice the concentration of overpressures at the axis of symmetry, according to the imposed conditions.

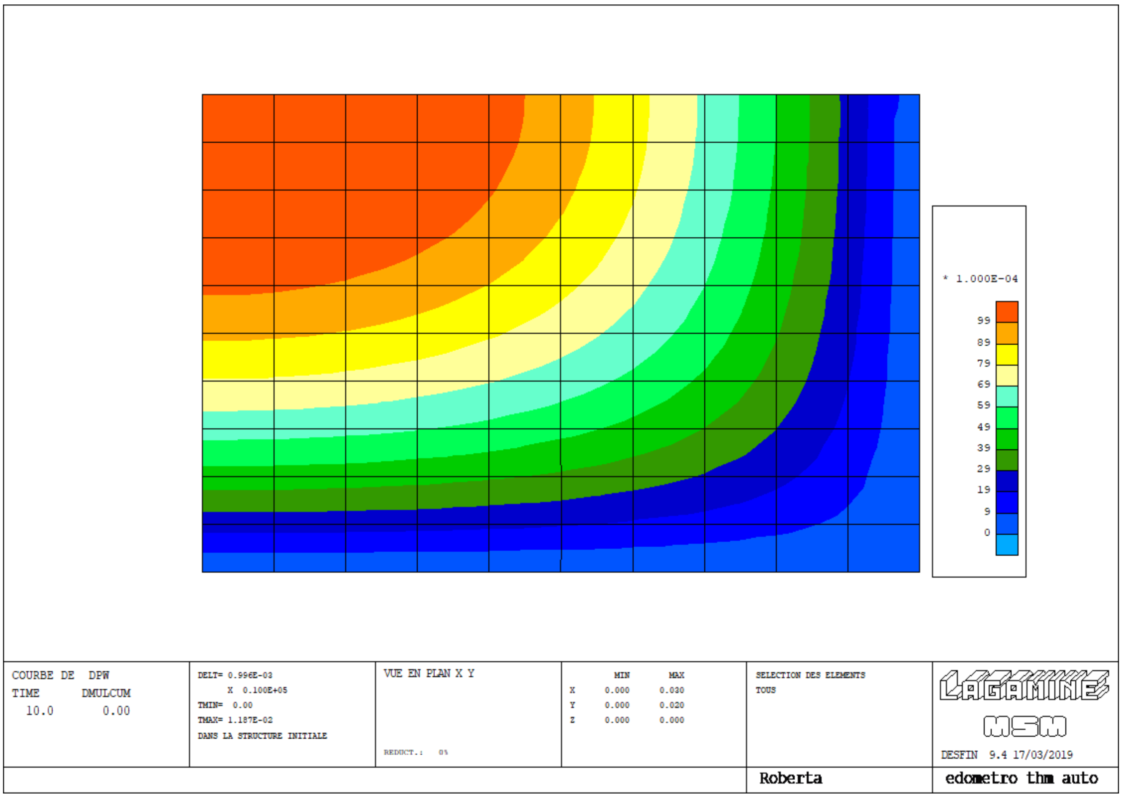

Figure 4.6 Interstitial pressures in a HM problem, at time 10 sec

At the end of the simulation, the water pressure is completely dissipated and, what is shown in the figure 4.7 is only a numerical trend because the overpressure has value of the order of 10^{-14}, i.e. zero.

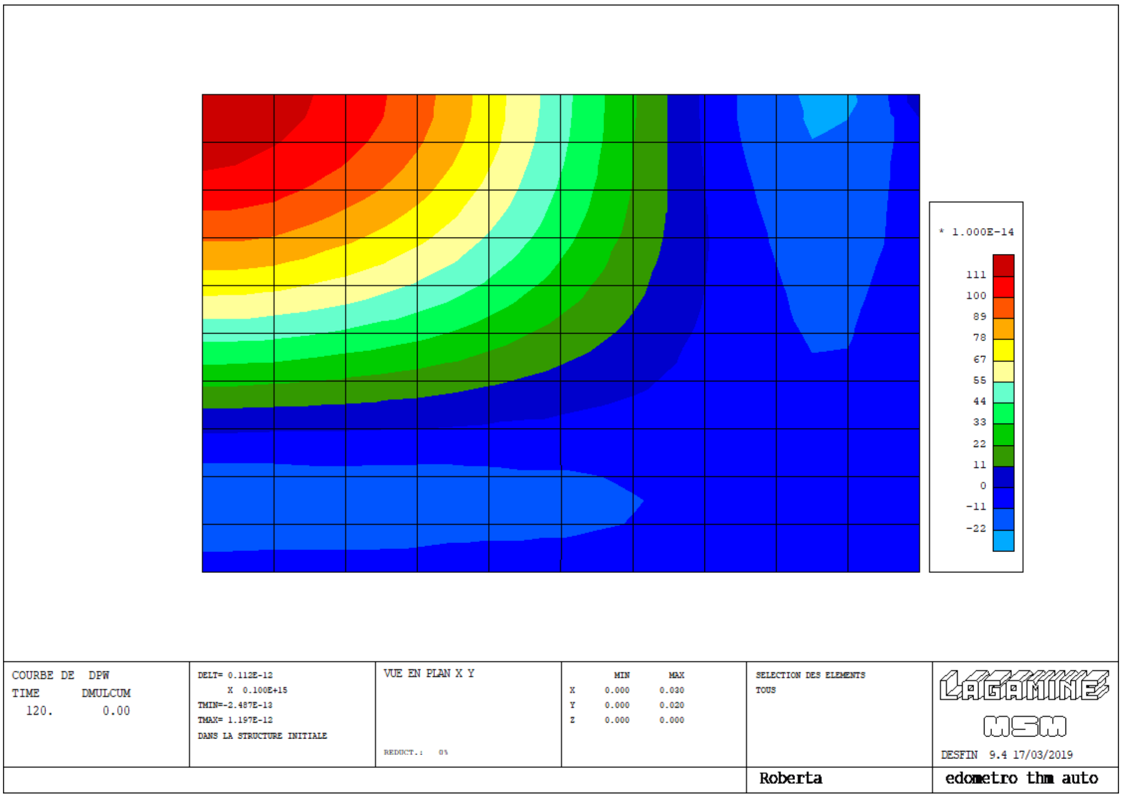

Figure 4.7 Interstitial pressures in a HM problem, at time 120 sec

4.4.3 Oedometer: thermo-hydro-mechanical problem

The last preliminary analysis is focused on the THM problem. The difference from the other analysis is that the variation of temperature is imposed only for the nodes of the right side, i.e. the right side is heated from 20°C to 40°C. The temperature is imposed equal to 20°C at time150 seconds, i.e. after the hydro-mechanical analysis, and equal to 40°C at time 500 seconds.

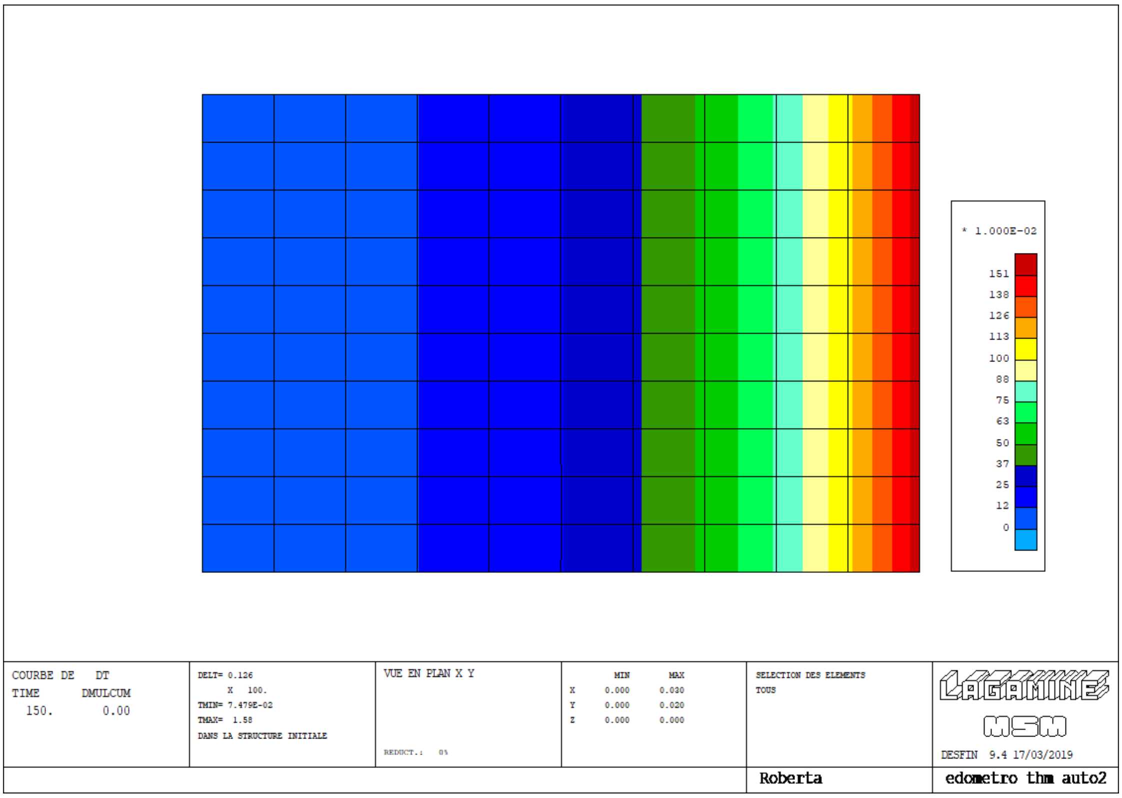

Figure 4.8 Variation of temperature in a THM problem, at 150 sec

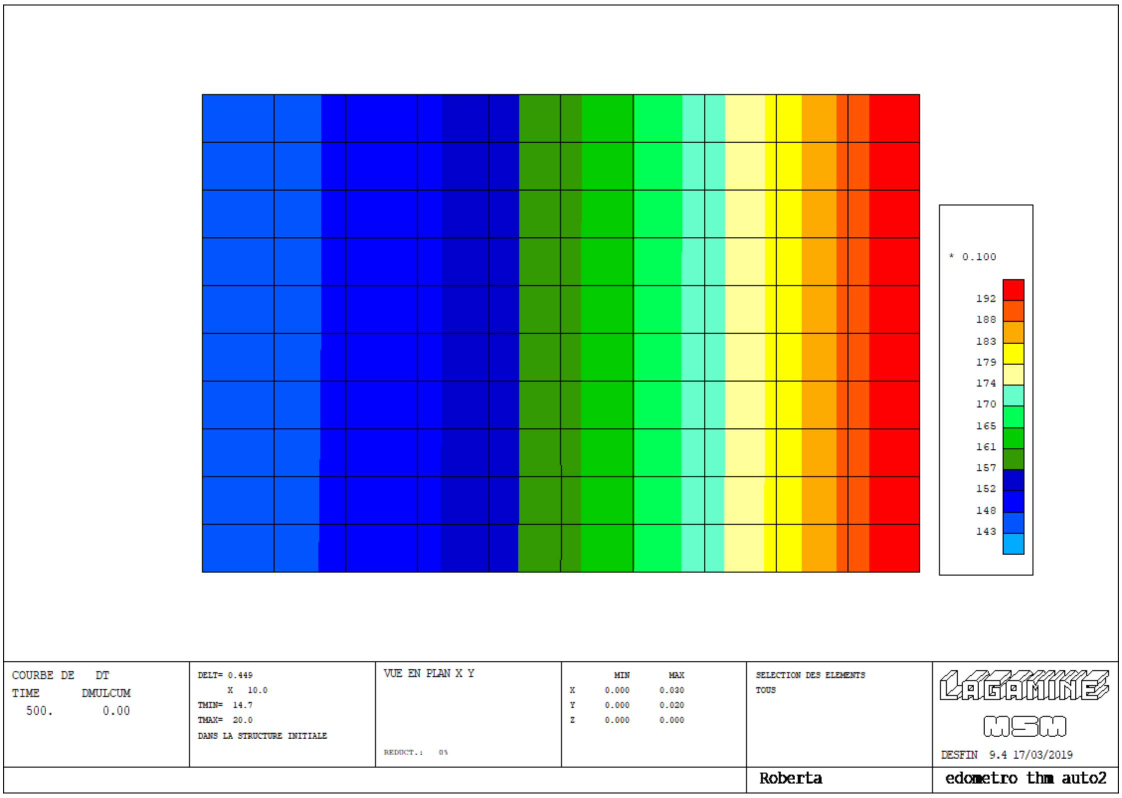

Figure 4.9 Variation of temperature in a THM problem, at 500 sec

The two figure above, show the heat diffusion through the sample at the two different time-steps, and the following one, highlights the variation of temperature as a function of time, for three point at the top of the sample: in the middle and in the two ends of it. Point 3 has a linear trend because the temperature there is imposed, on the other hand, point 4 and 52 present a non-linear trend because the variation of temperature is dictated by the thermal properties of the material.

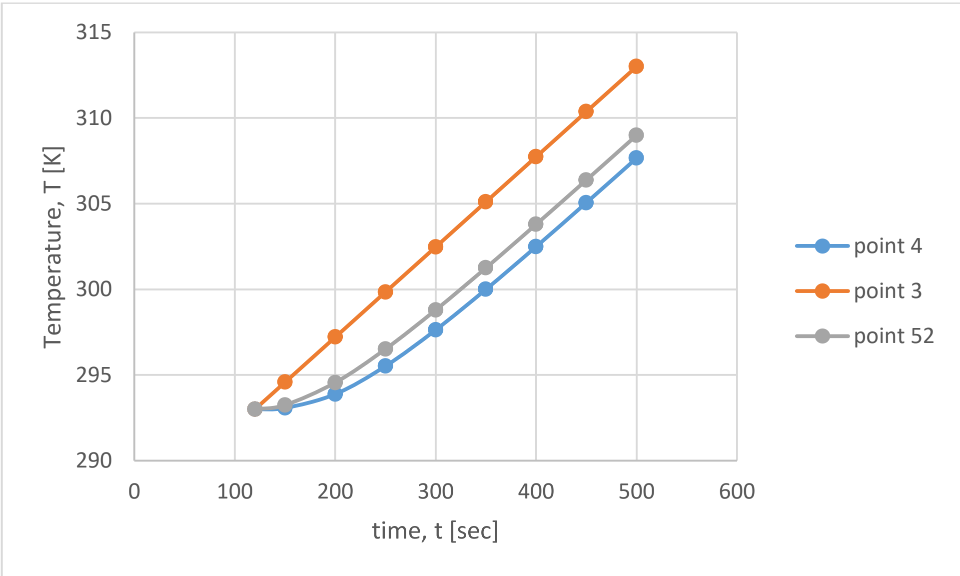

Figure 4.10 horizontal variation of temperature of points 4, 52, 3

Interesting observations can be made by observing the displacement graph of point 4, Figure 4.11. Indeed, the vertical displacements, understood as lowering of the specimen, decrease because of the heating that, instead, tends to make the soil expand.

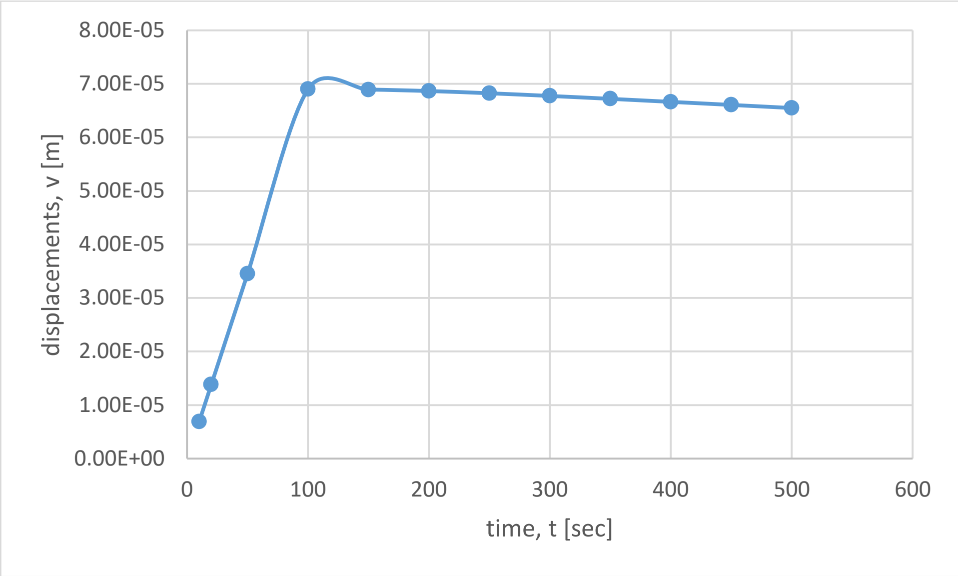

Figure 4.11 Displacements of point 4 in a THM problem

About the pressure, always of point 4, the same observations made for the displacements can be reported, i.e. the heating induces an increase of them as Figure 4.12 shows.

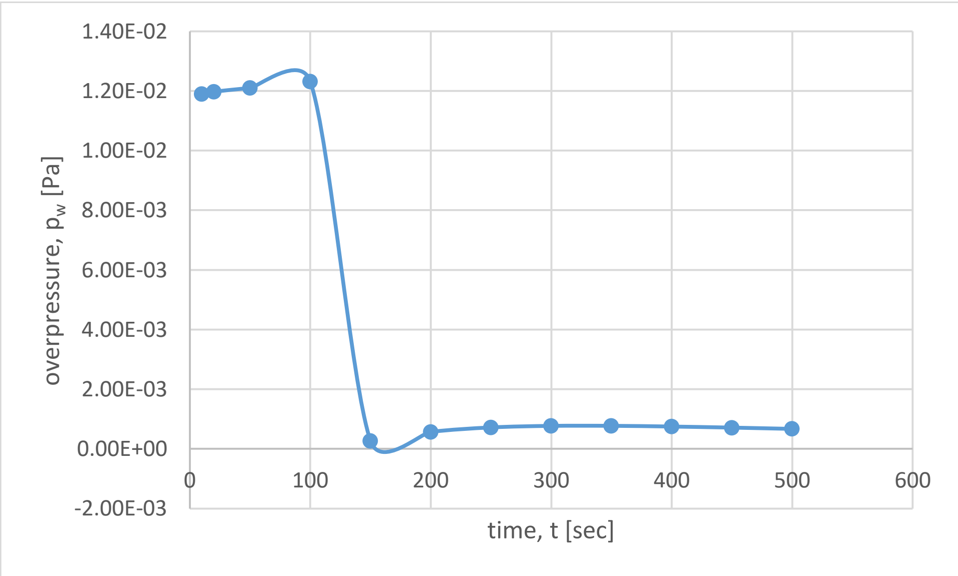

Figure 4.12 Interstitial pressure of point 4 for a THM problem

It is also worth bearing the variation in pressure as a function of temperature, and therefore indirectly of time. Indeed, as Figure 4.13 points out, the water pressure increases due to heating until around 27°C are reached. After this value, it is possible to notice decrees of the overpressure due to the fact that the sample is sand and it can easily dissipate the interstitial pressure until the imposed temperature of 40°C is reached and its value stops at 308 Pa.

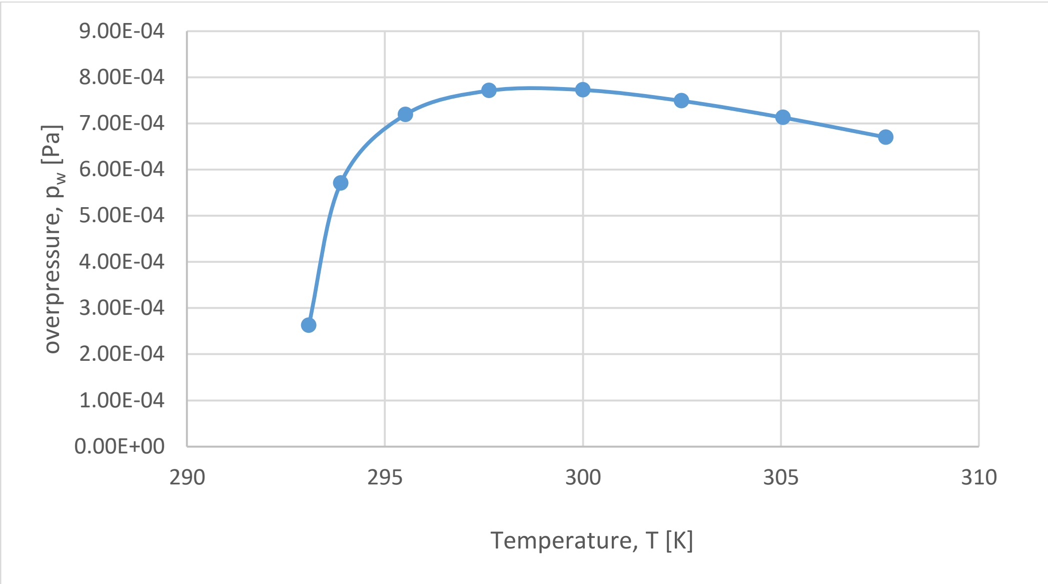

Figure 4.13 Overpressure of point 4 in function of temperature for a THM problem

5. Case study: thermo-mechanical analysis of the diaphragm wall of the underground car park in Turin

5.1 General overview

As explained in the previous chapters, e.g. 3.5, coupling the structural functionality with the geothermal one has various advantages. Especially, when considering structures embedded in the ground with an extended contact surface, such as diaphragm walls, the probability of success of the geothermal system is considerable.

For these particular structures, in addition to the geothermal study, required to monitor the exploitable thermal capacity, a thermo-mechanical analysis must be performed. The last one, it is fundamental to evaluate and control the stresses and deformations caused by the presence of an implant inside the diaphragm wall itself.

The aim of this thesis is to study the behaviour of an energy diaphragm wall, for this reason, the possible realization of the underground car park of via Ventimiglia, in Turin, will be analysed in this chapter, using the LAGAMINE software. Indeed, adjacent at the Unipolar Spinal Unit of the

T.O.C hospital (Turin Orthopedic Trauma Center), the idea of building an underground car park is being launched. The suggestion to introduce a geothermal system into the structure could represent added values as an incentive to carry on the work.

The underground car park, designed but not yet completed, will replace the current two-storey car park in front of the spinal unit of via Ventimiglia. To the study of the geothermal system and the foundation of the Ventimiglia parking lot, financed by the Piedmont Region - Enermhy Innovation Center, took part: the Polytechnic of Turin, Resolving srl and Teknema Progetti srl.

The geotechnical and structural project is supplied by Teknema Progetti srl and includes support structures along the entire external perimeter. About the geographical setting, the area is close to the Po river, i.e. presence of groundwater; on one side, the parking lot is in contact with the basement of another structure, the Unipolar Spinal Unit, but on the other three sides the diaphragm walls would be in contact with the ground and can be reasonably equipped with heat exchangers, as showed in figure 5.1.

Figure 5.1 Image 3D of current Ventimiglia car park (Google Maps 3D)

Referring to the analyses conducted by Barla & Barla (2012) and N_{spt} investigations conducted by *Arpa Piemonte*, it is possible to associate the area considered to the geotechnical unit GU2, according to the degree of cementation and the stratigraphy of the soil. Indeed, the material properties will be referred to unit GU2: gravel and weakly cemented sand.

Table 2 Mechanical parameter of geotechnical units (Barla & Barla 2012)

Geotechnical unit	GU1	GU2	GU3	GU4
C% [%]	-	0÷25	25÷50	50÷75
D_R [%]	50÷60	50÷70	60÷80	60÷80
γ [kN/m^3]	17÷19	18÷21	19÷22	19÷22
E_d [MPa]	10÷20	190÷240	240÷300	300÷370
ν [-]	0,35	0,30	0,30	0,30
σ_c [MPa]	0	0÷0,03	0,03÷0,14	0,14÷0,67
m [-]	-	3÷4,8	4,8÷7,8	7,8÷12,5
c [kPa]	0	0÷30	15÷80	50÷200
φ [°]	36÷37	37÷39	37÷42	39÷48

Hydraulic parameters are introduced to complete the characterization of the Turin soil, always referring to the geotechnical unit 2, showed in table 3, although our analysis does not involve a hydraulic aspect, but only the thermo-mechanical one.

Table 3 Hydraulic properties of the Turin subsoil (Barla 2017)

Parameter	Symbol	Unit	Value
Horizontal hydraulic conductivity	k_h	[m/s]	$4.15 \cdot 10^{-3}$
Vertical hydraulic conductivity	K_v	[m/s]	$0.21 \cdot 10^{-3}$

Porosity	n	[-]	0.25
Thermal capacity	Λ	$Wm^{-1}K^{-1}$	2.26
Thermal conductivity	ρ_s	$Jkg^{-1}K^{-1}$	1053
Longitudinal dispersion	α_L	[m]	3.1
Transverse dispersion	α_T	[m]	0.3

5.2 Technical description of the project

The project consists of a rectangular structure of external sides of 93.25x52.0 m, with three underground levels (Figure 5.2).

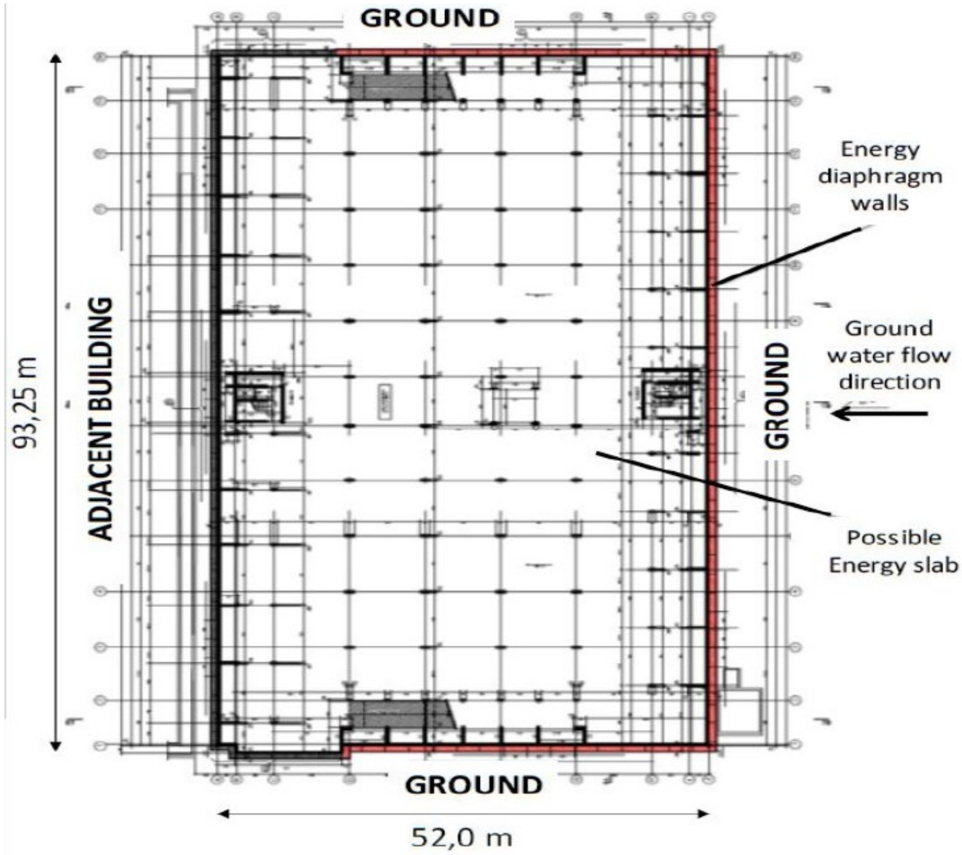

Figure 5.2 Underground car park plan (Di Donna, 2016)

The heights of the interpiano are equal to 2.45 m, with a horizontal covering thickness of 40 cm, intermediate horizontal of 25 cm thick and a bottom slab of 60 cm thick. The building, to support the altimetric variability of the countryside plan and of the surrounding road network, is designed with a slope perpendicular to the Via Ventimiglia of 1% to go down towards the T.C.O. The diaphragm wall are therefore 15.5 m deep, looking at the figure 5.3 it will be easy to understand the geometry.

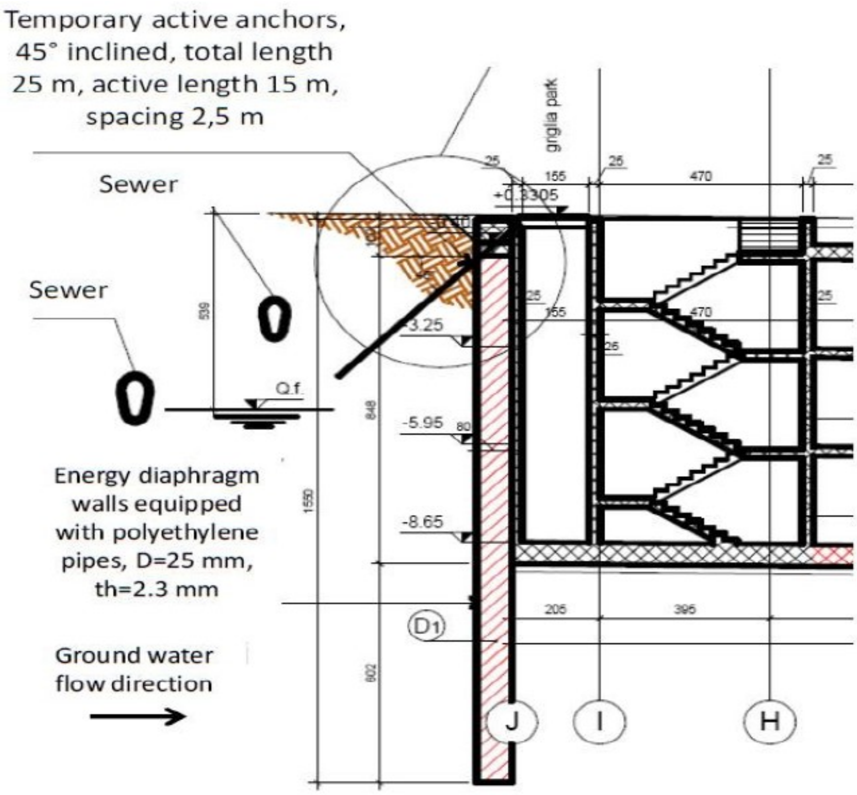

Figure 5.3 Vertical section of the underground car parking (A. Di Donna, 2016)

Regarding the materials used to construct the diaphragm and the bottom slab, concrete and steel were used. The concrete is a C32 / 40, while steel is a B450C. For the elastic modulus values of both materials, reference was made to the New Technical Standards for Construction (NTC; Ministry of Infrastructure and Transport, 2018).

In the diaphragm there are also reinforcements, both longitudinal and transversal. To consider their contribution, an equivalent elastic modulus of the concrete was calculated.

In the LAGAMINE software, concrete has been considered as an elastic, homogeneous and isotropic medium. The mechanical and thermal characterization parameters have been reported in Table 4.

Table 4 Mechanical and thermal properties of the concrete C32/40

Parameter	**Symbol**	**Unit**	**Value**
Young modulus	E_d	[MPa]	33 300
Poisson coefficient	v	[-]	0.2
Specific weight	γ	[kN/m^3]	25
Thermal conductivity	Λ_s	$Wm^{-1}K^{-1}$	2.3
Specific heat coefficient	ρ_s	$\mathrm{Jkg^{-1}K^{-1}}$	876
Coefficient of linear thermal expansion	c_s	[-]	$1.2 \cdot 10^{-5}$
Intrinsic permeability	k_p	[m^2]	10^{-16}
Porosity	n	[-]	0.12

In order to transform a simple diaphragm wall into an energy diaphragm wall capable of exchanging heat, polyethylene exchangers must be installed at the reinforcement cage before the concrete casting. In this case study, 13 exchanger tubes with the heat transfer fluid inside are assumed to have a diameter of 25 mm. The position of the tubes inside the diaphragms was selected based on a preliminary optimization study (Fig. 5.4); these are installed only on the three sides in contact with the ground, omitting the one in contact with the neighbouring structure (Fig. 5.4). The inlet and outlet of the tubes are supposed to be connected to a main circuit that connects the pipes to the heat pumps.

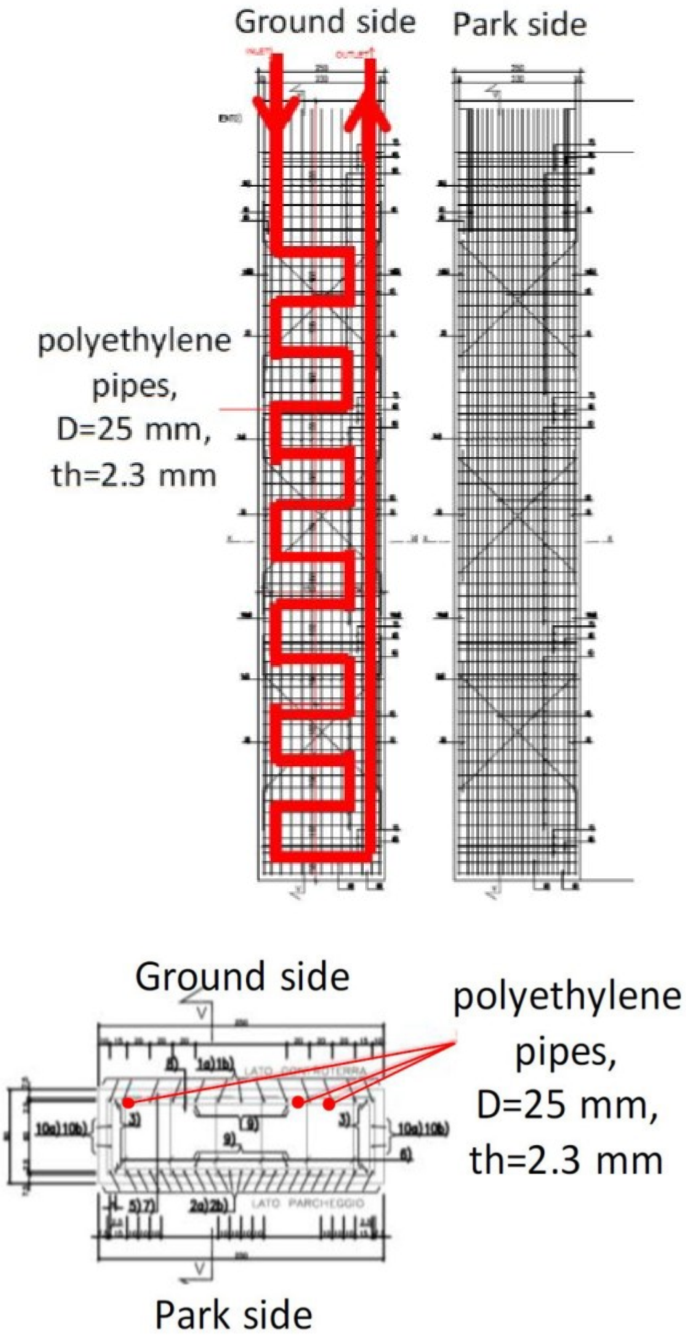

Figure 5.4 Position of the exchanger pipes and reinforcement cage

5.3 Identification of the diaphragm wall behavior with analicical calculation

To implement the model, a single section of the Ventimiglia underground car park was taken into consideration. The chosen section is oriented in the direction E-W and it is orthogonal to the long side of the car park. Furthermore, as a representative section, the one at the center of the diaphragm wall was selected.

It must be said that it was decided to simulate the thermo-mechanical behavior of the diaphragm wall without the surrounding soil. The choice was made to understand if it was possible to simplify the FE analysis in order to reach the purpose. Indeed, from an engineering point of view, the only behavior that matters is the one of the geostructure. Logically, the performance of a geostructure depends on the loading conditions to which it is located, i.e. on the soil. Indeed, after defining the geometry of the structure, the load due to the soil, was applied. Regarding the latter, the concept of active and passive thrust must be introduced.

5.3.1 Active and passive thrusts

Like all engineering works, retaining structures must be designed to meet safety and functionality requirements. When a retaining structure, or a part of it, does not meet these requirements, it has reached a limit state. The Rankine theory refers to limit state and hypothesize flat sliding surfaces, but due to the friction between the wall and the ground, the actual sliding surfaces are partially curved and the results are often non-precautionary. For this reason, must use precautions.

The hypotheses underlying the theory are:

- Homogeneous soil (γ=cost along the depth);
- Surface of the G.L. horizontal and infinitely extended;
- Inconsistent soil (c'=0);
- Absence of groundwater (u=0, $\sigma=\sigma'$);
- Validity of the Mohr-Coulomb failure criterion ($\tau_f = \sigma_n' tg\ \varphi'$);
- Absence of overloading at ground level;

All the hypotheses can be considered valid for our case. Indeed, the only two approximations made involve cohesion null, in favour of security, and no groundwater, in any case our analysis is the thermo-mechanical one that does not involve any water.

The Rankine theory presents notable analogies with the solutions deriving from the static theorem of the limit analysis. In it is assumed that the tensional state acting on a vertical wall is the existing one, in limit conditions, on the corresponding vertical arrangement thought to belong to an indefinite half-space. This hypothesis does not allow to take into account the friction at the wall-ground contact, this being a local phenomenon. The tensions acting on the vertical position in the boundary conditions assume a triangular distribution, with a line of action parallel to the ground plane, assumed horizontal.

The roughness of the wall-ground contact produces an inhomogeneous tension state in the ground that interacts with the retaining structure. In fact, while at great distances the friction between the wall and the ground is not affected and the main directions of tension are fixed (for example: vertical and horizontal directions for horizontal ground level), near the wall the presence of tangential tensions on the lying vertical produces a rotation of the main directions. Approaching the wall, therefore, there is a progressive rotation of the main directions of tension, which can be described by the composition of infinitesimal rotations, each of which can be thought to be produced by an infinitesimal discontinuity of the tension state between two contiguous regions. Once assumed a distribution of tensions congruent with this physical intuition, and compatible with the balance and the law of plasticity, the static theorem of the limit analysis ensures its validity. The solution can be expressed by providing the effective tension acting in the normal direction to the wall-ground contact as a function of the effective tension evaluated in the region distant from the wall (Lancellotta, 2002; Mylonakis et al., 2007). These solutions provide a precautionary estimate of the actions transmitted to the wall in boundary conditions and also have the advantage of being expressed in a closed form.

Wanting to take into account the roughness of the soil - wall contact, a cautionary estimate of the thrusts is obtained by applying the static theorem of the limit analysis (Lancellotta, 2002; Mylonakis et al. 2007) and so the limit effective tensions agents in the normal direction to the wall are expressed in form:

$$\sigma'_{a,p} = \cos\delta \cdot \left[\frac{\cos\delta \mp \sqrt{\text{sen}^2\varphi' - \text{sen}^2\delta}}{\cos i \pm \sqrt{\text{sen}^2\varphi' - \text{sen}^2 i}} \right] \cdot e^{\mp 2\psi \tan\varphi'} \cdot \left(\gamma' z \cdot \cos i\right) = K_{a,p} \cdot \cos\delta \cdot \gamma' z \qquad (5.1)$$

With

$$2\psi = \text{sen}^{-1}\left(\frac{\text{sen}\ \delta}{\text{sen}\ \varphi'}\right) \mp \text{sen}^{-1}\left(\frac{\text{sen}\ i}{\text{sen}\ \varphi'}\right) \mp \delta + i \qquad (5.2)$$

where ψ represents the rotation of the principal directions of tension between the regions distant and close to the wall, and i·z·cos·γ' is the effective vertical tension acting, in the region distant from the wall, on a position parallel to the ground plane indefinitely inclined and δ is the angle of friction wall-ground chosen as 2/3 of the friction angle of the soil (38°).

Table 4 reports the parameters of the soil, according to the geotechnical unit 2 define in chapter 5.1, and the corresponding active and passive thrust coefficients, calculated as per formula (5.1).

Table 5 Properties of the soil

Parameter	**Symbol**	**Unit**	**Value**
Young modulus	E_d	[MPa]	215
Poisson coefficient	v	[-]	0.3
Specific weight	γ	[kN/m^3]	19.5
Porosity	n	[-]	0.25
Friction angle	φ	[°]	38
Friction angle wall-ground	δ	[°]	25.3
Active thrust coefficient	K_a	[-]	0.24
Passive thrust coefficient	K_p	[-]	8.15

The diaphragm considered is unconstrained, i.e. fixed Earth support is the condition considered. In this particular case, the stability is entrusted to the ground detachable. The analysis is to limit state, thus the breaking mechanism is a rotation around a point O called the interlocking section (Figure 5.5).

Aat the moment of collapse, above O active stress is the one on the side of the ground to support (left side), passive stress is the one offered by the ground below the excavation (right side). Below O the stresses are exchanged and in figure 5.5 it is possible to recognize the active action as the red one and the passive soil action as the green one.

Furthermore, it can be established that the piling depth D is 20% of the depth of the point O, from inverse formula the depth of rotation point O is obtained:

$$y_o = \frac{D}{1.2} = \frac{6}{1.2} = 5\,m \quad (5.3)$$

To verify that this approximation is correct, a simple check is made through the equilibrium of horizontal translation, in order to obtain the reaction R_{eq} that will be compared with the real one, i.e. $R_{real} \geq R_{eq}$. Where R is the resultant of active and passive stresses below the point O.

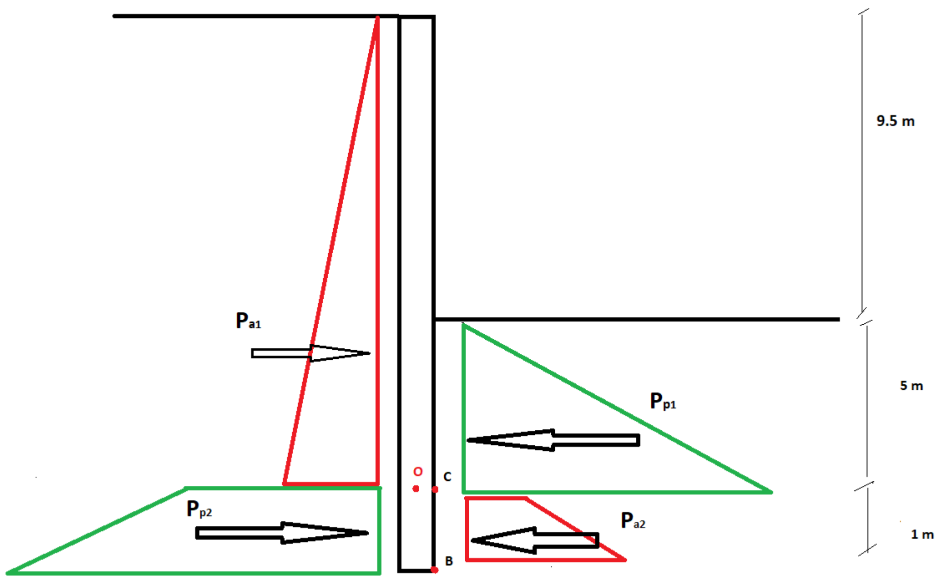

Figure 5.5 Active and passive thrust of the soil

To obtain R_{eq} the active thrust P_{a1} and the passive thrust P_{p1} must be calculated:

$$P_{a1} = \frac{1}{2}\,\sigma_a H = \frac{1}{2}\gamma K_a H^2 = \frac{1}{2} 19.5 \cdot 0.24 \cdot (9.5+5)^2 = 492\ \frac{kN}{m} \tag{5.4}$$

$$P_{p1} = \frac{1}{2}\,\sigma_p y_0 = \frac{1}{2}\gamma K_p {y_0}^2 = \frac{1}{2} 19.5 \cdot 8.15 \cdot (5)^2 = 1986.56\ \frac{kN}{m} \tag{5.5}$$

$$R_{eq} = P_{p1} - P_{a1} = 1986.56 - 492 = 1494.6\ \frac{kN}{m} \tag{5.6}$$

The real resultant R is calculated considering the thrust below point O as:

$$\sigma_{a2C} = \gamma K_a H^2 = 19.5 \cdot 0.24 \cdot (5)^2 = 23.4\ \frac{kN}{m^2} \tag{5.7}$$

$$\sigma_{a2B} = \gamma K_a H^2 = 19.5 \cdot 0.24 \cdot (6)^2 = 28.08\ \frac{kN}{m^2} \tag{5.8}$$

$$P_{a2} = \frac{1}{2}(\,\sigma_{a2B} - \sigma_{a2C})(D - y_0) + \sigma_{a2C}\,(D - y_0) = 25.38\ \frac{kN}{m} \tag{5.9}$$

$$\sigma_{p2C} = \gamma K_p\, H = 19.5 \cdot 8.15 \cdot (9.5+5) = 2304.41\ \frac{kN}{m^2} \tag{5.10}$$

$$\sigma_{p2B} = \gamma K_p H_{tot} = 19.5 \cdot 0.24 \cdot 15.5 = 2463.33\ \frac{kN}{m^2} \tag{5.11}$$

$$P_{p2} = \frac{1}{2}\big(\,\sigma_{p2B} - \sigma_{p2C}\big)(D - y_0) + \sigma_{p2C}\,(D - y_0) = 2383.9\ \frac{kN}{m} \tag{5.12}$$

$$R_{real} = P_{p2} - P_{a2} = 2383.9 - 25.83 = 2358.1\ \frac{kN}{m} \tag{5.13}$$

$$R_{real} \geq R_{eq} \qquad 2358.1\ \frac{kN}{m} \geq 1494.6\ \frac{kN}{m} \tag{5.14}$$

The check is satisfied, thus the rotation point can be considered, with a good approximation, the real one.

Knowing the thrusts and the rotation point, it is possible to chart the bending moment (Figure 5.6), useful for doing comparison with the results given by the LAGAMINE software.

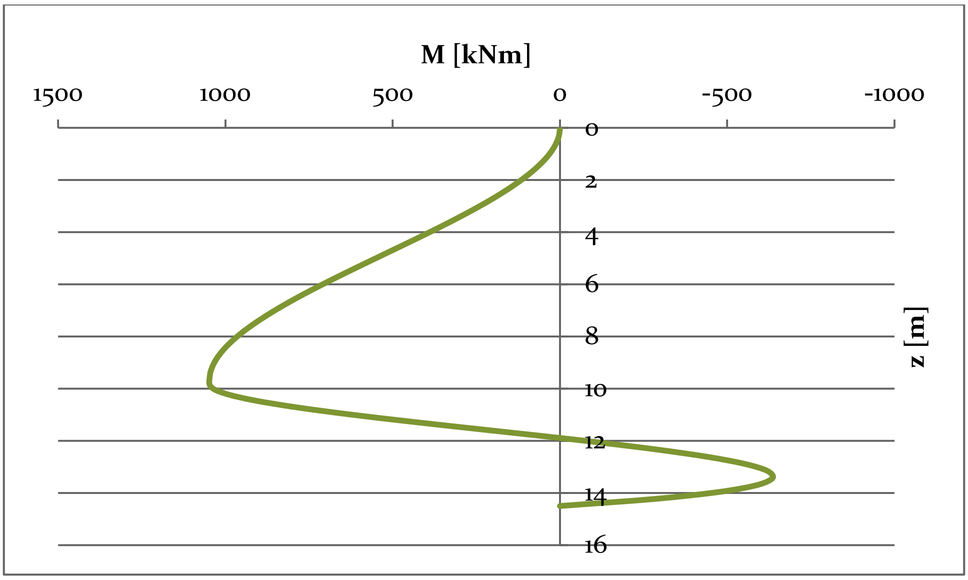

Figure 5.6 Bending moment calculated by active and passive thrusts

5.4 Finite element numerical modeling

The knowledge of the geometry of the diaphragm wall, paragraph 5.2, and the loads acting on it, allows to create the model using the LAGAMINE software. Thus, the geometry and boundary conditions were set into the "*GMAIL file*". The mesh was created dividing the several segments into an appropriate number to create finite elements of 0.20x0.25 m. Indeed, the upper and lower ends of the diaphragm, 0.8 m thick, have been divided into 4 segments each of 0.20 m. On the other hand, the lateral ends, 15.5 m of the overall length, have been divided into 58 parts. The final mesh is represented in the figure 5.7.

Afterwards, the diaphragm wall has been loaded with the load distributed linearly due to the soil actions, obtained in chapter 5.3.1. In addition, boundary conditions have been settled, i.e. the translation of point O in the two directions has been fixed and two rollers have been placed at the bottom of the diaphragm wall to simulate the "fixed Earth support" condition (Figure 5.7).

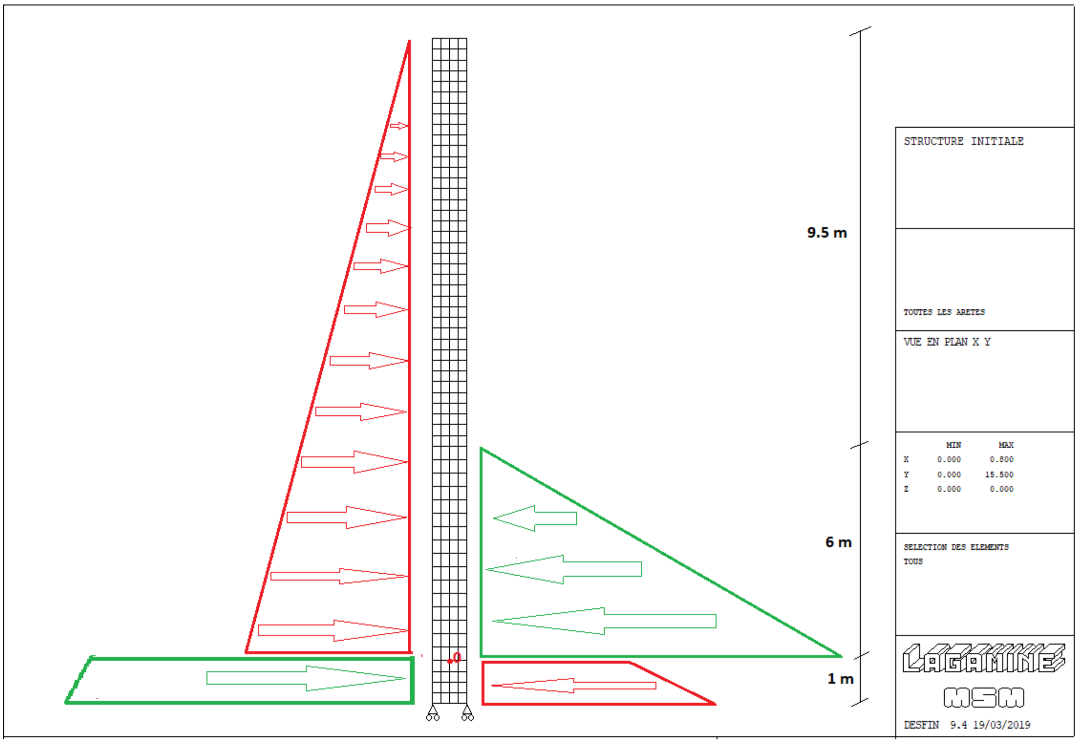

Figure 5.7 Mesh of the initial structure

The next step was to set the properties of the diaphragm wall into the "*DATA file*". The type of concrete used has been define in chapter 5.2, table 4. Moreover, the initial condition of temperature has been fixed for all the nodes equal to 14°, according to the Torino subsoil conditions (Di Donna, 2016). Lastly the elements has been defined as "*MWAT2*", that allows to do a complete THM analysis, even though only TM analysis will be done.

To be sure that all the information written is correct, *Prepro* button is made to run.

The "*LOADING file*" is the one where all created files are called up to run the software and get the results. Indeed, into the *LOADING file* are defined the time steps that are wanted to be reported into the results, the increment of the time calculation decided and here it is imposed to read the *"LIC and DEP files"*.

The *LIC* file is where load times are imposed. As a matter of fact, at time 0 second no load is imposed. Then, to simulate the excavation, the linear distributed loads are made to grow linearly. In fact, at time $8.64E^{04}$ seconds (1 day), it is imposed a increment of imposed force multiplier equal to 1, i.e. at that time all the loads defined into the *DATA file* are applied to the maximum value.

The "*DEP file*" it is proper to the thermal analysis. The file dictates the times of thermal variation imposed to the nodes chosen, in this case on the exchanger tubes. For the initial mechanical analysis this file is not used.

Another useful file is the "*PRI file*". Here it is possible to select the values wanted, referred to the chosen nodes and elements, to print them later.

After setting the several files, the program can be run pushing on the *Lagamine* button.

All the files described above can be viewed in the Appendix 1.

5.5 Interpretation of the results

Now that the LAGAMINE software has all the needed files, it is possible to pull out the desired results, export them on Excel and thus analyse them.

5.5.1 Mechanical results

The first analysis made is the mechanical one. The simulation of the excavation, on the right side, is done controlling the active and passive thrust of the soil, letting them vary linearly from time 0 sec to time $8.64\ E^{04}$

sec (1day). The value and trend of the trusts is the one reported in the paragraph 5.3.1.

Due to the actions of the soil, the diaphragm wall will suffer a deformation like in Figure 5.8. Moreover, a changing in stress will appear and of course a bending moment will characterize the geostructure.

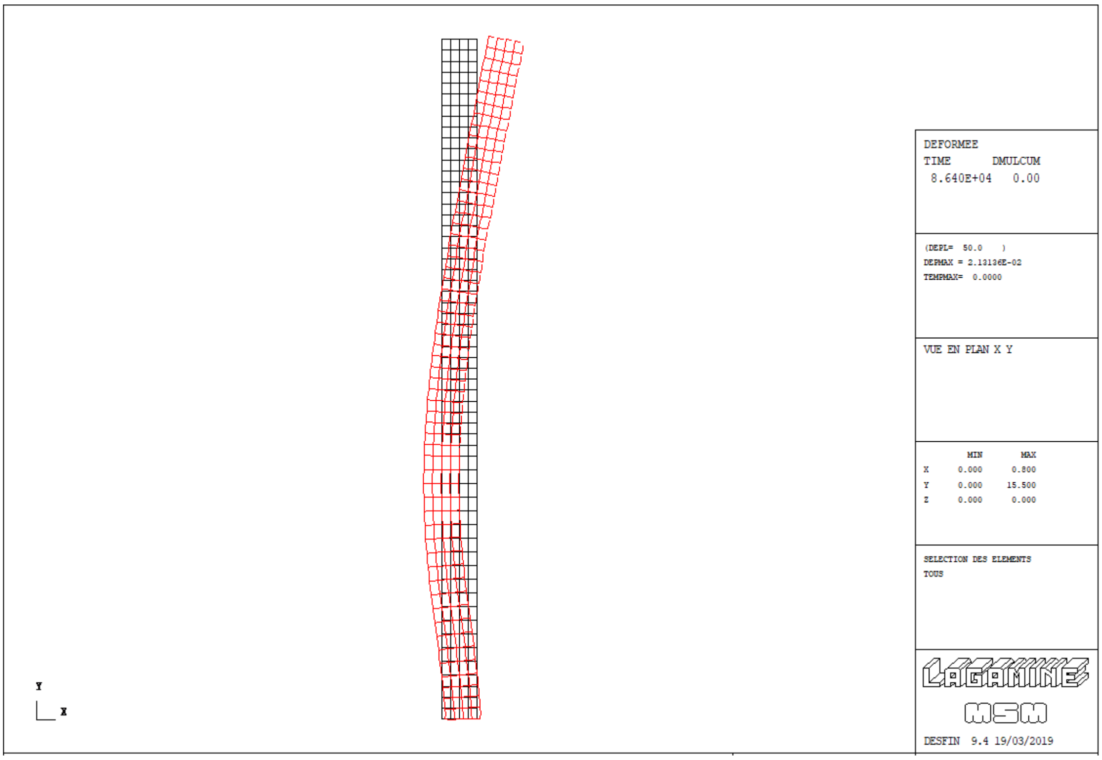

Figure 5.8 Deformed structure due to soil thrusts

When the excavation is finished, the maximum displacement occurs at the top of the structure and it is equal to 20.6 mm, as shown in Figure 5.9.

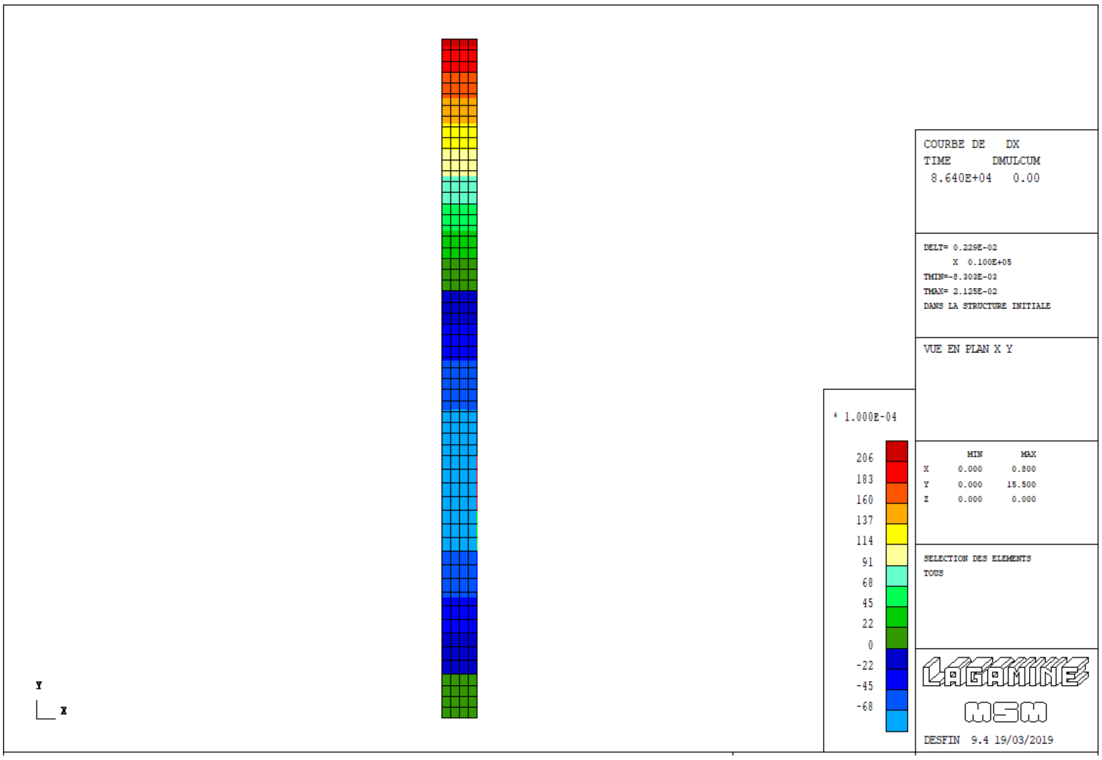

Figure 5.9 Horizontal displacements of the diaphragm wall for the mechanical analysis

Besides the displacements directly provided by the software, it is possible to plot horizontal displacements and bending moment from the value of variation of the coordinate x and the variation of stresses, printed through PRI file (Figures 5.10, 5.11).

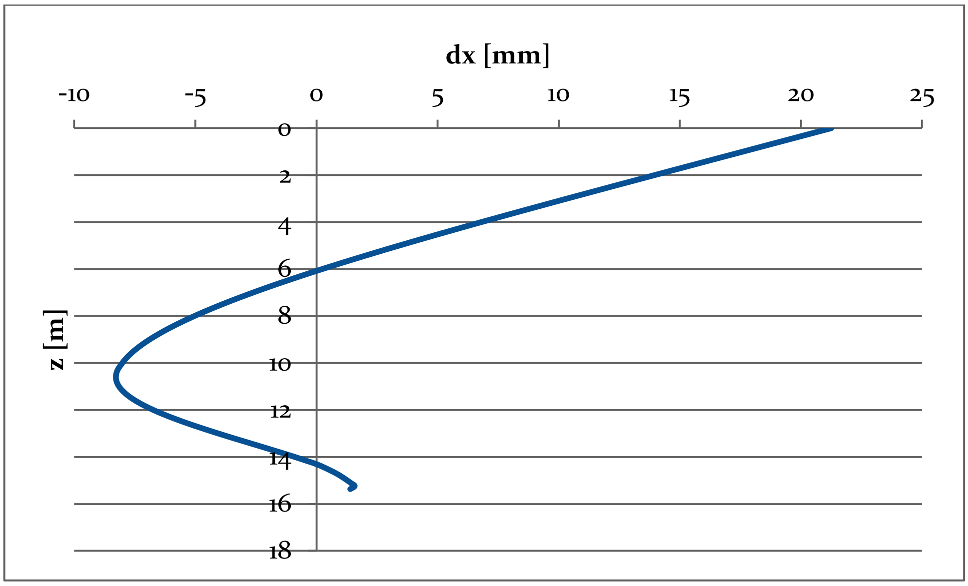

Figure 5.10 Horizontal displacements obtained

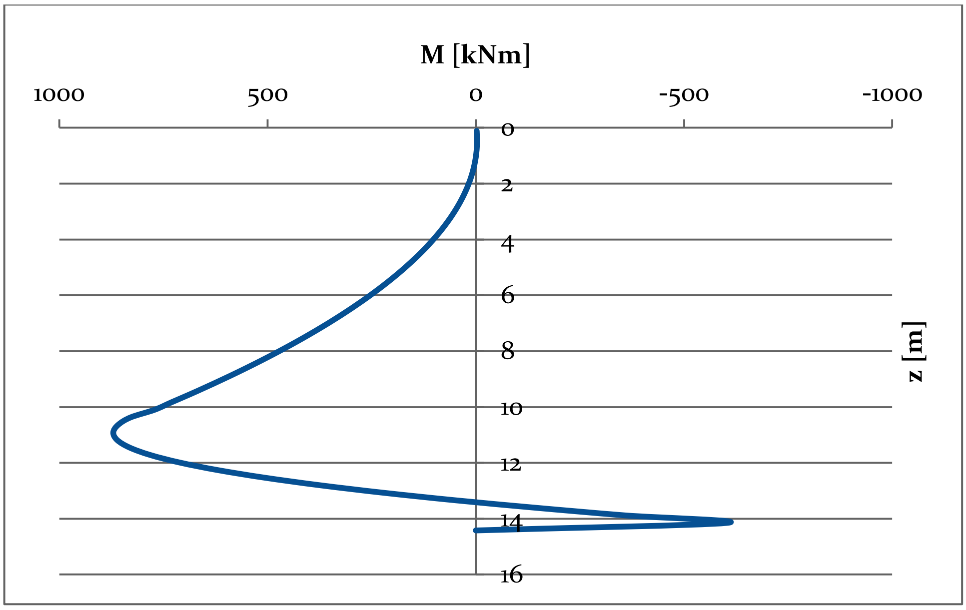

Figure 5.11 Bending moment from mechanical analysis

It is possible to do a comparison with the analysis made by Barla et al. (2018). The paper studies the same diaphragm wall, in the same context, but in the total complex, i.e. with surrounding soil and bottom slab. Even if the constraint conditions are different, i.e. bottom slab, an interesting comparison can be made. Indeed, with the complete model, the displacement at the top of the structure, due to the only excavation, are equal to 17 mm, comparable in order of magnitude with the result just obtained (Figure 5.12).

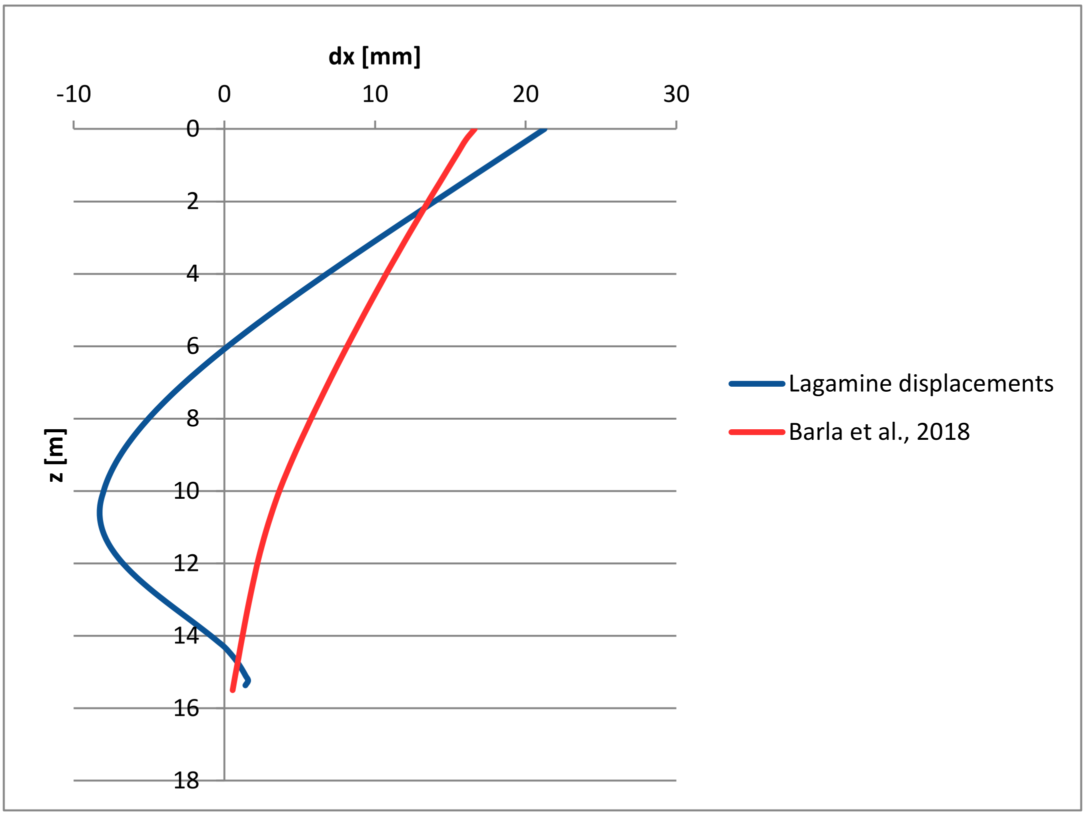

Figure 5.12 Comparison of displacements between Lagamine software and Barla et al. (2018)

Moreover, it is evident that an acceptable comparison can be made by referring to the diagram obtained from the analytical way, the Lagamine analysis and the analysis led by Barla et al. (2018) (Figure 5.13). An important observation must be made about the difference between the three bending moments. Indeed, because of the different boundary conditions, the behavior of the diaphragm wall must be different. The presence of the soil and the bottom slab considered in the anlysis of Barla et al. (2018), guarantees a reduced bending moment. Instead, the difference in value of the analytical calculation and the FE analysis, is accettable due to the thickness of the wall considered in the FEM calculation.

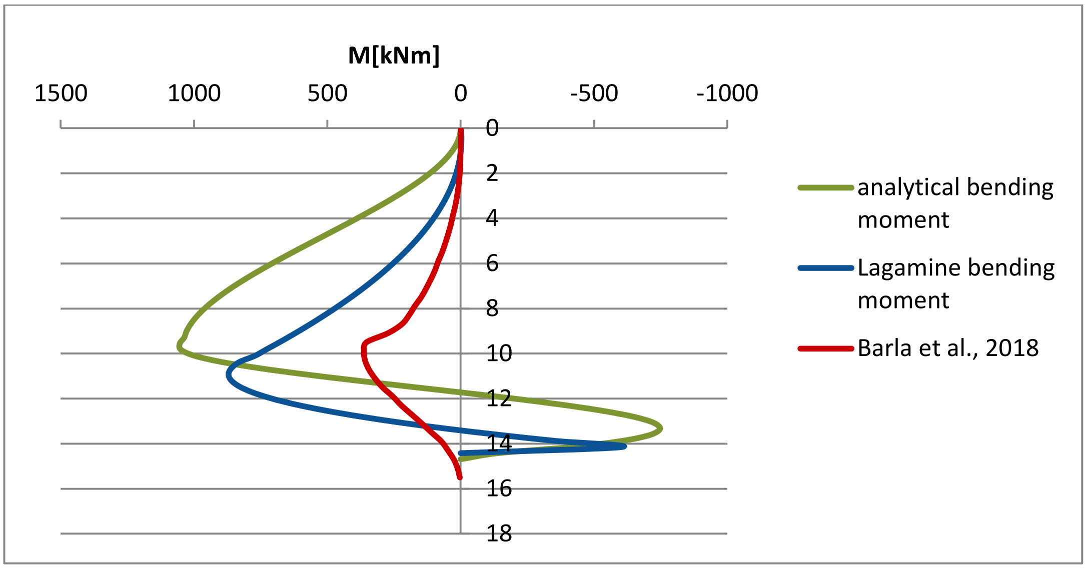

Figure 5.13 Comparison of bending moment between analytical calculation, Lagamine alysis and Barla et al. (2018)

5.5.2. Thermal results: activation of the geothermal probes

For the simulation of the geothermal plant, a thermal variation was inserted inside the exchanger tubes, through a time-dependent temperature setting on the nodes where the tubes are supposed to be. Indeed, the 13 pipes are positioned from 2 m below the top of the diaphragm wall, with an interaxis of 1 m one to another. In order to take into account the real position of the tubes, i.e. considering concreate cover, the nodes selected are distant 20 cm from the side (Figure 5.14).

In winter, heat is extracted from the circulating fluid in the pipes, while in summer the reverse process takes place, i.e. the heat is transferred to the fluid. Therefore the temperature trend in the pipes was modeled in a manner consistent with this consideration.

Specifically, a solar year of thermal variation within the probes was divided as follows:

- from day 1 to day 60: constant temperature of 4° C;
- from day 60 to day 90: temperature variable linearly increasing from 4 ° C to 14 ° C;
- from day 90 to day 120: constant temperature of 14 ° C;
- from day 120 to day 150: temperature variable linearly increasing from 14 ° C to 26.5 ° C;
- from day 150 to day 240: constant temperature of 26.5 ° C;
- from day 240 to day 270: temperature variable linearly in a decreasing way from 26.5 ° C to 14 ° C;
- from day 270 to day 300: constant temperature of 14 ° C;
- from day 300 to day 330: temperature linearly decreasing from 14 ° C to 4°C;
- from day 330 to day 365: constant temperature of 4 ° C.

To perform the input in the probes for two solar years, 18 analyses cycles were therefore carried out, using the *DEP files* before described, and following reported.

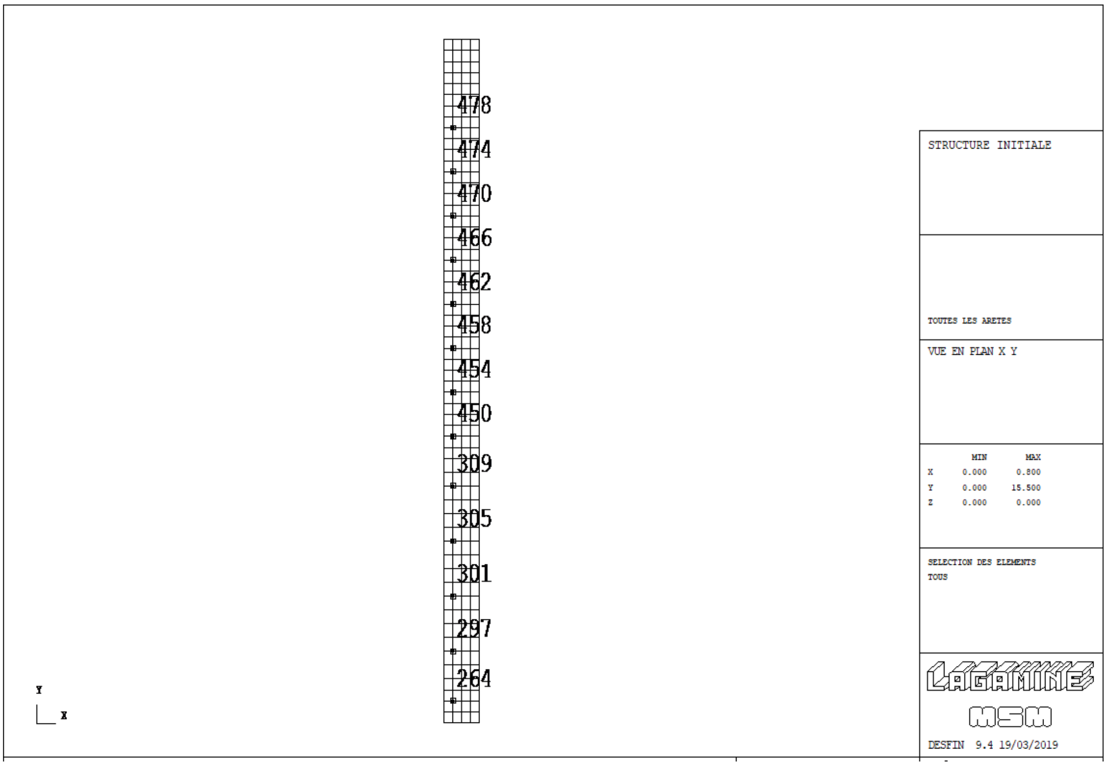

Figure 5.14 Position of the tube into the diaphragms

At day 1, when the exchanger tubes are activated, the temperature of the probes is 4°C (January) and the initial temperature of the structure is 14°C, as agreed by Di Donna (2016). For the difference in temperature, it is possible to locate the pipes in Figure 5.15.

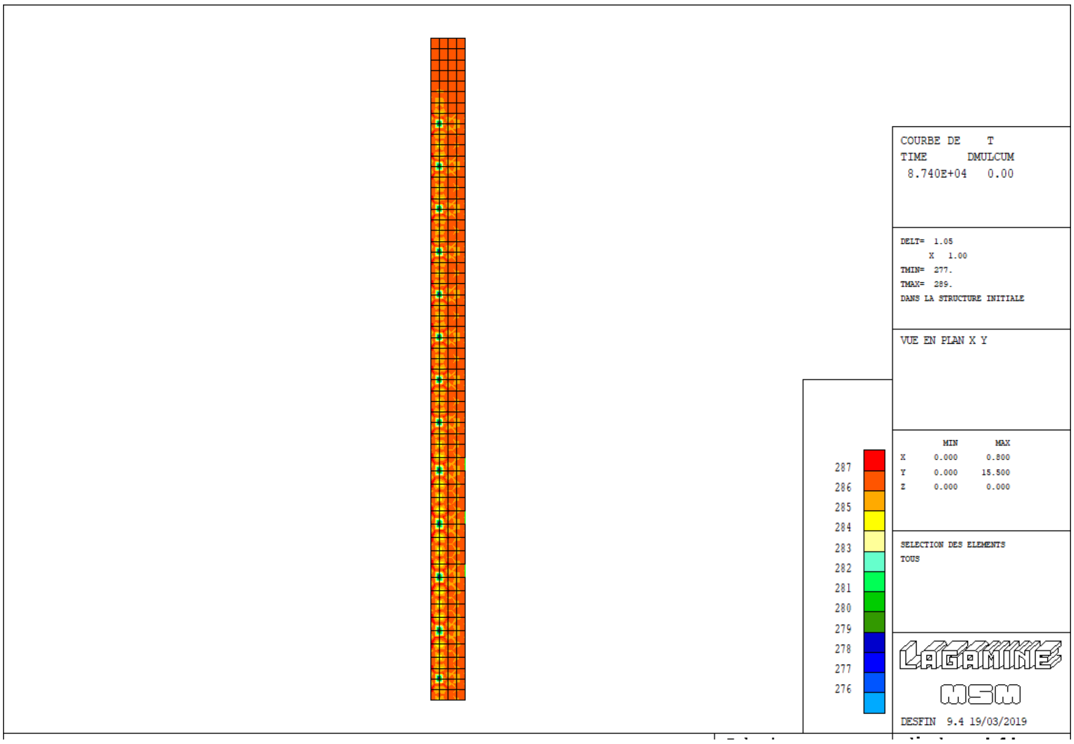

Figure 5.15 Temperature (in kelvin) inside the diaphragm wall at day 1

At day 60 (2 months), are evaluated the bending moment and the displacements, compared with the mechanical ones. As we can see from Figure 5.16 it is possible to highlighting the similarity between the two curves. Indeed, the difference between bending moments is almost perceptible inasmuch is of the order of Newtoon (Table 6).

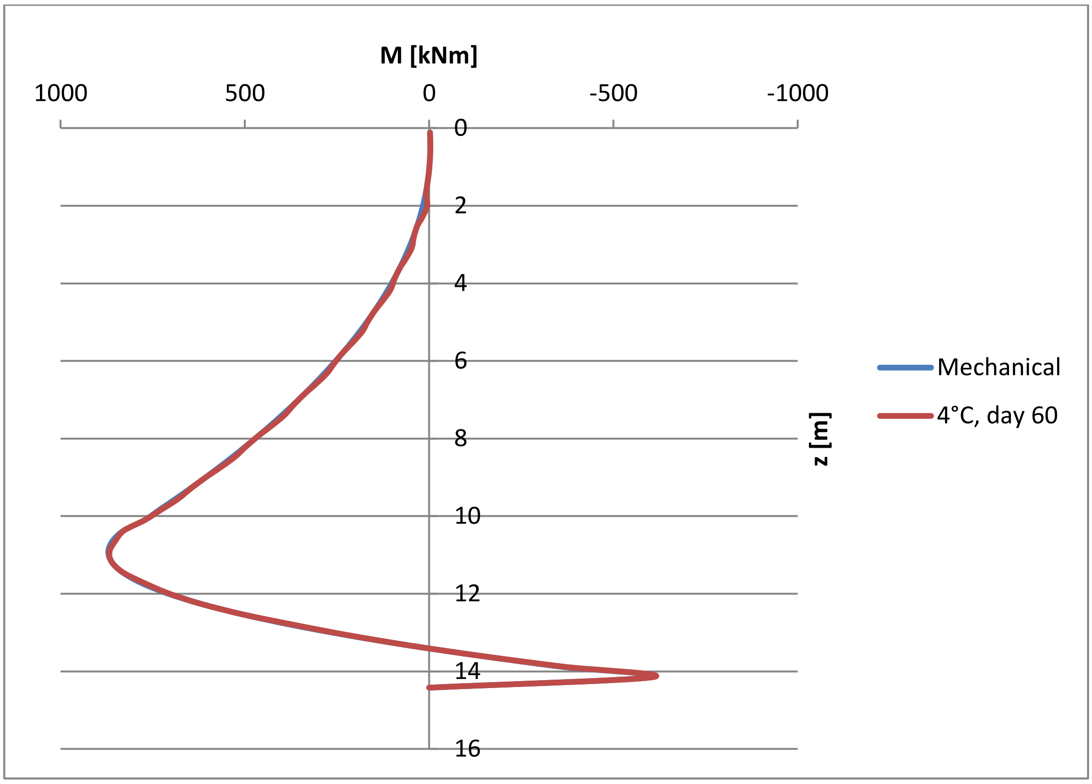

Figure 5.16 Comparison between bending moments at day 1 and day 60 from the activation

Regarding displacements, the difference is more marked as Figure 5.17 shows. Furthermore, because the system is cooled, from 14°C to 4°C, there is a contraction of the diaphragm wall, i.e. head displacement is reduced. Everything is consistent with what is expected from a "Fixed Earth support".

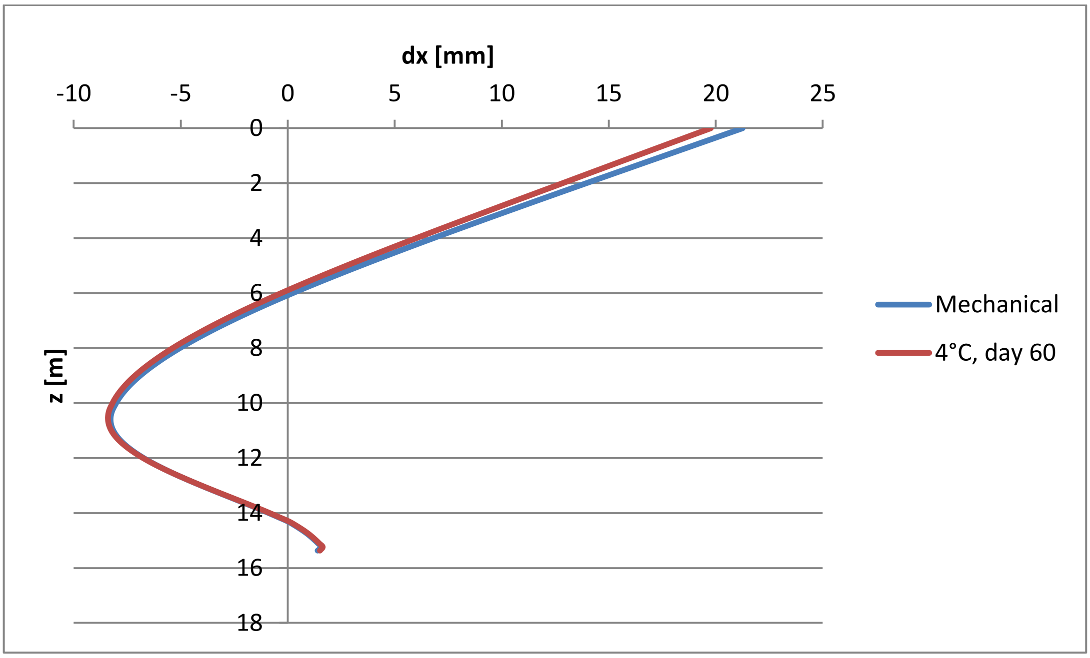

Figure 5.17 Comparison between horizontal displacements at day 1 and day 60 from activation

The comparison in terms of displacements and bending moment, can be done for the whole year, thus the results are reported in the following diagrams. As it is evident, bending moment is quite the same, but the horizontal displacement although change appreciably.

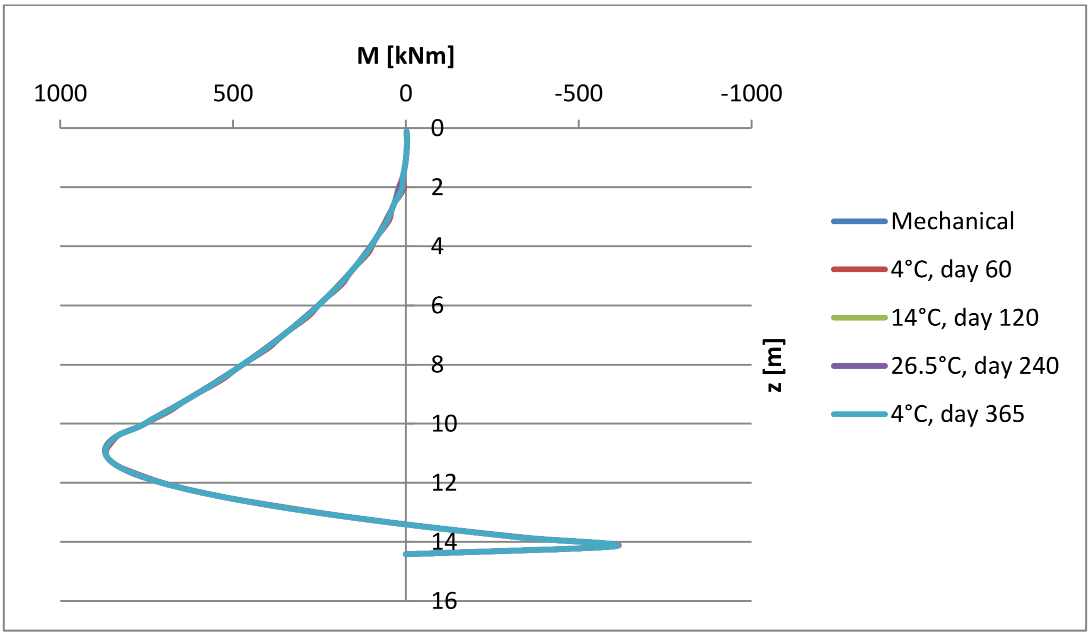

Figure 5.18 Comparison between bending moments in the whole first year of activation

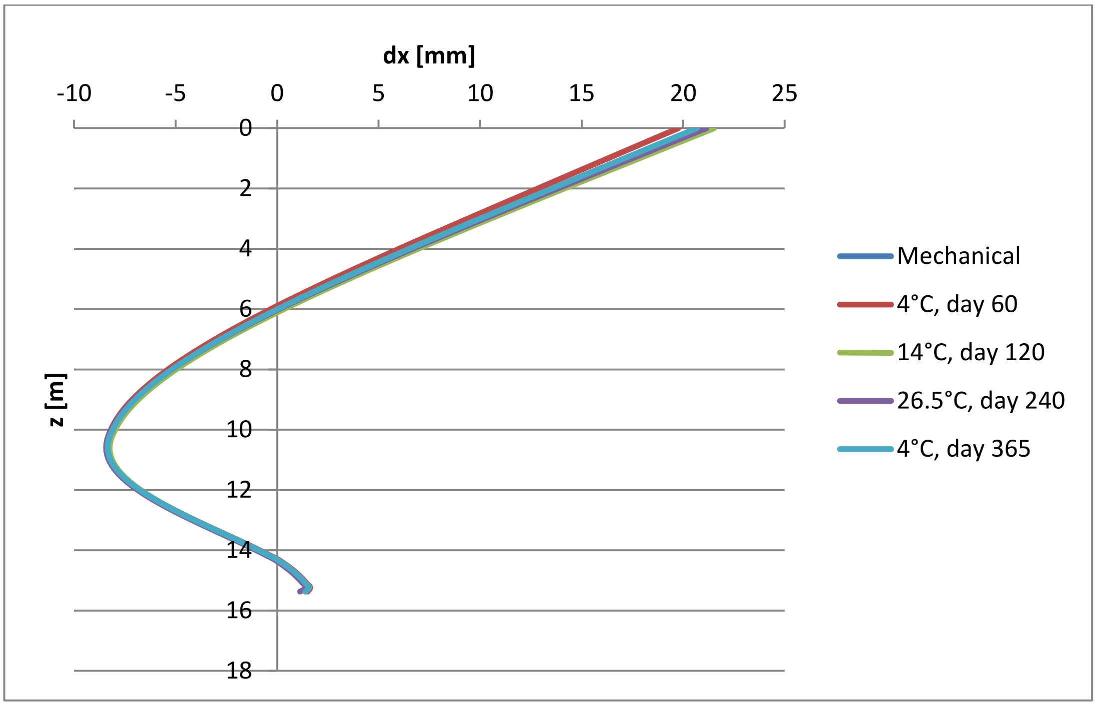

Figure 5.19 Comparison between horizontal displacements in the whole first year of activation

In summer and at the end of the first year, the temperature inside the diaphragm wall is almost uniform along it, due to the presence of the tubes with interaxis of 1 m. In both cases, the temperature is almost everywhere close to the one set by the probes. Obviously, in the area close to the top the temperature is higher inasmuch the geothermal system starts 2 m below (Figures 5.20, 5.21).

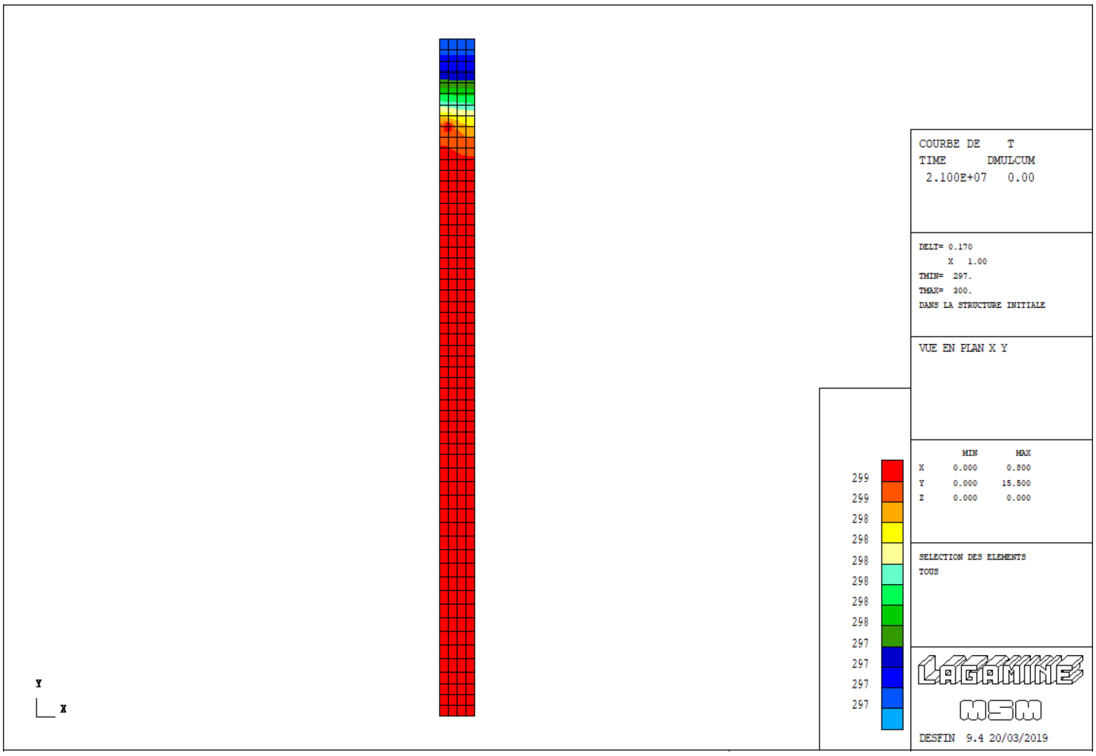

Figure 5.20 Temperature (in kelvin) inside the wall at 240 days (summer)

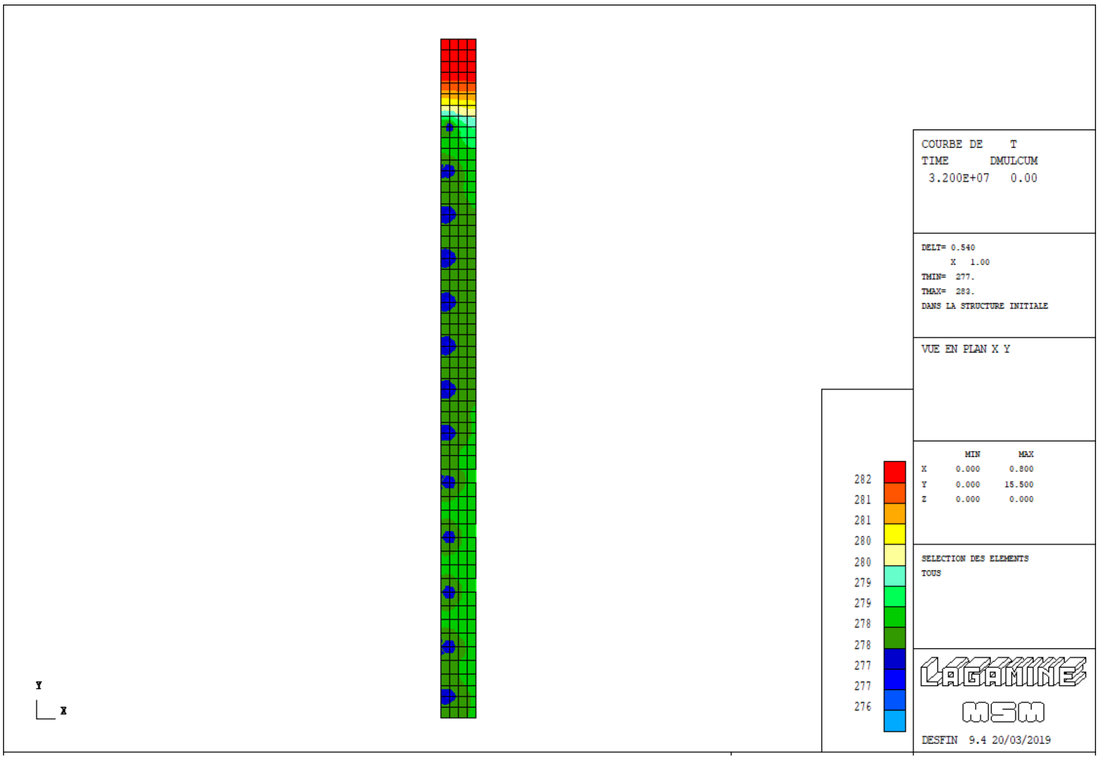

Figure 5.21 Temperature (in kelvin) inside the wall at the end of the first year of activation

The same observations can be made during the second year of the system activation. Thus, bending moment in the second year, is reported in Figure 5.22 and all the horizontal displacement occurred in the two years of activation are plotted in Figure 5.23.

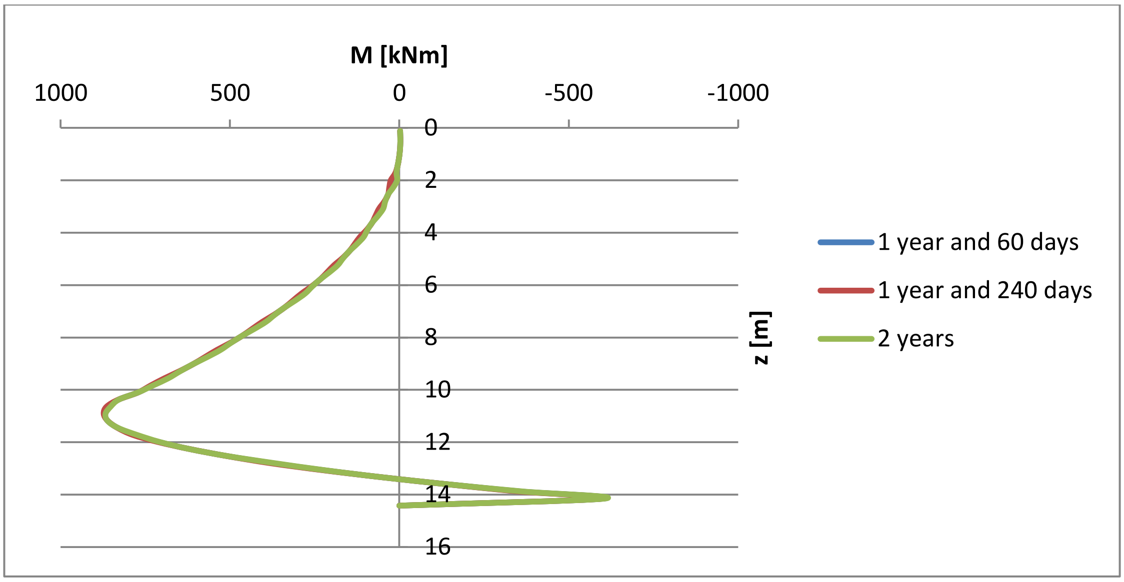

Figure 5.22 Comparison between bending moment in the second year of activation

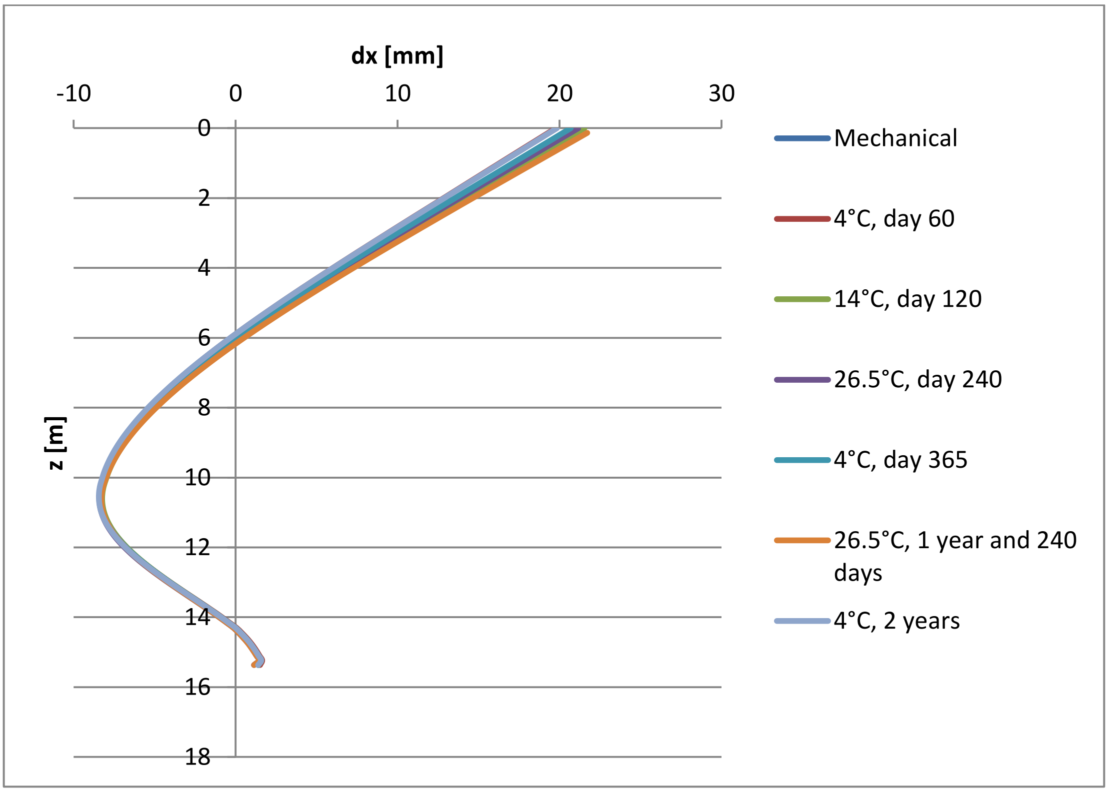

Figure 5.23 Horizontal displacements during the two years of system activation

Similarly to the first year is the temperature along the diaphragm wall during the second year of activation (Figure 5.24, 5.25). Only one interesting observation is that, during the summer of 2 year, the temperature inside the diaphragm is not as uniform as in the first year, even though the difference between the tubes and the wall is just 1 K. Same observation and same difference is noted at the end of the second year.

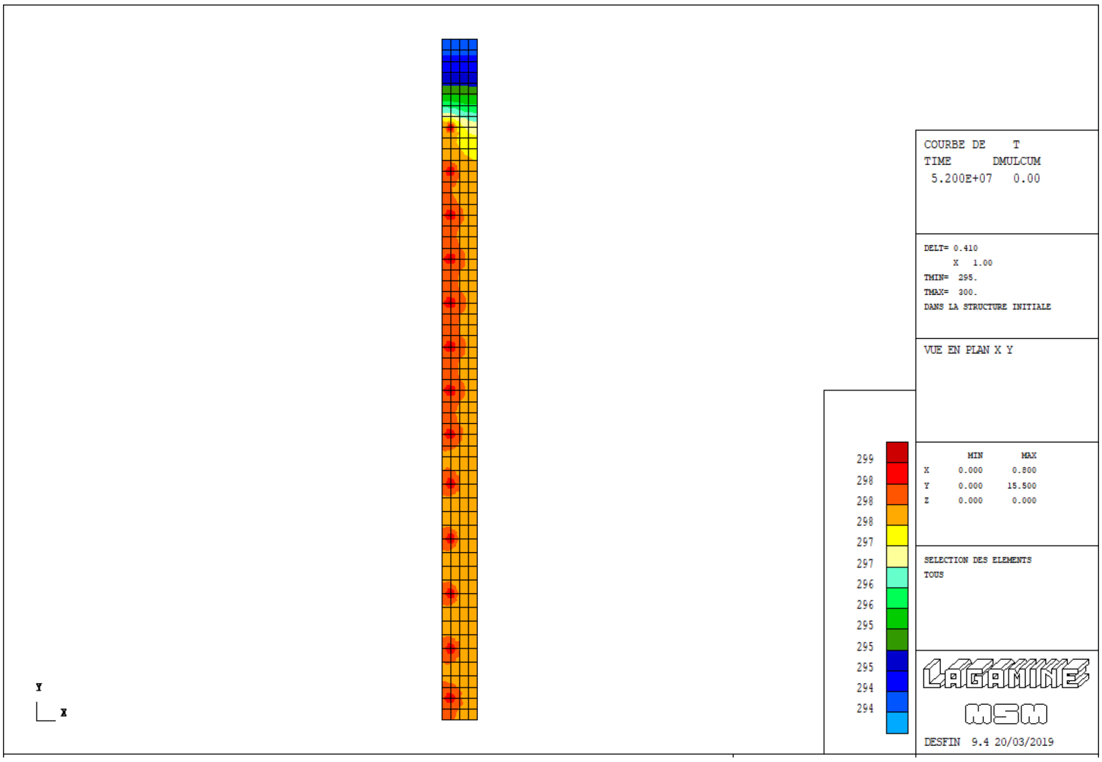

Figure 5.24 Temperature (in kelvin) inside the wall at 1 year and 240 days (summer)

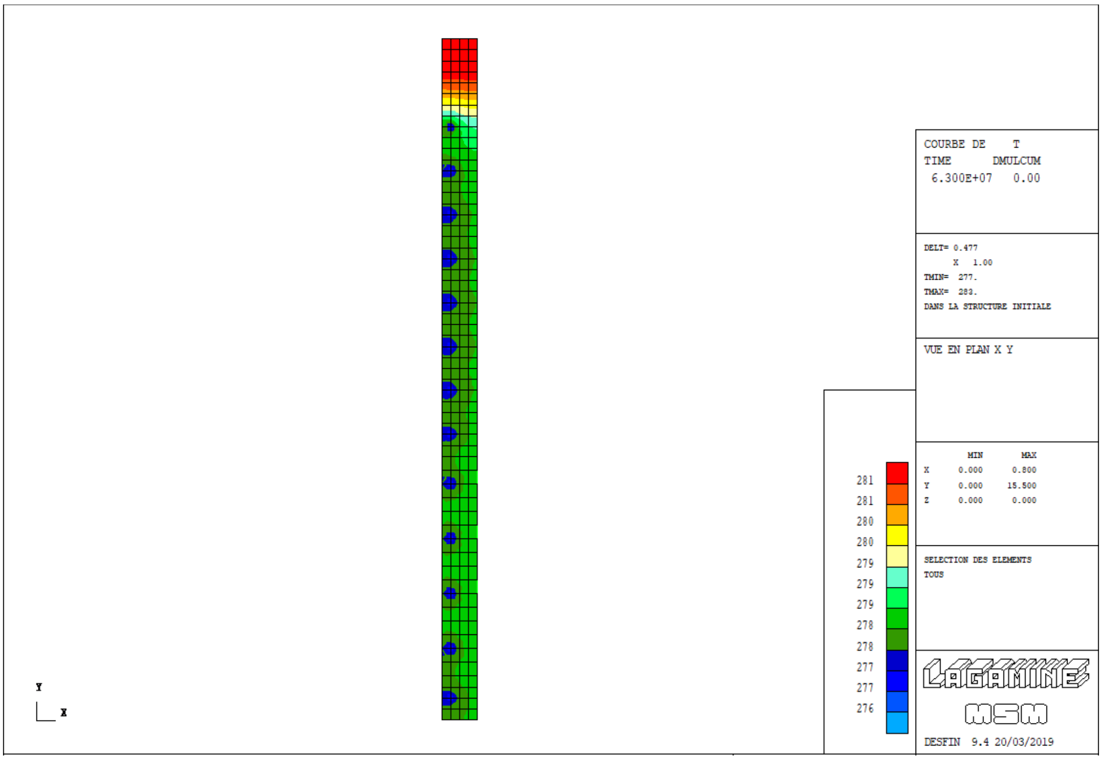

Figure 5.25 Temperature (in kelvin) inside the wall at the end of the second year of activation

5.5.3 Comparison of results

From the graphs it is difficult to appreciate the variations undergone by the wall, consequently Tables 6 and 7 show the numerical values that characterize the activation phases of the tubes. To this comparison is added the one referring to the analysis performed by Barla et al. (2018) (see chapter 3.4) so as to be able to draw conclusions later.

Table 6 Comparison with Barla et al. (2018) analysis of the first year of activation

	M_{max} [kNm]	$M_{max\ Barla}$ [kNm]	d_{head} [mm]	$d_{head\ Barla}$ [mm]
Mechanical (14°C)	870.4	380	21.25	17
Winter (4°C, day 60)	867.1	460	19.77	16
Summer (26.5°C, day 240)	870.5	352	21.5	22
Winter (4°C, 1 year)	869.3	-	20.7	-

Table 7 Comparison with Barla et al. (2018) analysis of the second year of activation

	M_{max} [kNm]	$M_{max\ Barla}$ [kNm]	d_{head} [mm]	$d_{head\ Barla}$ [mm]
Winter (4°C, 1 year and 60 days)	869.9	450	20.69	17
Summer (26.5°C, 1 year and 240 days)	872.7	354	22.21	22
Winter (4°C, 2 years)	867.4	470	19.82	18

The greatest discrepancy between the results obtained by the model presented in this thesis and the ones from Barla et al. (2018), can be seen in the values of bending moments. It is not particularly surprising because of the constraint conditions, which are very different even if the diaphragm wall is actually the same. Indeed, the structure here studied, presents just two rollers at the bottom of the wall to simulate the "Fixed Earth support" condition and a rotation point on the axis of the structure at 1 m from the bottom of it. On the other hand, the analysis conducted by Barla et al. (2018) involves the same diaphragm wall where a bottom slab is presents. Moreover, the surrounding soil is simulated, i.e. the interaction between soil and wall is different from the one simulated with active and passive thrusts.

For this reasons, it is easy to perceive by intuition that the results must be different. Nevertheless, it is interesting to notice that a comparison between the two analyses can be made regarding the displacements. Indeed, when the geothermal system is not yet active, i.e. only the actions of the soil urges the wall, the difference, in terms of horizontal displacements, is only of 4 mm (Figure 5.12). In addition, the same trend during the years can be noticed: in summer the displacement increases and in winter is reduced (respectively Figure 5.26 and Figure 5.27).

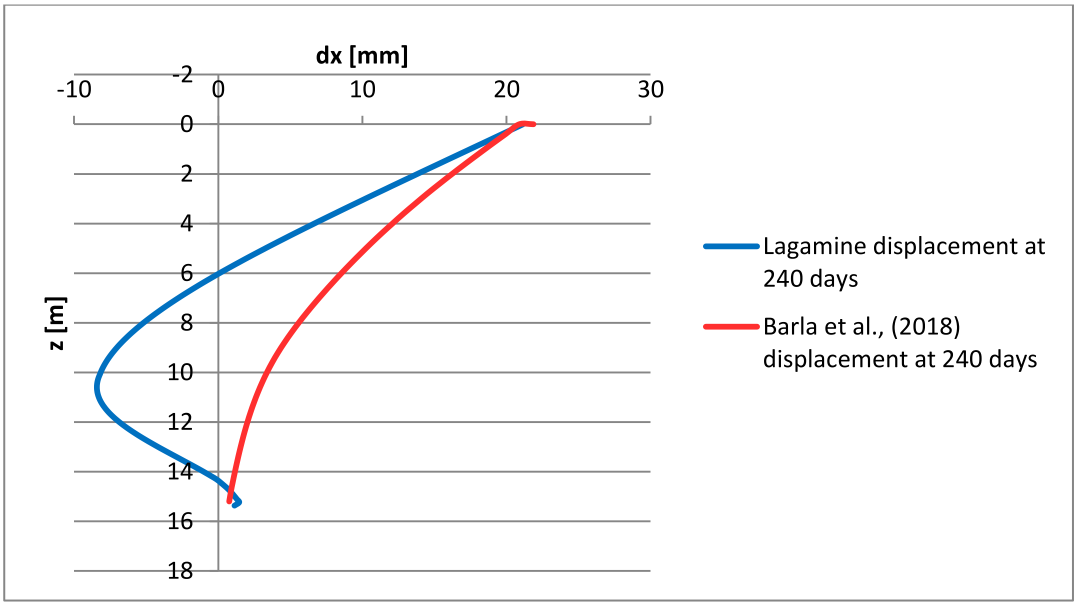

Figure 5.26 Comparison of displacements between Lagamine software and Barla et al. (2018) at 240 days of activation (end of summer)

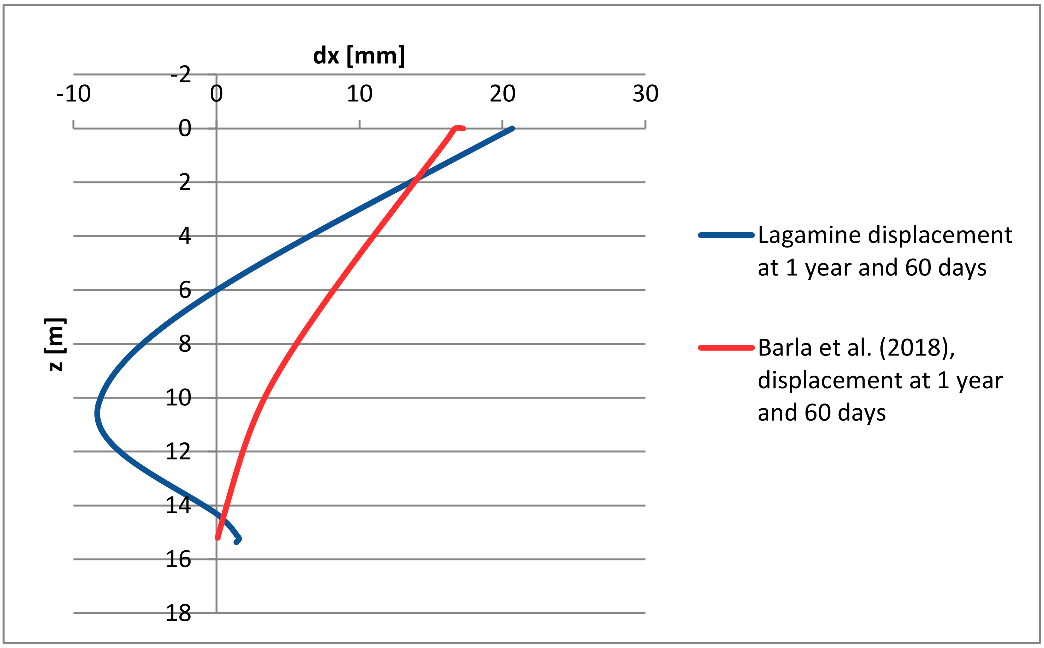

Figure 5.27 Comparison of displacements between Lagamine software and Barla et al., (2018) at 1 year and 60 days of activation (end of winter)

Especially, between the summer and the end of the second year, the variation of displacement to the head is around the 60% of the one proposed by Barla et al. (2018) (Figure 5.28 and Figure 5.29).

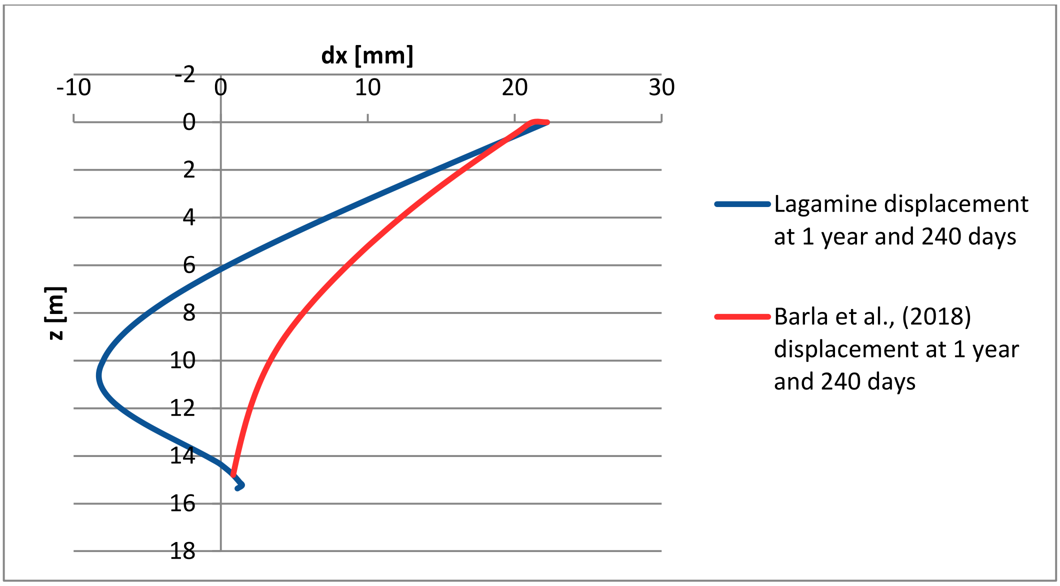

Figure 5.28 Comparison of displacements between Lagamine software and Barla et al. (2018) at 1 year and 240 days of activation (end of summer)

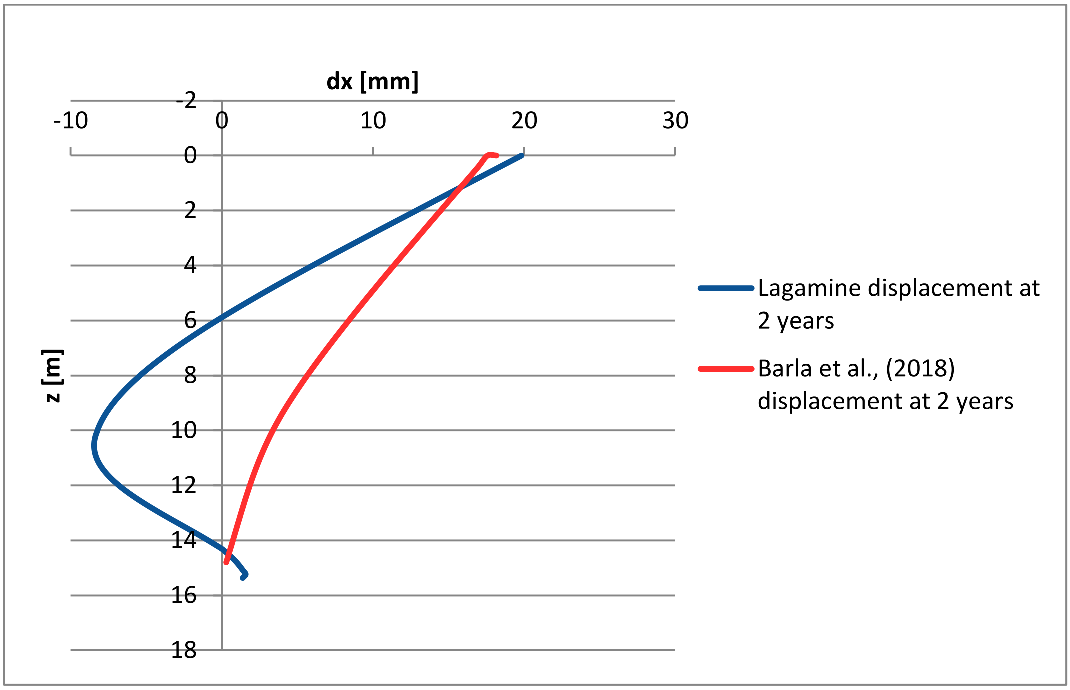

Figure 5.29 Comparison of displacements between Lagamine software and Barla et al., (2018) at 2 years of activation (end of winter)

Important observations must be done regarding the case study of this thesis.

After the mechanical phase, can be noticed a decrease in the maximum head displacement of about 1.5 mm at the end of the first winter phase (after 60 days); subsequently the maximum value at the head of the diaphragm is reached and it is equal to 21.5 mm at the end of the first summer phase (after 240 days) and later, after a year and 60 days (end of winter period) value decreases and so on cyclically. Furthermore, an interesting observation can be made concerning displacements. In the first year of the system activation, the decrease (winter) and increase (summer) of the head displacement is equal to 7%. Nevertheless, during the second year, it is highlighted an increase of 6.8% in displacement between winter (1 year and 60 days) and summer (1 year and 240 days), but at the end of the second year a decrease of 10% shows up. This suggests that increasing cycles and the transition from summer to winter tend to make the wall more sensitive to displacements. To confirm this statement, an increase between 4.25% and 4.5% in displacements is noted between the same seasons in the two years of system activation.

Thus, in subsequent cycles, i.e. years, the percentages of increase in displacement may increase as well, or can stay constant too. Further analysis would be appropriate.

The results of the analysis brigs to conclude that:

- as the temperature increases, the horizontal displacements of the diaphragm wall increase;
- with the continuation of the application cycles of the thermal inputs the values at the end of each period are greater than the previous one; also here it must be reiterated that this observation refers to two years of simulation with activated implant and does not ensure the same progression for the years to come.

6. Conclusions

This thesis is based on the study of the thermo-mechanical behavior of a diaphragm wall, part of the underground car park of via Ventimiglia, Turin. The aim was to analyze the effects that a geothermal system induces within a geostructure from a thermo-mechanical point of view.

The geothermal system as the one considered, allows to heat and cool the concerned area, in this case the inside of the car park, just exchanging heat with the soil. The technology exploits the shallow geothermal resource reducing dependence on fossil fuels.

Introducing the concept of geothermal energy and its different forms was fundamental to understand how the technology works. At the base of this, energy geostructure has been described. Thanks to the huge surface in contact with the ground, tunnels are perhaps the ones that can best exploit the geothermal system. Nevertheless, energy pipes and energy diaphragm wall are widely used around the world.

Diaphragm wall represents an excellent solution for exchanging heat with the ground given the particularly large surfaces. The key point of the energy geostructures is that are able to combine structural function with the energy one. Thus, with just one structure is possible to merge two really important functions. Indeed, a great saving in construction is guaranteed because only an additional operation to install the circuit is required. The pipes must be bound on the reinforcement cage and connect to the main pipeline which will join the geothermal heat pump.

It is not enough to study the energy aspect in terms of heat transfer capacity. To use a system like this, which requires an appropriate project and an initial expenditure of money, stresses and displacements must also be taken into account.

Although a similar analysis already exists of the same diaphragm wall, it has been thought to use different software and to study only the decontextualized diaphragm wall. For this reason, no soil and no slab was modelized. The only action taken into consideration was the one of the soil, acting as a result of the excavation.

After studying the mechanical behavior due to the action of the thrusts, thermo-mechanical analysis was started. Thus, the 13 pipes were activated, causing the internal temperature to vary according to the season considered. The analysis forecasted two years of observation, with a total of 18 cycles. The results showed constancy in bending moment but an increase of displacement at the head of the diaphragm around 5%, compared to the values obtained by mechanical analysis only, going from 21.25 mm to 22.3 mm. The same percentage was noticed between the displacements of the head in the same season of the two years considered.

From this thesis work, it emerged that taking into account only the diaphragm wall without the actual in situ conditions, allows to overestimate the mechanical displacements and in any case to have the same order of magnitude of displacements in system activation. Moreover, even if the variation of the bending moment is not appreciable, it is always in favor of safety, since the bending moment is higher than the one of the real case.

Possible developments of this work could take into account the several constraint conditions to which a real diaphragm wall is subjected. For example, more than the bottom slab, an upper slab could be considered in order to simulate the car parking roof. From a thermic point of view, the observation period can be extended to understand if the variations in displacement will stabilize or will continue to increase.

Certainly the technology deserves attention and further studies, as the benefits offered are not negligible and for sure it is an excellent to solution against the pollution problem that today more than ever afflicts our society.

Appendix 1

Gmail file : Geometry and boundary conditions

```
npts nseg nlis mxpl nzon mxzn nden  NEL TYPE PROG SMTH
  8  10   0   0   5   4   0 200   4   0   8   0   0   0   0   4
  N        X_coor       Y_coord
  1          0.0          0.0
  2          0.8          0.0
  3          0.0          1.0
  4          0.8          1.0
  5          0.0          6.0
  6          0.8          6.0
  7          0.0         15.5
  8          0.8         15.5
  N Type   N1   N2   N3   N4
  1   1   1   2   0   0   4
  2   1   2   4   0   0   4
  3   1   4   6   0   0  16
  4   1   6   8   0   0  38
  5   1   8   7   0   0   4
  6   1   7   5   0   0  38
  7   1   5   3   0   0  16
  8   1   3   1   0   0   4
  9   1   4   3   0   0   4
 10   1   6   5   0   0   4
  N TYPC NSEG jtyp nint mate geom      young nu thick/LISZ
  1   2   4 205   4   1   2   0   0
    0.0      0.0      0.0      0.0
  1   2   9   8
  2   2   4 205   4   1   2   0   0
    0.0      0.0      0.0      0.0
 -9   3  10   7
  3   2   4 205   4   1   2   0   0
    0.0      0.0      0.0      0.0
-10   4   5   6
  4  11   3  15   2   3   0   0   0
    0.0      0.0      0.0      0.0
  6   7   8
  5  11   2  15   2   4   0   0   0
    0.0      0.0      0.0      0.0
  2   3
```

Data file : Properties, elements, nodes and laws

```
  5   2 821   7 310   0   0   0   0   6   0   0   0   0
  1   1   0 100   40   18   80   1


NODES
  1      0.0      0.0      0.0      0.0277.000000
  2.800000011      0.0      0.0      0.0277.000000
  3.8000000111.00000000      0.0      0.0277.000000
  4.8000000116.00000000      0.0      0.0277.000000
  5.80000001115.5000000      0.0      0.0277.000000
  6      0.015.5000000      0.0      0.0277.000000
  7      0.06.00000000      0.0      0.0277.000000
  8      0.01.00000000      0.0      0.0277.000000
  9.100000001      0.0      0.0      0.0277.000000
 10.200000002      0.0      0.0      0.0277.000000
 11.300000011      0.0      0.0      0.0277.000000
 12.400000005      0.0      0.0      0.0277.000000
 13.500000000      0.0      0.0      0.0277.000000
 14.600000023      0.0      0.0      0.0277.000000
 15.699999988      0.0      0.0      0.0277.000000
 16.800000011.125000000      0.0      0.0277.000000
 17.800000011.250000000      0.0      0.0277.000000
 18.800000011.375000000      0.0      0.0277.000000
 19.800000011.500000000      0.0      0.0277.000000
 20.800000011.625000000      0.0      0.0277.000000
 21.800000011.750000000      0.0      0.0277.000000
 22.800000011.875000000      0.0      0.0277.000000
 23.8000000111.15625000      0.0      0.0277.000000
 24.8000000111.31250000      0.0      0.0277.000000
 25.8000000111.46875000      0.0      0.0277.000000
 26.8000000111.62500000      0.0      0.0277.000000
 27.8000000111.78125000      0.0      0.0277.000000
 28.8000000111.93750000      0.0      0.0277.000000
 29.8000000112.09375000      0.0      0.0277.000000
 30.8000000112.25000000      0.0      0.0277.000000
 31.8000000112.40625000      0.0      0.0277.000000
```

32.8000000112.56250000	0.0	0.0277.000000
33.8000000112.71875000	0.0	0.0277.000000
34.8000000112.87500000	0.0	0.0277.000000
35.8000000113.03125000	0.0	0.0277.000000
36.8000000113.18750000	0.0	0.0277.000000
37.8000000113.34375000	0.0	0.0277.000000
38.8000000113.50000000	0.0	0.0277.000000
39.8000000113.65625000	0.0	0.0277.000000
40.8000000113.81250000	0.0	0.0277.000000
41.8000000113.96875000	0.0	0.0277.000000
42.8000000114.12500000	0.0	0.0277.000000
43.8000000114.28125000	0.0	0.0277.000000
44.8000000114.43750000	0.0	0.0277.000000
45.8000000114.59375000	0.0	0.0277.000000
46.8000000114.75000000	0.0	0.0277.000000
47.8000000114.90625000	0.0	0.0277.000000
48.8000000115.06250000	0.0	0.0277.000000
49.8000000115.21875000	0.0	0.0277.000000
50.8000000115.37500000	0.0	0.0277.000000
51.8000000115.53125000	0.0	0.0277.000000
52.8000000115.68750000	0.0	0.0277.000000
53.8000000115.84375000	0.0	0.0277.000000
54.8000000116.12500000	0.0	0.0277.000000
55.8000000116.25000000	0.0	0.0277.000000
56.8000000116.37500000	0.0	0.0277.000000
57.8000000116.50000000	0.0	0.0277.000000
58.8000000116.62500000	0.0	0.0277.000000
59.8000000116.75000000	0.0	0.0277.000000
60.8000000116.87500000	0.0	0.0277.000000
61.8000000117.00000000	0.0	0.0277.000000
62.8000000117.12500000	0.0	0.0277.000000
63.8000000117.25000000	0.0	0.0277.000000
64.8000000117.37500000	0.0	0.0277.000000
65.8000000117.50000000	0.0	0.0277.000000
66.8000000117.62500000	0.0	0.0277.000000
67.8000000117.75000000	0.0	0.0277.000000
68.8000000117.87500000	0.0	0.0277.000000
69.8000000117.99999952	0.0	0.0277.000000
70.8000000118.12500000	0.0	0.0277.000000
71.8000000118.25000000	0.0	0.0277.000000
72.8000000118.37500000	0.0	0.0277.000000
73.8000000118.50000000	0.0	0.0277.000000
74.8000000118.62500000	0.0	0.0277.000000
75.8000000118.75000000	0.0	0.0277.000000
76.8000000118.87500000	0.0	0.0277.000000
77.8000000119.00000000	0.0	0.0277.000000
78.8000000119.12500000	0.0	0.0277.000000
79.8000000119.25000000	0.0	0.0277.000000
80.8000000119.37500000	0.0	0.0277.000000
81.8000000119.50000000	0.0	0.0277.000000
82.8000000119.62500000	0.0	0.0277.000000
83.8000000119.75000000	0.0	0.0277.000000
84.8000000119.87500095	0.0	0.0277.000000
85.80000001110.0000009	0.0	0.0277.000000
86.80000001110.1250009	0.0	0.0277.000000
87.80000001110.2500009	0.0	0.0277.000000
88.80000001110.3750009	0.0	0.0277.000000
89.80000001110.5000009	0.0	0.0277.000000
90.80000001110.6250009	0.0	0.0277.000000
91.80000001110.7500009	0.0	0.0277.000000
92.80000001110.8750009	0.0	0.0277.000000
93.80000001111.0000009	0.0	0.0277.000000
94.80000001111.1250009	0.0	0.0277.000000
95.80000001111.2500019	0.0	0.0277.000000
96.80000001111.3750019	0.0	0.0277.000000
97.80000001111.5000019	0.0	0.0277.000000
98.80000001111.6250019	0.0	0.0277.000000
99.80000001111.7500019	0.0	0.0277.000000
100.80000001111.8750019	0.0	0.0277.000000
101.80000001112.0000019	0.0	0.0277.000000
102.80000001112.1250019	0.0	0.0277.000000
103.80000001112.2500019	0.0	0.0277.000000
104.80000001112.3750019	0.0	0.0277.000000
105.80000001112.5000019	0.0	0.0277.000000
106.80000001112.6250028	0.0	0.0277.000000
107.80000001112.7500028	0.0	0.0277.000000
108.80000001112.8750028	0.0	0.0277.000000
109.80000001113.0000028	0.0	0.0277.000000
110.80000001113.1250028	0.0	0.0277.000000
111.80000001113.2500028	0.0	0.0277.000000
112.80000001113.3750028	0.0	0.0277.000000
113.80000001113.5000028	0.0	0.0277.000000
114.80000001113.6250028	0.0	0.0277.000000
115.80000001113.7500028	0.0	0.0277.000000
116.80000001113.8750038	0.0	0.0277.000000
117.80000001114.0000038	0.0	0.0277.000000
118.80000001114.1250038	0.0	0.0277.000000
119.80000001114.2500038	0.0	0.0277.000000
120.80000001114.3750038	0.0	0.0277.000000
121.80000001114.5000038	0.0	0.0277.000000
122.80000001114.6250038	0.0	0.0277.000000

```
123.80000001114.7500038	0.0	0.0277.000000
124.80000001114.8750038	0.0	0.0277.000000
125.80000001115.0000038	0.0	0.0277.000000
126.80000001115.1250038	0.0	0.0277.000000
127.80000001115.2500047	0.0	0.0277.000000
128.80000001115.3750047	0.0	0.0277.000000
129.69999998815.5000000	0.0	0.0277.000000
130.60000002315.5000000	0.0	0.0277.000000
131.50000000015.5000000	0.0	0.0277.000000
132.40000000515.5000000	0.0	0.0277.000000
133.30000001115.5000000	0.0	0.0277.000000
134.20000000215.5000000	0.0	0.0277.000000
135.10000000115.5000000	0.0	0.0277.000000
136	0.015.3750000	0.0	0.0277.000000
137	0.015.2500000	0.0	0.0277.000000
138	0.015.1250000	0.0	0.0277.000000
139	0.015.0000000	0.0	0.0277.000000
140	0.014.8750000	0.0	0.0277.000000
141	0.014.7500000	0.0	0.0277.000000
142	0.014.6250000	0.0	0.0277.000000
143	0.014.5000000	0.0	0.0277.000000
144	0.014.3750000	0.0	0.0277.000000
145	0.014.2500000	0.0	0.0277.000000
146	0.014.1250000	0.0	0.0277.000000
147	0.014.0000000	0.0	0.0277.000000
148	0.013.8750000	0.0	0.0277.000000
149	0.013.7500000	0.0	0.0277.000000
150	0.013.6250000	0.0	0.0277.000000
151	0.013.5000000	0.0	0.0277.000000
152	0.013.3750000	0.0	0.0277.000000
153	0.013.2500000	0.0	0.0277.000000
154	0.013.1250000	0.0	0.0277.000000
155	0.013.0000000	0.0	0.0277.000000
156	0.012.8750000	0.0	0.0277.000000
157	0.012.7500000	0.0	0.0277.000000
158	0.012.6250000	0.0	0.0277.000000
159	0.012.5000000	0.0	0.0277.000000
160	0.012.3750000	0.0	0.0277.000000
161	0.012.2500000	0.0	0.0277.000000
162	0.012.1250000	0.0	0.0277.000000
163	0.012.0000000	0.0	0.0277.000000
164	0.011.8750000	0.0	0.0277.000000
165	0.011.7500000	0.0	0.0277.000000
166	0.011.6249990	0.0	0.0277.000000
167	0.011.4999990	0.0	0.0277.000000
168	0.011.3749990	0.0	0.0277.000000
169	0.011.2499990	0.0	0.0277.000000
170	0.011.1249990	0.0	0.0277.000000
171	0.010.9999990	0.0	0.0277.000000
172	0.010.8749990	0.0	0.0277.000000
173	0.010.7499990	0.0	0.0277.000000
174	0.010.6249990	0.0	0.0277.000000
175	0.010.4999990	0.0	0.0277.000000
176	0.010.3749990	0.0	0.0277.000000
177	0.010.2499980	0.0	0.0277.000000
178	0.010.1249980	0.0	0.0277.000000
179	0.09.99999809	0.0	0.0277.000000
180	0.09.87499809	0.0	0.0277.000000
181	0.09.74999809	0.0	0.0277.000000
182	0.09.62499809	0.0	0.0277.000000
183	0.09.49999809	0.0	0.0277.000000
184	0.09.37499809	0.0	0.0277.000000
185	0.09.24999809	0.0	0.0277.000000
186	0.09.12499809	0.0	0.0277.000000
187	0.08.99999809	0.0	0.0277.000000
188	0.08.87499713	0.0	0.0277.000000
189	0.08.74999713	0.0	0.0277.000000
190	0.08.62499713	0.0	0.0277.000000
191	0.08.49999713	0.0	0.0277.000000
192	0.08.37499713	0.0	0.0277.000000
193	0.08.24999713	0.0	0.0277.000000
194	0.08.12499713	0.0	0.0277.000000
195	0.07.99999712	0.0	0.0277.000000
196	0.07.87499665	0.0	0.0277.000000
197	0.07.74999665	0.0	0.0277.000000
198	0.07.62499665	0.0	0.0277.000000
199	0.07.49999665	0.0	0.0277.000000
200	0.07.37499665	0.0	0.0277.000000
201	0.07.24999618	0.0	0.0277.000000
202	0.07.12499618	0.0	0.0277.000000
203	0.06.99999618	0.0	0.0277.000000
204	0.06.87499618	0.0	0.0277.000000
205	0.06.74999618	0.0	0.0277.000000
206	0.06.62499570	0.0	0.0277.000000
207	0.06.49999570	0.0	0.0277.000000
208	0.06.37499570	0.0	0.0277.000000
209	0.06.24999570	0.0	0.0277.000000
210	0.06.12499570	0.0	0.0277.000000
211	0.05.84375000	0.0	0.0277.000000
212	0.05.68750000	0.0	0.0277.000000
213	0.05.53125000	0.0	0.0277.000000
```

214	0.05.37500000	0.0	0.0277.000000
215	0.05.21875000	0.0	0.0277.000000
216	0.05.06250000	0.0	0.0277.000000
217	0.04.90625000	0.0	0.0277.000000
218	0.04.75000000	0.0	0.0277.000000
219	0.04.59375000	0.0	0.0277.000000
220	0.04.43750000	0.0	0.0277.000000
221	0.04.28125000	0.0	0.0277.000000
222	0.04.12500000	0.0	0.0277.000000
223	0.03.96875000	0.0	0.0277.000000
224	0.03.81250000	0.0	0.0277.000000
225	0.03.65625000	0.0	0.0277.000000
226	0.03.50000000	0.0	0.0277.000000
227	0.03.34375000	0.0	0.0277.000000
228	0.03.18750000	0.0	0.0277.000000
229	0.03.03125000	0.0	0.0277.000000
230	0.02.87500000	0.0	0.0277.000000
231	0.02.71875000	0.0	0.0277.000000
232	0.02.56250000	0.0	0.0277.000000
233	0.02.40625000	0.0	0.0277.000000
234	0.02.25000000	0.0	0.0277.000000
235	0.02.09375000	0.0	0.0277.000000
236	0.01.93750000	0.0	0.0277.000000
237	0.01.78125000	0.0	0.0277.000000
238	0.01.62500000	0.0	0.0277.000000
239	0.01.46875000	0.0	0.0277.000000
240	0.01.31250000	0.0	0.0277.000000
241	0.01.15625000	0.0	0.0277.000000
242	0.0.125000000	0.0	0.0277.000000
243	0.0.250000000	0.0	0.0277.000000
244	0.0.375000000	0.0	0.0277.000000
245	0.0.500000000	0.0	0.0277.000000
246	0.0.625000000	0.0	0.0277.000000
247	0.0.750000000	0.0	0.0277.000000
248	0.0.875000000	0.0	0.0277.000000

249.6999999881.00000000	0.0	0.0277.000000
250.6000000231.00000000	0.0	0.0277.000000
251.5000000001.00000000	0.0	0.0277.000000
252.4000000051.00000000	0.0	0.0277.000000
253.3000000111.00000000	0.0	0.0277.000000
254.2000000021.00000000	0.0	0.0277.000000
255.1000000011.00000000	0.0	0.0277.000000
256.6999999886.00000000	0.0	0.0277.000000
257.6000000236.00000000	0.0	0.0277.000000
258.5000000006.00000000	0.0	0.0277.000000
259.4000000056.00000000	0.0	0.0277.000000
260.3000000116.00000000	0.0	0.0277.000000
261.2000000026.00000000	0.0	0.0277.000000
262.1000000016.00000000	0.0	0.0277.000000
263.200000017.250000000	0.0	0.0277.000000
264.200000017.500000000	0.0	0.0277.000000
265.200000017.750000000	0.0	0.0277.000000
266.400000035.250000000	0.0	0.0277.000000
267.400000035.500000000	0.0	0.0277.000000
268.400000035.750000000	0.0	0.0277.000000
269.600000023.250000000	0.0	0.0277.000000
270.600000023.500000000	0.0	0.0277.000000
271.600000023.750000000	0.0	0.0277.000000
272.200000017.125000000	0.0	0.0277.000000
273.200000017.375000000	0.0	0.0277.000000
274.200000017.625000000	0.0	0.0277.000000
275.200000017.875000000	0.0	0.0277.000000
276.400000035.125000000	0.0	0.0277.000000
277.400000035.375000000	0.0	0.0277.000000
278.400000035.625000000	0.0	0.0277.000000
279.400000035.875000000	0.0	0.0277.000000
280.600000023.125000000	0.0	0.0277.000000
281.600000023.375000000	0.0	0.0277.000000
282.600000023.625000000	0.0	0.0277.000000
283.600000023.875000000	0.0	0.0277.000000
284.100000008.250000000	0.0	0.0277.000000
285.300000011.250000000	0.0	0.0277.000000
286.500000000.250000000	0.0	0.0277.000000
287.700000047.250000000	0.0	0.0277.000000
288.100000008.500000000	0.0	0.0277.000000
289.300000011.500000000	0.0	0.0277.000000
290.500000000.500000000	0.0	0.0277.000000
291.700000047.500000000	0.0	0.0277.000000
292.100000008.750000000	0.0	0.0277.000000
293.300000011.750000000	0.0	0.0277.000000
294.500000000.750000000	0.0	0.0277.000000
295.700000047.750000000	0.0	0.0277.000000
296.2000000171.31250000	0.0	0.0277.000000
297.2000000171.62500000	0.0	0.0277.000000
298.2000000171.93750000	0.0	0.0277.000000
299.2000000172.25000000	0.0	0.0277.000000
300.2000000172.56250000	0.0	0.0277.000000
301.2000000172.87500000	0.0	0.0277.000000
302.2000000173.18750000	0.0	0.0277.000000
303.2000000173.50000000	0.0	0.0277.000000
304.2000000173.81250000	0.0	0.0277.000000

305.2000000174.12500000	0.0	0.0277.000000
306.2000000174.43750000	0.0	0.0277.000000
307.2000000174.75000000	0.0	0.0277.000000
308.2000000175.06250000	0.0	0.0277.000000
309.2000000175.37500000	0.0	0.0277.000000
310.2000000175.68750000	0.0	0.0277.000000
311.4000000351.31250000	0.0	0.0277.000000
312.4000000351.62500000	0.0	0.0277.000000
313.4000000351.93750000	0.0	0.0277.000000
314.4000000352.25000000	0.0	0.0277.000000
315.4000000352.56250000	0.0	0.0277.000000
316.4000000352.87500000	0.0	0.0277.000000
317.4000000353.18750000	0.0	0.0277.000000
318.4000000353.50000000	0.0	0.0277.000000
319.4000000353.81250000	0.0	0.0277.000000
320.4000000354.12500000	0.0	0.0277.000000
321.4000000354.43750000	0.0	0.0277.000000
322.4000000354.75000000	0.0	0.0277.000000
323.4000000355.06250000	0.0	0.0277.000000
324.4000000355.37500000	0.0	0.0277.000000
325.4000000355.68750000	0.0	0.0277.000000
326.6000000231.31250000	0.0	0.0277.000000
327.6000000231.62500000	0.0	0.0277.000000
328.6000000231.93750000	0.0	0.0277.000000
329.6000000232.25000000	0.0	0.0277.000000
330.6000000232.56250000	0.0	0.0277.000000
331.6000000232.87500000	0.0	0.0277.000000
332.6000000233.18750000	0.0	0.0277.000000
333.6000000233.50000000	0.0	0.0277.000000
334.6000000233.81250000	0.0	0.0277.000000
335.6000000234.12500000	0.0	0.0277.000000
336.6000000234.43750000	0.0	0.0277.000000
337.6000000234.75000000	0.0	0.0277.000000
338.6000000235.06250000	0.0	0.0277.000000
339.6000000235.37500000	0.0	0.0277.000000
340.6000000235.68750000	0.0	0.0277.000000
341.2000000171.15625000	0.0	0.0277.000000
342.2000000171.46875000	0.0	0.0277.000000
343.2000000171.78125000	0.0	0.0277.000000
344.2000000172.09375000	0.0	0.0277.000000
345.2000000172.40625000	0.0	0.0277.000000
346.2000000172.71875000	0.0	0.0277.000000
347.2000000173.03125000	0.0	0.0277.000000
348.2000000173.34375000	0.0	0.0277.000000
349.2000000173.65625000	0.0	0.0277.000000
350.2000000173.96875000	0.0	0.0277.000000
351.2000000174.28125000	0.0	0.0277.000000
352.2000000174.59375000	0.0	0.0277.000000
353.2000000174.90625000	0.0	0.0277.000000
354.2000000175.21875000	0.0	0.0277.000000
355.2000000175.53125000	0.0	0.0277.000000
356.2000000175.84375000	0.0	0.0277.000000
357.4000000351.15625000	0.0	0.0277.000000
358.4000000351.46875000	0.0	0.0277.000000
359.4000000351.78125000	0.0	0.0277.000000
360.4000000352.09375000	0.0	0.0277.000000
361.4000000352.40625000	0.0	0.0277.000000
362.4000000352.71875000	0.0	0.0277.000000
363.4000000353.03125000	0.0	0.0277.000000
364.4000000353.34375000	0.0	0.0277.000000
365.4000000353.65625000	0.0	0.0277.000000
366.4000000353.96875000	0.0	0.0277.000000
367.4000000354.28125000	0.0	0.0277.000000
368.4000000354.59375000	0.0	0.0277.000000
369.4000000354.90625000	0.0	0.0277.000000
370.4000000355.21875000	0.0	0.0277.000000
371.4000000355.53125000	0.0	0.0277.000000
372.4000000355.84375000	0.0	0.0277.000000
373.6000000231.15625000	0.0	0.0277.000000
374.6000000231.46875000	0.0	0.0277.000000
375.6000000231.78125000	0.0	0.0277.000000
376.6000000232.09375000	0.0	0.0277.000000
377.6000000232.40625000	0.0	0.0277.000000
378.6000000232.71875000	0.0	0.0277.000000
379.6000000233.03125000	0.0	0.0277.000000
380.6000000233.34375000	0.0	0.0277.000000
381.6000000233.65625000	0.0	0.0277.000000
382.6000000233.96875000	0.0	0.0277.000000
383.6000000234.28125000	0.0	0.0277.000000
384.6000000234.59375000	0.0	0.0277.000000
385.6000000234.90625000	0.0	0.0277.000000
386.6000000235.21875000	0.0	0.0277.000000
387.6000000235.53125000	0.0	0.0277.000000
388.6000000235.84375000	0.0	0.0277.000000
389.1000000081.31250000	0.0	0.0277.000000
390.3000000111.31250000	0.0	0.0277.000000
391.5000000001.31250000	0.0	0.0277.000000
392.7000000471.31250000	0.0	0.0277.000000
393.1000000081.62500000	0.0	0.0277.000000
394.3000000111.62500000	0.0	0.0277.000000
395.5000000001.62500000	0.0	0.0277.000000

396.7000000471.62500000	0.0	0.0277.000000
397.1000000081.93750000	0.0	0.0277.000000
398.3000000111.93750000	0.0	0.0277.000000
399.5000000001.93750000	0.0	0.0277.000000
400.7000000471.93750000	0.0	0.0277.000000
401.1000000082.25000000	0.0	0.0277.000000
402.3000000112.25000000	0.0	0.0277.000000
403.5000000002.25000000	0.0	0.0277.000000
404.7000000472.25000000	0.0	0.0277.000000
405.1000000082.56250000	0.0	0.0277.000000
406.3000000112.56250000	0.0	0.0277.000000
407.5000000002.56250000	0.0	0.0277.000000
408.7000000472.56250000	0.0	0.0277.000000
409.1000000082.87500000	0.0	0.0277.000000
410.3000000112.87500000	0.0	0.0277.000000
411.5000000002.87500000	0.0	0.0277.000000
412.7000000472.87500000	0.0	0.0277.000000
413.1000000083.18750000	0.0	0.0277.000000
414.3000000113.18750000	0.0	0.0277.000000
415.5000000003.18750000	0.0	0.0277.000000
416.7000000473.18750000	0.0	0.0277.000000
417.1000000083.50000000	0.0	0.0277.000000
418.3000000113.50000000	0.0	0.0277.000000
419.5000000003.50000000	0.0	0.0277.000000
420.7000000473.50000000	0.0	0.0277.000000
421.1000000083.81250000	0.0	0.0277.000000
422.3000000113.81250000	0.0	0.0277.000000
423.5000000003.81250000	0.0	0.0277.000000
424.7000000473.81250000	0.0	0.0277.000000
425.1000000084.12500000	0.0	0.0277.000000
426.3000000114.12500000	0.0	0.0277.000000
427.5000000004.12500000	0.0	0.0277.000000
428.7000000474.12500000	0.0	0.0277.000000
429.1000000084.43750000	0.0	0.0277.000000
430.3000000114.43750000	0.0	0.0277.000000
431.5000000004.43750000	0.0	0.0277.000000
432.7000000474.43750000	0.0	0.0277.000000
433.1000000084.75000000	0.0	0.0277.000000
434.3000000114.75000000	0.0	0.0277.000000
435.5000000004.75000000	0.0	0.0277.000000
436.7000000474.75000000	0.0	0.0277.000000
437.1000000085.06250000	0.0	0.0277.000000
438.3000000115.06250000	0.0	0.0277.000000
439.5000000005.06250000	0.0	0.0277.000000
440.7000000475.06250000	0.0	0.0277.000000
441.1000000085.37500000	0.0	0.0277.000000
442.3000000115.37500000	0.0	0.0277.000000
443.5000000005.37500000	0.0	0.0277.000000
444.7000000475.37500000	0.0	0.0277.000000
445.1000000085.68750000	0.0	0.0277.000000
446.3000000115.68750000	0.0	0.0277.000000
447.5000000005.68750000	0.0	0.0277.000000
448.7000000475.68750000	0.0	0.0277.000000
449.2000000176.24999809	0.0	0.0277.000000
450.2000000176.49999712	0.0	0.0277.000000
451.2000000176.74999618	0.0	0.0277.000000
452.2000000176.99999665	0.0	0.0277.000000
453.2000000177.24999809	0.0	0.0277.000000
454.2000000177.49999809	0.0	0.0277.000000
455.2000000177.74999809	0.0	0.0277.000000
456.2000000177.99999809	0.0	0.0277.000000
457.2000000178.24999809	0.0	0.0277.000000
458.2000000178.49999809	0.0	0.0277.000000
459.2000000178.74999809	0.0	0.0277.000000
460.2000000178.99999809	0.0	0.0277.000000
461.2000000179.24999809	0.0	0.0277.000000
462.2000000179.49999809	0.0	0.0277.000000
463.2000000179.74999809	0.0	0.0277.000000
464.2000000179.99999904	0.0	0.0277.000000
465.20000001710.2499990	0.0	0.0277.000000
466.20000001710.5000000	0.0	0.0277.000000
467.20000001710.7500000	0.0	0.0277.000000
468.20000001711.0000000	0.0	0.0277.000000
469.20000001711.2500000	0.0	0.0277.000000
470.20000001711.5000000	0.0	0.0277.000000
471.20000001711.7500000	0.0	0.0277.000000
472.20000001712.0000000	0.0	0.0277.000000
473.20000001712.2500000	0.0	0.0277.000000
474.20000001712.5000000	0.0	0.0277.000000
475.20000001712.7500000	0.0	0.0277.000000
476.20000001713.0000000	0.0	0.0277.000000
477.20000001713.2500000	0.0	0.0277.000000
478.20000001713.5000000	0.0	0.0277.000000
479.20000001713.7500000	0.0	0.0277.000000
480.20000001714.0000000	0.0	0.0277.000000
481.20000001714.2500000	0.0	0.0277.000000
482.20000001714.5000000	0.0	0.0277.000000
483.20000001714.7500000	0.0	0.0277.000000
484.20000001715.0000000	0.0	0.0277.000000
485.20000001715.2500000	0.0	0.0277.000000
486.4000000356.24999903	0.0	0.0277.000000

487.4000000356.49999809	0.0	0.0277.000000
488.4000000356.74999809	0.0	0.0277.000000
489.4000000356.99999809	0.0	0.0277.000000
490.4000000357.24999903	0.0	0.0277.000000
491.4000000357.49999903	0.0	0.0277.000000
492.4000000357.74999903	0.0	0.0277.000000
493.4000000357.99999903	0.0	0.0277.000000
494.4000000358.24999809	0.0	0.0277.000000
495.4000000358.49999809	0.0	0.0277.000000
496.4000000358.74999809	0.0	0.0277.000000
497.4000000358.99999904	0.0	0.0277.000000
498.4000000359.24999904	0.0	0.0277.000000
499.4000000359.49999904	0.0	0.0277.000000
500.4000000359.74999904	0.0	0.0277.000000
501.40000003510.0000000	0.0	0.0277.000000
502.40000003510.2500000	0.0	0.0277.000000
503.40000003510.5000000	0.0	0.0277.000000
504.40000003510.7500000	0.0	0.0277.000000
505.40000003511.0000000	0.0	0.0277.000000
506.40000003511.2500000	0.0	0.0277.000000
507.40000003511.5000000	0.0	0.0277.000000
508.40000003511.7500000	0.0	0.0277.000000
509.40000003512.0000000	0.0	0.0277.000000
510.40000003512.2500000	0.0	0.0277.000000
511.40000003512.5000000	0.0	0.0277.000000
512.40000003512.7500000	0.0	0.0277.000000
513.40000003513.0000000	0.0	0.0277.000000
514.40000003513.2500000	0.0	0.0277.000000
515.40000003513.5000000	0.0	0.0277.000000
516.40000003513.7500000	0.0	0.0277.000000
517.40000003514.0000000	0.0	0.0277.000000
518.40000003514.2500000	0.0	0.0277.000000
519.40000003514.5000000	0.0	0.0277.000000
520.40000003514.7500000	0.0	0.0277.000000
521.40000003515.0000000	0.0	0.0277.000000
522.40000003515.2500000	0.0	0.0277.000000
523.6000000236.24999903	0.0	0.0277.000000
524.6000000236.49999903	0.0	0.0277.000000
525.6000000236.74999903	0.0	0.0277.000000
526.6000000236.99999903	0.0	0.0277.000000
527.6000000237.24999903	0.0	0.0277.000000
528.6000000237.49999903	0.0	0.0277.000000
529.6000000237.74999903	0.0	0.0277.000000
530.6000000237.99999903	0.0	0.0277.000000
531.6000000238.24999904	0.0	0.0277.000000
532.6000000238.49999904	0.0	0.0277.000000
533.6000000238.74999904	0.0	0.0277.000000
534.6000000239.00000000	0.0	0.0277.000000
535.6000000239.25000000	0.0	0.0277.000000
536.6000000239.50000000	0.0	0.0277.000000
537.6000000239.75000000	0.0	0.0277.000000
538.60000002310.0000000	0.0	0.0277.000000
539.60000002310.2500000	0.0	0.0277.000000
540.60000002310.5000000	0.0	0.0277.000000
541.60000002310.7500000	0.0	0.0277.000000
542.60000002311.0000000	0.0	0.0277.000000
543.60000002311.2500000	0.0	0.0277.000000
544.60000002311.5000000	0.0	0.0277.000000
545.60000002311.7500000	0.0	0.0277.000000
546.60000002312.0000000	0.0	0.0277.000000
547.60000002312.2500000	0.0	0.0277.000000
548.60000002312.5000000	0.0	0.0277.000000
549.60000002312.7500000	0.0	0.0277.000000
550.60000002313.0000000	0.0	0.0277.000000
551.60000002313.2500000	0.0	0.0277.000000
552.60000002313.5000000	0.0	0.0277.000000
553.60000002313.7500000	0.0	0.0277.000000
554.60000002314.0000000	0.0	0.0277.000000
555.60000002314.2500000	0.0	0.0277.000000
556.60000002314.5000000	0.0	0.0277.000000
557.60000002314.7500000	0.0	0.0277.000000
558.60000002315.0000000	0.0	0.0277.000000
559.60000002315.2500019	0.0	0.0277.000000
560.2000000176.12499903	0.0	0.0277.000000
561.2000000176.37499761	0.0	0.0277.000000
562.2000000176.62499665	0.0	0.0277.000000
563.2000000176.87499618	0.0	0.0277.000000
564.2000000177.12499712	0.0	0.0277.000000
565.2000000177.37499809	0.0	0.0277.000000
566.2000000177.62499809	0.0	0.0277.000000
567.2000000177.87499809	0.0	0.0277.000000
568.2000000178.12499809	0.0	0.0277.000000
569.2000000178.37499809	0.0	0.0277.000000
570.2000000178.62499809	0.0	0.0277.000000
571.2000000178.87499809	0.0	0.0277.000000
572.2000000179.12499809	0.0	0.0277.000000
573.2000000179.37499809	0.0	0.0277.000000
574.2000000179.62499809	0.0	0.0277.000000
575.2000000179.87499809	0.0	0.0277.000000
576.20000001710.1249990	0.0	0.0277.000000
577.20000001710.3750000	0.0	0.0277.000000

578.20000001710.6250000	0.0	0.0277.000000
579.20000001710.8750000	0.0	0.0277.000000
580.20000001711.1250000	0.0	0.0277.000000
581.20000001711.3750000	0.0	0.0277.000000
582.20000001711.6250000	0.0	0.0277.000000
583.20000001711.8750000	0.0	0.0277.000000
584.20000001712.1250000	0.0	0.0277.000000
585.20000001712.3750000	0.0	0.0277.000000
586.20000001712.6250000	0.0	0.0277.000000
587.20000001712.8750000	0.0	0.0277.000000
588.20000001713.1250000	0.0	0.0277.000000
589.20000001713.3750000	0.0	0.0277.000000
590.20000001713.6250000	0.0	0.0277.000000
591.20000001713.8750000	0.0	0.0277.000000
592.20000001714.1250000	0.0	0.0277.000000
593.20000001714.3750000	0.0	0.0277.000000
594.20000001714.6250000	0.0	0.0277.000000
595.20000001714.8750000	0.0	0.0277.000000
596.20000001715.1250000	0.0	0.0277.000000
597.20000001715.3750000	0.0	0.0277.000000
598.4000000356.12499952	0.0	0.0277.000000
599.4000000356.37499855	0.0	0.0277.000000
600.4000000356.62499809	0.0	0.0277.000000
601.4000000356.87499809	0.0	0.0277.000000
602.4000000357.12499855	0.0	0.0277.000000
603.4000000357.37499903	0.0	0.0277.000000
604.4000000357.62499903	0.0	0.0277.000000
605.4000000357.87499903	0.0	0.0277.000000
606.4000000358.12499809	0.0	0.0277.000000
607.4000000358.37499809	0.0	0.0277.000000
608.4000000358.62499809	0.0	0.0277.000000
609.4000000358.87499809	0.0	0.0277.000000
610.4000000359.12499904	0.0	0.0277.000000
611.4000000359.37499904	0.0	0.0277.000000
612.4000000359.62499904	0.0	0.0277.000000
613.4000000359.87500000	0.0	0.0277.000000
614.40000003510.1250000	0.0	0.0277.000000
615.40000003510.3750000	0.0	0.0277.000000
616.40000003510.6250000	0.0	0.0277.000000
617.40000003510.8750000	0.0	0.0277.000000
618.40000003511.1250000	0.0	0.0277.000000
619.40000003511.3750000	0.0	0.0277.000000
620.40000003511.6250000	0.0	0.0277.000000
621.40000003511.8750000	0.0	0.0277.000000
622.40000003512.1250000	0.0	0.0277.000000
623.40000003512.3750000	0.0	0.0277.000000
624.40000003512.6250000	0.0	0.0277.000000
625.40000003512.8750000	0.0	0.0277.000000
626.40000003513.1250000	0.0	0.0277.000000
627.40000003513.3750000	0.0	0.0277.000000
628.40000003513.6250000	0.0	0.0277.000000
629.40000003513.8750000	0.0	0.0277.000000
630.40000003514.1250000	0.0	0.0277.000000
631.40000003514.3750000	0.0	0.0277.000000
632.40000003514.6250000	0.0	0.0277.000000
633.40000003514.8750000	0.0	0.0277.000000
634.40000003515.1250000	0.0	0.0277.000000
635.40000003515.3750000	0.0	0.0277.000000
636.6000000236.12499952	0.0	0.0277.000000
637.6000000236.37499903	0.0	0.0277.000000
638.6000000236.62499903	0.0	0.0277.000000
639.6000000236.87499903	0.0	0.0277.000000
640.6000000237.12499903	0.0	0.0277.000000
641.6000000237.37499903	0.0	0.0277.000000
642.6000000237.62499903	0.0	0.0277.000000
643.6000000237.87499903	0.0	0.0277.000000
644.6000000238.12499904	0.0	0.0277.000000
645.6000000238.37499904	0.0	0.0277.000000
646.6000000238.62499904	0.0	0.0277.000000
647.6000000238.87500000	0.0	0.0277.000000
648.6000000239.12500000	0.0	0.0277.000000
649.6000000239.37500000	0.0	0.0277.000000
650.6000000239.62500000	0.0	0.0277.000000
651.6000000239.87500000	0.0	0.0277.000000
652.60000002310.1250000	0.0	0.0277.000000
653.60000002310.3750000	0.0	0.0277.000000
654.60000002310.6250000	0.0	0.0277.000000
655.60000002310.8750000	0.0	0.0277.000000
656.60000002311.1250000	0.0	0.0277.000000
657.60000002311.3750000	0.0	0.0277.000000
658.60000002311.6250000	0.0	0.0277.000000
659.60000002311.8750000	0.0	0.0277.000000
660.60000002312.1250000	0.0	0.0277.000000
661.60000002312.3750000	0.0	0.0277.000000
662.60000002312.6250000	0.0	0.0277.000000
663.60000002312.8750000	0.0	0.0277.000000
664.60000002313.1250000	0.0	0.0277.000000
665.60000002313.3750000	0.0	0.0277.000000
666.60000002313.6250000	0.0	0.0277.000000
667.60000002313.8750000	0.0	0.0277.000000
668.60000002314.1250000	0.0	0.0277.000000

669.60000002314.3750000	0.0	0.0277.000000
670.60000002314.6250000	0.0	0.0277.000000
671.60000002314.8750000	0.0	0.0277.000000
672.60000002315.1250009	0.0	0.0277.000000
673.60000002315.3750009	0.0	0.0277.000000
674.1000000086.24999712	0.0	0.0277.000000
675.3000000116.24999855	0.0	0.0277.000000
676.5000000006.24999903	0.0	0.0277.000000
677.7000000476.24999952	0.0	0.0277.000000
678.1000000086.49999618	0.0	0.0277.000000
679.3000000116.49999761	0.0	0.0277.000000
680.5000000006.49999855	0.0	0.0277.000000
681.7000000476.49999952	0.0	0.0277.000000
682.1000000086.74999618	0.0	0.0277.000000
683.3000000116.74999712	0.0	0.0277.000000
684.5000000006.74999855	0.0	0.0277.000000
685.7000000476.74999952	0.0	0.0277.000000
686.1000000086.99999618	0.0	0.0277.000000
687.3000000116.99999712	0.0	0.0277.000000
688.5000000006.99999855	0.0	0.0277.000000
689.7000000476.99999952	0.0	0.0277.000000
690.1000000087.24999712	0.0	0.0277.000000
691.3000000117.24999855	0.0	0.0277.000000
692.5000000007.24999903	0.0	0.0277.000000
693.7000000477.24999952	0.0	0.0277.000000
694.1000000087.49999712	0.0	0.0277.000000
695.3000000117.49999855	0.0	0.0277.000000
696.5000000007.49999903	0.0	0.0277.000000
697.7000000477.49999952	0.0	0.0277.000000
698.1000000087.74999712	0.0	0.0277.000000
699.3000000117.74999855	0.0	0.0277.000000
700.5000000007.74999903	0.0	0.0277.000000
701.7000000477.74999952	0.0	0.0277.000000
702.1000000087.99999761	0.0	0.0277.000000
703.3000000117.99999855	0.0	0.0277.000000
704.5000000007.99999903	0.0	0.0277.000000
705.7000000477.99999903	0.0	0.0277.000000
706.1000000088.24999809	0.0	0.0277.000000
707.3000000118.24999809	0.0	0.0277.000000
708.5000000008.24999809	0.0	0.0277.000000
709.7000000478.25000000	0.0	0.0277.000000
710.1000000088.49999809	0.0	0.0277.000000
711.3000000118.49999809	0.0	0.0277.000000
712.5000000008.49999809	0.0	0.0277.000000
713.7000000478.50000000	0.0	0.0277.000000
714.1000000088.74999809	0.0	0.0277.000000
715.3000000118.74999809	0.0	0.0277.000000
716.5000000008.74999809	0.0	0.0277.000000
717.7000000478.75000000	0.0	0.0277.000000
718.1000000088.99999809	0.0	0.0277.000000
719.3000000118.99999809	0.0	0.0277.000000
720.5000000009.00000000	0.0	0.0277.000000
721.7000000479.00000000	0.0	0.0277.000000
722.1000000089.24999809	0.0	0.0277.000000
723.3000000119.24999809	0.0	0.0277.000000
724.5000000009.25000000	0.0	0.0277.000000
725.7000000479.25000000	0.0	0.0277.000000
726.1000000089.49999809	0.0	0.0277.000000
727.3000000119.49999809	0.0	0.0277.000000
728.5000000009.50000000	0.0	0.0277.000000
729.7000000479.50000000	0.0	0.0277.000000
730.1000000089.74999809	0.0	0.0277.000000
731.3000000119.74999809	0.0	0.0277.000000
732.5000000009.75000000	0.0	0.0277.000000
733.7000000479.75000000	0.0	0.0277.000000
734.1000000089.99999809	0.0	0.0277.000000
735.30000001110.0000000	0.0	0.0277.000000
736.50000000010.0000000	0.0	0.0277.000000
737.70000004710.0000000	0.0	0.0277.000000
738.10000000810.2499980	0.0	0.0277.000000
739.30000001110.2500000	0.0	0.0277.000000
740.50000000010.2500000	0.0	0.0277.000000
741.70000004710.2500000	0.0	0.0277.000000
742.10000000810.5000000	0.0	0.0277.000000
743.30000001110.5000000	0.0	0.0277.000000
744.50000000010.5000000	0.0	0.0277.000000
745.70000004710.5000000	0.0	0.0277.000000
746.10000000810.7500000	0.0	0.0277.000000
747.30000001110.7500000	0.0	0.0277.000000
748.50000000010.7500000	0.0	0.0277.000000
749.70000004710.7500000	0.0	0.0277.000000
750.10000000811.0000000	0.0	0.0277.000000
751.30000001111.0000000	0.0	0.0277.000000
752.50000000011.0000000	0.0	0.0277.000000
753.70000004711.0000000	0.0	0.0277.000000
754.10000000811.2500000	0.0	0.0277.000000
755.30000001111.2500000	0.0	0.0277.000000
756.50000000011.2500000	0.0	0.0277.000000
757.70000004711.2500009	0.0	0.0277.000000
758.10000000811.5000000	0.0	0.0277.000000
759.30000001111.5000000	0.0	0.0277.000000

```
  760.50000000011.5000000      0.0      0.0277.000000
  761.70000004711.5000009      0.0      0.0277.000000
  762.10000000811.7500000      0.0      0.0277.000000
  763.30000001111.7500000      0.0      0.0277.000000
  764.50000000011.7500000      0.0      0.0277.000000
  765.70000004711.7500009      0.0      0.0277.000000
  766.10000000812.0000000      0.0      0.0277.000000
  767.30000001112.0000000      0.0      0.0277.000000
  768.50000000012.0000000      0.0      0.0277.000000
  769.70000004712.0000009      0.0      0.0277.000000
  770.10000000812.2500000      0.0      0.0277.000000
  771.30000001112.2500000      0.0      0.0277.000000
  772.50000000012.2500000      0.0      0.0277.000000
  773.70000004712.2500009      0.0      0.0277.000000
  774.10000000812.5000000      0.0      0.0277.000000
  775.30000001112.5000000      0.0      0.0277.000000
  776.50000000012.5000000      0.0      0.0277.000000
  777.70000004712.5000009      0.0      0.0277.000000
  778.10000000812.7500000      0.0      0.0277.000000
  779.30000001112.7500000      0.0      0.0277.000000
  780.50000000012.7500000      0.0      0.0277.000000
  781.70000004712.7500019      0.0      0.0277.000000
  782.10000000813.0000000      0.0      0.0277.000000
  783.30000001113.0000000      0.0      0.0277.000000
  784.50000000013.0000000      0.0      0.0277.000000
  785.70000004713.0000019      0.0      0.0277.000000
  786.10000000813.2500000      0.0      0.0277.000000
  787.30000001113.2500000      0.0      0.0277.000000
  788.50000000013.2500000      0.0      0.0277.000000
  789.70000004713.2500019      0.0      0.0277.000000
  790.10000000813.5000000      0.0      0.0277.000000
  791.30000001113.5000000      0.0      0.0277.000000
  792.50000000013.5000000      0.0      0.0277.000000
  793.70000004713.5000019      0.0      0.0277.000000
  794.10000000813.7500000      0.0      0.0277.000000
  795.30000001113.7500000      0.0      0.0277.000000
  796.50000000013.7500000      0.0      0.0277.000000
  797.70000004713.7500019      0.0      0.0277.000000
  798.10000000814.0000000      0.0      0.0277.000000
  799.30000001114.0000000      0.0      0.0277.000000
  800.50000000014.0000000      0.0      0.0277.000000
  801.70000004714.0000019      0.0      0.0277.000000
  802.10000000814.2500000      0.0      0.0277.000000
  803.30000001114.2500000      0.0      0.0277.000000
  804.50000000014.2500000      0.0      0.0277.000000
  805.70000004714.2500019      0.0      0.0277.000000
  806.10000000814.5000000      0.0      0.0277.000000
  807.30000001114.5000000      0.0      0.0277.000000
  808.50000000014.5000000      0.0      0.0277.000000
  809.70000004714.5000019      0.0      0.0277.000000
  810.10000000814.7500000      0.0      0.0277.000000
  811.30000001114.7500000      0.0      0.0277.000000
  812.50000000014.7500000      0.0      0.0277.000000
  813.70000004714.7500019      0.0      0.0277.000000
  814.10000000815.0000000      0.0      0.0277.000000
  815.30000001115.0000000      0.0      0.0277.000000
  816.50000000015.0000000      0.0      0.0277.000000
  817.70000004715.0000019      0.0      0.0277.000000
  818.10000000815.2500000      0.0      0.0277.000000
  819.30000001115.2500000      0.0      0.0277.000000
  820.50000000015.2500009      0.0      0.0277.000000
  821.70000004715.2500038      0.0      0.0277.000000
GRAVI
        -9.81
RENUM
  210   0   0   0   2      0.
FIXED
    1  252
    2   1   2  252
    3   1 -821
    4   1 -821
    5   1 -821

FORCE

COLAW
    1   1
    0   1
   3.33E10     0.2     2500.
    2  171
    0   0   0   0   1   0   0   1   1   1   0   0   0   1
    1.E-16
     0.12      0.     293.     1.E4     1.E5
     0.001    0.019    1000.  4.54E-10    2.E-4      0.6      0.
     4186.     0.      0.
    1.8E-5     0.     1.18      0.      0.     1000.      0.
    1.2E-5     1.7      0.     930.      0.
       0.      0.      0.
       0.      0.      0.
       0.      0.      0.      0.      0.      0.      0.
       0.      0.      0.      0.      0.
```

```
    0.    0.    2.    3.
  3  95  spinta attiva lato terreno
  6  0
    0.    0.    0.    0.
  6.73E4    0.    0.    0.
  4  95  spinta passiva lato terreno
  6  0
  2.30E6    0.    0.    0.
  2.46E6    0.    0.    0.
  5  95   spinta passiva lato scavo
  6  0
  7.94E5    0.    0.    0.
    0.    0.    0.    0.
  6  95   spinta attiva lato scavo
  6  0
  2.81E4    0.    0.    0.
  2.34E4    0.    0.    0.
MWAT2
  16  0  1
-2.046E+05   13200   0.25    0.
  8  4  1  8  4  2
  1  9  10 272 263 284 243 242
  8  4  1  8  4  2
 243 284 263 273 264 288 245 244
  8  4  1  8  4  2
 245 288 264 274 265 292 247 246
  8  4  1  8  4  2
 247 292 265 275 254 255  8 248
  8  4  1  8  4  2
  10  11  12 276 266 285 263 272
  8  4  1  8  4  2
 263 285 266 277 267 289 264 273
  8  4  1  8  4  2
 264 289 267 278 268 293 265 274
  8  4  1  8  4  2
 265 293 268 279 252 253 254 275
  8  4  1  8  4  2
  12  13  14 280 269 286 266 276
  8  4  1  8  4  2
 266 286 269 281 270 290 267 277
  8  4  1  8  4  2
 267 290 270 282 271 294 268 278
  8  4  1  8  4  2
 268 294 271 283 250 251 252 279
  8  4  1  8  4  2
  14  15  2  16  17 287 269 280
  8  4  1  8  4  2
 269 287  17  18  19 291 270 281
  8  4  1  8  4  2
 270 291  19  20  21 295 271 282
  8  4  1  8  4  2
 271 295  21  22  3 249 250 283
MWAT2
  64  0  1
-2.046E+05   13200   0.25    0.
  8  4  1  8  4  2
  8 255 254 341 296 389 240 241
  8  4  1  8  4  2
 240 389 296 342 297 393 238 239
  8  4  1  8  4  2
 238 393 297 343 298 397 236 237
  8  4  1  8  4  2
 236 397 298 344 299 401 234 235
  8  4  1  8  4  2
 234 401 299 345 300 405 232 233
  8  4  1  8  4  2
 232 405 300 346 301 409 230 231
  8  4  1  8  4  2
 230 409 301 347 302 413 228 229
  8  4  1  8  4  2
 228 413 302 348 303 417 226 227
  8  4  1  8  4  2
 226 417 303 349 304 421 224 225
  8  4  1  8  4  2
 224 421 304 350 305 425 222 223
  8  4  1  8  4  2
 222 425 305 351 306 429 220 221
  8  4  1  8  4  2
 220 429 306 352 307 433 218 219
  8  4  1  8  4  2
 218 433 307 353 308 437 216 217
  8  4  1  8  4  2
 216 437 308 354 309 441 214 215
  8  4  1  8  4  2
 214 441 309 355 310 445 212 213
  8  4  1  8  4  2
 212 445 310 356 261 262  7 211
  8  4  1  8  4  2
 254 253 252 357 311 390 296 341
  8  4  1  8  4  2
 296 390 311 358 312 394 297 342
```

```
 8  4  1  8  4  2
297 394 312 359 313 398 298 343
 8  4  1  8  4  2
298 398 313 360 314 402 299 344
 8  4  1  8  4  2
299 402 314 361 315 406 300 345
 8  4  1  8  4  2
300 406 315 362 316 410 301 346
 8  4  1  8  4  2
301 410 316 363 317 414 302 347
 8  4  1  8  4  2
302 414 317 364 318 418 303 348
 8  4  1  8  4  2
303 418 318 365 319 422 304 349
 8  4  1  8  4  2
304 422 319 366 320 426 305 350
 8  4  1  8  4  2
305 426 320 367 321 430 306 351
 8  4  1  8  4  2
306 430 321 368 322 434 307 352
 8  4  1  8  4  2
307 434 322 369 323 438 308 353
 8  4  1  8  4  2
308 438 323 370 324 442 309 354
 8  4  1  8  4  2
309 442 324 371 325 446 310 355
 8  4  1  8  4  2
310 446 325 372 259 260 261 356
 8  4  1  8  4  2
252 251 250 373 326 391 311 357
 8  4  1  8  4  2
311 391 326 374 327 395 312 358
 8  4  1  8  4  2
312 395 327 375 328 399 313 359
 8  4  1  8  4  2
313 399 328 376 329 403 314 360
 8  4  1  8  4  2
314 403 329 377 330 407 315 361
 8  4  1  8  4  2
315 407 330 378 331 411 316 362
 8  4  1  8  4  2
316 411 331 379 332 415 317 363
 8  4  1  8  4  2
317 415 332 380 333 419 318 364
 8  4  1  8  4  2
318 419 333 381 334 423 319 365
 8  4  1  8  4  2
319 423 334 382 335 427 320 366
 8  4  1  8  4  2
320 427 335 383 336 431 321 367
 8  4  1  8  4  2
321 431 336 384 337 435 322 368
 8  4  1  8  4  2
322 435 337 385 338 439 323 369
 8  4  1  8  4  2
323 439 338 386 339 443 324 370
 8  4  1  8  4  2
324 443 339 387 340 447 325 371
 8  4  1  8  4  2
325 447 340 388 257 258 259 372
 8  4  1  8  4  2
250 249   3  23  24 392 326 373
 8  4  1  8  4  2
326 392  24  25  26 396 327 374
 8  4  1  8  4  2
327 396  26  27  28 400 328 375
 8  4  1  8  4  2
328 400  28  29  30 404 329 376
 8  4  1  8  4  2
329 404  30  31  32 408 330 377
 8  4  1  8  4  2
330 408  32  33  34 412 331 378
 8  4  1  8  4  2
331 412  34  35  36 416 332 379
 8  4  1  8  4  2
332 416  36  37  38 420 333 380
 8  4  1  8  4  2
333 420  38  39  40 424 334 381
 8  4  1  8  4  2
334 424  40  41  42 428 335 382
 8  4  1  8  4  2
335 428  42  43  44 432 336 383
 8  4  1  8  4  2
336 432  44  45  46 436 337 384
 8  4  1  8  4  2
337 436  46  47  48 440 338 385
 8  4  1  8  4  2
338 440  48  49  50 444 339 386
 8  4  1  8  4  2
339 444  50  51  52 448 340 387
 8  4  1  8  4  2
```

```
 340 448  52  53   4 256 257 388
MWAT2
 152   0   1
-2.046E+05    13200     0.25      0.
   8   4   1   8   4   2
   7  262  261  560  449  674  209  210
   8   4   1   8   4   2
 209 674 449 561 450 678 207 208
   8   4   1   8   4   2
 207 678 450 562 451 682 205 206
   8   4   1   8   4   2
 205 682 451 563 452 686 203 204
   8   4   1   8   4   2
 203 686 452 564 453 690 201 202
   8   4   1   8   4   2
 201 690 453 565 454 694 199 200
   8   4   1   8   4   2
 199 694 454 566 455 698 197 198
   8   4   1   8   4   2
 197 698 455 567 456 702 195 196
   8   4   1   8   4   2
 195 702 456 568 457 706 193 194
   8   4   1   8   4   2
 193 706 457 569 458 710 191 192
   8   4   1   8   4   2
 191 710 458 570 459 714 189 190
   8   4   1   8   4   2
 189 714 459 571 460 718 187 188
   8   4   1   8   4   2
 187 718 460 572 461 722 185 186
   8   4   1   8   4   2
 185 722 461 573 462 726 183 184
   8   4   1   8   4   2
 183 726 462 574 463 730 181 182
   8   4   1   8   4   2
 181 730 463 575 464 734 179 180
   8   4   1   8   4   2
 179 734 464 576 465 738 177 178
   8   4   1   8   4   2
 177 738 465 577 466 742 175 176
   8   4   1   8   4   2
 175 742 466 578 467 746 173 174
   8   4   1   8   4   2
 173 746 467 579 468 750 171 172
   8   4   1   8   4   2
 171 750 468 580 469 754 169 170
   8   4   1   8   4   2
 169 754 469 581 470 758 167 168
   8   4   1   8   4   2
 167 758 470 582 471 762 165 166
   8   4   1   8   4   2
 165 762 471 583 472 766 163 164
   8   4   1   8   4   2
 163 766 472 584 473 770 161 162
   8   4   1   8   4   2
 161 770 473 585 474 774 159 160
   8   4   1   8   4   2
 159 774 474 586 475 778 157 158
   8   4   1   8   4   2
 157 778 475 587 476 782 155 156
   8   4   1   8   4   2
 155 782 476 588 477 786 153 154
   8   4   1   8   4   2
 153 786 477 589 478 790 151 152
   8   4   1   8   4   2
 151 790 478 590 479 794 149 150
   8   4   1   8   4   2
 149 794 479 591 480 798 147 148
   8   4   1   8   4   2
 147 798 480 592 481 802 145 146
   8   4   1   8   4   2
 145 802 481 593 482 806 143 144
   8   4   1   8   4   2
 143 806 482 594 483 810 141 142
   8   4   1   8   4   2
 141 810 483 595 484 814 139 140
   8   4   1   8   4   2
 139 814 484 596 485 818 137 138
   8   4   1   8   4   2
 137 818 485 597 134 135   6 136
   8   4   1   8   4   2
 261 260 259 598 486 675 449 560
   8   4   1   8   4   2
 449 675 486 599 487 679 450 561
   8   4   1   8   4   2
 450 679 487 600 488 683 451 562
   8   4   1   8   4   2
 451 683 488 601 489 687 452 563
   8   4   1   8   4   2
 452 687 489 602 490 691 453 564
   8   4   1   8   4   2
```

```
453 691 490 603 491 695 454 565
 8  4  1  8  4  2
454 695 491 604 492 699 455 566
 8  4  1  8  4  2
455 699 492 605 493 703 456 567
 8  4  1  8  4  2
456 703 493 606 494 707 457 568
 8  4  1  8  4  2
457 707 494 607 495 711 458 569
 8  4  1  8  4  2
458 711 495 608 496 715 459 570
 8  4  1  8  4  2
459 715 496 609 497 719 460 571
 8  4  1  8  4  2
460 719 497 610 498 723 461 572
 8  4  1  8  4  2
461 723 498 611 499 727 462 573
 8  4  1  8  4  2
462 727 499 612 500 731 463 574
 8  4  1  8  4  2
463 731 500 613 501 735 464 575
 8  4  1  8  4  2
464 735 501 614 502 739 465 576
 8  4  1  8  4  2
465 739 502 615 503 743 466 577
 8  4  1  8  4  2
466 743 503 616 504 747 467 578
 8  4  1  8  4  2
467 747 504 617 505 751 468 579
 8  4  1  8  4  2
468 751 505 618 506 755 469 580
 8  4  1  8  4  2
469 755 506 619 507 759 470 581
 8  4  1  8  4  2
470 759 507 620 508 763 471 582
 8  4  1  8  4  2
471 763 508 621 509 767 472 583
 8  4  1  8  4  2
472 767 509 622 510 771 473 584
 8  4  1  8  4  2
473 771 510 623 511 775 474 585
 8  4  1  8  4  2
474 775 511 624 512 779 475 586
 8  4  1  8  4  2
475 779 512 625 513 783 476 587
 8  4  1  8  4  2
476 783 513 626 514 787 477 588
 8  4  1  8  4  2
477 787 514 627 515 791 478 589
 8  4  1  8  4  2
478 791 515 628 516 795 479 590
 8  4  1  8  4  2
479 795 516 629 517 799 480 591
 8  4  1  8  4  2
480 799 517 630 518 803 481 592
 8  4  1  8  4  2
481 803 518 631 519 807 482 593
 8  4  1  8  4  2
482 807 519 632 520 811 483 594
 8  4  1  8  4  2
483 811 520 633 521 815 484 595
 8  4  1  8  4  2
484 815 521 634 522 819 485 596
 8  4  1  8  4  2
485 819 522 635 132 133 134 597
 8  4  1  8  4  2
259 258 257 636 523 676 486 598
 8  4  1  8  4  2
486 676 523 637 524 680 487 599
 8  4  1  8  4  2
487 680 524 638 525 684 488 600
 8  4  1  8  4  2
488 684 525 639 526 688 489 601
 8  4  1  8  4  2
489 688 526 640 527 692 490 602
 8  4  1  8  4  2
490 692 527 641 528 696 491 603
 8  4  1  8  4  2
491 696 528 642 529 700 492 604
 8  4  1  8  4  2
492 700 529 643 530 704 493 605
 8  4  1  8  4  2
493 704 530 644 531 708 494 606
 8  4  1  8  4  2
494 708 531 645 532 712 495 607
 8  4  1  8  4  2
495 712 532 646 533 716 496 608
 8  4  1  8  4  2
496 716 533 647 534 720 497 609
 8  4  1  8  4  2
497 720 534 648 535 724 498 610
```

```
 8   4   1   8   4   2
498 724 535 649 536 728 499 611
 8   4   1   8   4   2
499 728 536 650 537 732 500 612
 8   4   1   8   4   2
500 732 537 651 538 736 501 613
 8   4   1   8   4   2
501 736 538 652 539 740 502 614
 8   4   1   8   4   2
502 740 539 653 540 744 503 615
 8   4   1   8   4   2
503 744 540 654 541 748 504 616
 8   4   1   8   4   2
504 748 541 655 542 752 505 617
 8   4   1   8   4   2
505 752 542 656 543 756 506 618
 8   4   1   8   4   2
506 756 543 657 544 760 507 619
 8   4   1   8   4   2
507 760 544 658 545 764 508 620
 8   4   1   8   4   2
508 764 545 659 546 768 509 621
 8   4   1   8   4   2
509 768 546 660 547 772 510 622
 8   4   1   8   4   2
510 772 547 661 548 776 511 623
 8   4   1   8   4   2
511 776 548 662 549 780 512 624
 8   4   1   8   4   2
512 780 549 663 550 784 513 625
 8   4   1   8   4   2
513 784 550 664 551 788 514 626
 8   4   1   8   4   2
514 788 551 665 552 792 515 627
 8   4   1   8   4   2
515 792 552 666 553 796 516 628
 8   4   1   8   4   2
516 796 553 667 554 800 517 629
 8   4   1   8   4   2
517 800 554 668 555 804 518 630
 8   4   1   8   4   2
518 804 555 669 556 808 519 631
 8   4   1   8   4   2
519 808 556 670 557 812 520 632
 8   4   1   8   4   2
520 812 557 671 558 816 521 633
 8   4   1   8   4   2
521 816 558 672 559 820 522 634
 8   4   1   8   4   2
522 820 559 673 130 131 132 635
 8   4   1   8   4   2
257 256   4  54  55 677 523 636
 8   4   1   8   4   2
523 677  55  56  57 681 524 637
 8   4   1   8   4   2
524 681  57  58  59 685 525 638
 8   4   1   8   4   2
525 685  59  60  61 689 526 639
 8   4   1   8   4   2
526 689  61  62  63 693 527 640
 8   4   1   8   4   2
527 693  63  64  65 697 528 641
 8   4   1   8   4   2
528 697  65  66  67 701 529 642
 8   4   1   8   4   2
529 701  67  68  69 705 530 643
 8   4   1   8   4   2
530 705  69  70  71 709 531 644
 8   4   1   8   4   2
531 709  71  72  73 713 532 645
 8   4   1   8   4   2
532 713  73  74  75 717 533 646
 8   4   1   8   4   2
533 717  75  76  77 721 534 647
 8   4   1   8   4   2
534 721  77  78  79 725 535 648
 8   4   1   8   4   2
535 725  79  80  81 729 536 649
 8   4   1   8   4   2
536 729  81  82  83 733 537 650
 8   4   1   8   4   2
537 733  83  84  85 737 538 651
 8   4   1   8   4   2
538 737  85  86  87 741 539 652
 8   4   1   8   4   2
539 741  87  88  89 745 540 653
 8   4   1   8   4   2
540 745  89  90  91 749 541 654
 8   4   1   8   4   2
541 749  91  92  93 753 542 655
 8   4   1   8   4   2
```

```
542 753  93  94  95 757 543 656
  8   4   1   8   4   2
543 757  95  96  97 761 544 657
  8   4   1   8   4   2
544 761  97  98  99 765 545 658
  8   4   1   8   4   2
545 765  99 100 101 769 546 659
  8   4   1   8   4   2
546 769 101 102 103 773 547 660
  8   4   1   8   4   2
547 773 103 104 105 777 548 661
  8   4   1   8   4   2
548 777 105 106 107 781 549 662
  8   4   1   8   4   2
549 781 107 108 109 785 550 663
  8   4   1   8   4   2
550 785 109 110 111 789 551 664
  8   4   1   8   4   2
551 789 111 112 113 793 552 665
  8   4   1   8   4   2
552 793 113 114 115 797 553 666
  8   4   1   8   4   2
553 797 115 116 117 801 554 667
  8   4   1   8   4   2
554 801 117 118 119 805 555 668
  8   4   1   8   4   2
555 805 119 120 121 809 556 669
  8   4   1   8   4   2
556 809 121 122 123 813 557 670
  8   4   1   8   4   2
557 813 123 124 125 817 558 671
  8   4   1   8   4   2
558 817 125 126 127 821 559 672
  8   4   1   8   4   2
559 821 127 128   5 129 130 673
LICHA
 54   0
  2   3
  6 136 137
  2   3
137 138 139
  2   3
139 140 141
  2   3
141 142 143
  2   3
143 144 145
  2   3
145 146 147
  2   3
147 148 149
  2   3
149 150 151
  2   3
151 152 153
  2   3
153 154 155
  2   3
155 156 157
  2   3
157 158 159
  2   3
159 160 161
  2   3
161 162 163
  2   3
163 164 165
  2   3
165 166 167
  2   3
167 168 169
  2   3
169 170 171
  2   3
171 172 173
  2   3
173 174 175
  2   3
175 176 177
  2   3
177 178 179
  2   3
179 180 181
  2   3
181 182 183
  2   3
183 184 185
  2   3
185 186 187
  2   3
187 188 189
```

```
  2   3
 189  190  191
  2   3
 191  192  193
  2   3
 193  194  195
  2   3
 195  196  197
  2   3
 197  198  199
  2   3
 199  200  201
  2   3
 201  202  203
  2   3
 203  204  205
  2   3
 205  206  207
  2   3
 207  208  209
  2   3
 209  210    7
  2   3
  7  211  212
  2   3
 212  213  214
  2   3
 214  215  216
  2   3
 216  217  218
  2   3
 218  219  220
  2   3
 220  221  222
  2   3
 222  223  224
  2   3
 224  225  226
  2   3
 226  227  228
  2   3
 228  229  230
  2   3
 230  231  232
  2   3
 232  233  234
  2   3
 234  235  236
  2   3
 236  237  238
  2   3
 238  239  240
  2   3
 240  241    8
LICHA
  4   0
  2   4
  8  248  247
  2   4
 247  246  245
  2   4
 245  244  243
  2   4
 243  242    1
LICHA
 16   0
  2   5
  3   23   24
  2   5
 24   25   26
  2   5
 26   27   28
  2   5
 28   29   30
  2   5
 30   31   32
  2   5
 32   33   34
  2   5
 34   35   36
  2   5
 36   37   38
  2   5
 38   39   40
  2   5
 40   41   42
  2   5
 42   43   44
  2   5
 44   45   46
  2   5
```

```
  46  47  48
  2   5
  48  49  50
  2   5
  50  51  52
  2   5
  52  53   4
LICHA
  4   0
  2   6
  2  16  17
  2   6
  17  18  19
  2   6
  19  20  21
  2   6
  21  22   3
```

***Loading File*: steps of calculation (1-60 days)**

```
  2   3   4   8   0   0   0

  1  -1 9999   1   1   1   2   1  30   0   0   1
  3   0      0   0   0   0   0   0   0
 1.0E-05     1.0      0.0      0.0      0.0      0.0      0.0
    2.0  5.2E+06    0.001     10.      0.0      0.0


 1.30E+06      0.0      0.0    0.001    0.001   0   0   0   0   1

0.00000000      0.0   0
1300000.00      0.0   0
2600000.00      0.0   0
3900000.00      0.0   0
5200000.00      0.0   0
```

***Loading File*: steps of calculation (60- 120 days)**

```
  3   2   4  18   0   0   0

  1  -1 9999   1   1   1   2   1  30   0   0   1
  3   0      0   0   0   0   0   0   0
 1.0E-05     1.0      0.0      0.0      0.0      0.0      0.0
    1.0   1.00E7    0.001     10.0      0.0      0.0


  5.20E6     0.1      0.0    0.001    0.001   0   0   0   0   1

5200000.00      0.0   0
6500000.00      0.0   0
7800000.00      0.0   0
8900000.00      0.0   0
10000000.0      0.0   0
```

***Loading File*: steps of calculation (120-240 days)**

```
  3   2   4  18   0   0   0

  1  -1 9999   1   1   1   2   1  30   0   0   1
  3   0      0   0   0   0   0   0   0
 1.0E-05     1.0      0.0      0.0      0.0      0.0      0.0
    1.0   2.10E7    0.001     10.0      0.0      0.0


  1.00E7     0.1      0.0    0.001    0.001   0   0   0   0   1

10000000.0      0.0   0
13000000.0      0.0   0
16000000.0      0.0   0
18000000.0      0.0   0
21000000.0      0.0   0
```

***Loading File*: steps of calculation (240-365 days)**

```
  3   2   4  18   0   0   0

  1  -1 9999   1   1   1   2   1  30   0   0   1
  3   0      0   0   0   0   0   0   0
 1.0E-05     1.0      0.0      0.0      0.0      0.0      0.0
    1.0   3.20E7    0.001     10.0      0.0      0.0


  2.10E7     0.1      0.0    0.001    0.001   0   0   0   0   1

21000000.0      0.0   0
24000000.0      0.0   0
26000000.0      0.0   0
29000000.0      0.0   0
32000000.0      0.0   0
```

***LIC file*: loading steps**

```
  4
     0
    0.0      0.0
```

```
 1.30E+06
    0.0      0.0
 2.60E+06
    0.5      0.0
 5.20E+06
    1.0      0.0
```

***PRI file*: printed nodes and elements**

```
NODES
   1   1   6  -8  136 -248
   2   1   6  -8  136 -248
   3   1   6  -8  136 -248
   5   1   6  -8  136 -248
  16   1   6  -8  136 -248
  17   1   6  -8  136 -248

ELEMT
   1   1 -310
   2   1 -310
   3   1 -310

REACT

TIMES
```

***DEP file*: temperature steps (4°C-14°C)**

```
   3  13
 5.20E+06
 264   5    277.0
 297   5    277.0
 301   5    277.0
 305   5    277.0
 309   5    277.0
 450   5    277.0
 454   5    277.0
 458   5    277.0
 462   5    277.0
 466   5    277.0
 470   5    277.0
 474   5    277.0
 478   5    277.0
 7.80E+06
 264   5    287.0
 297   5    287.0
 301   5    287.0
 305   5    287.0
 309   5    287.0
 450   5    287.0
 454   5    287.0
 458   5    287.0
 462   5    287.0
 466   5    287.0
 470   5    287.0
 474   5    287.0
 478   5    287.0
 1.00E+07
 264   5    287.0
 297   5    287.0
 301   5    287.0
 305   5    287.0
 309   5    287.0
 450   5    287.0
 454   5    287.0
 458   5    287.0
 462   5    287.0
 466   5    287.0
 470   5    287.0
 474   5    287.0
 478   5    287.0
```

***DEP file*: temperature steps (14°C-26.5°C)**

```
   3  13
 1.00E+07
 264   5    287.0
 297   5    287.0
 301   5    287.0
 305   5    287.0
 309   5    287.0
 450   5    287.0
 454   5    287.0
 458   5    287.0
 462   5    287.0
 466   5    287.0
 470   5    287.0
 474   5    287.0
 478   5    287.0
 1.30E+07
 264   5    299.5
 297   5    299.5
 301   5    299.5
```

305 5 299.5
309 5 299.5
450 5 299.5
454 5 299.5
458 5 299.5
462 5 299.5
466 5 299.5
470 5 299.5
474 5 299.5
478 5 299.5
2.10E+07
264 5 299.5
297 5 299.5
301 5 299.5
305 5 299.5
309 5 299.5
450 5 299.5
454 5 299.5
458 5 299.5
462 5 299.5
466 5 299.5
470 5 299.5
474 5 299.5
478 5 299.5

***DEP file*: temperature steps (26.5°C-14°C)**

5 13
2.10E+07
264 5 299.5
297 5 299.5
301 5 299.5
305 5 299.5
309 5 299.5
450 5 299.5
454 5 299.5
458 5 299.5
462 5 299.5
466 5 299.5
470 5 299.5
474 5 299.5
478 5 299.5
2.40E+07
264 5 287.0
297 5 287.0
301 5 287.0
305 5 287.0
309 5 287.0
450 5 287.0
454 5 287.0
458 5 287.0
462 5 287.0
466 5 287.0
470 5 287.0
474 5 287.0
478 5 287.0
2.60E+07
264 5 287.0
297 5 287.0
301 5 287.0
305 5 287.0
309 5 287.0
450 5 287.0
454 5 287.0
458 5 287.0
462 5 287.0
466 5 287.0
470 5 287.0
474 5 287.0
478 5 287.0
2.90E+07
264 5 277.0
297 5 277.0
301 5 277.0
305 5 277.0
309 5 277.0
450 5 277.0
454 5 277.0
458 5 277.0
462 5 277.0
466 5 277.0
470 5 277.0
474 5 277.0
478 5 277.0
3.20E+07
264 5 277.0
297 5 277.0
301 5 277.0
305 5 277.0
309 5 277.0
450 5 277.0
454 5 277.0

```
458   5   277.0
462   5   277.0
466   5   277.0
470   5   277.0
474   5   277.0
478   5   277.0
```

DEP file: temperature steps (2th year)

```
 10  13
3.20E+07
264   5   277.0
297   5   277.0
301   5   277.0
305   5   277.0
309   5   277.0
450   5   277.0
454   5   277.0
458   5   277.0
462   5   277.0
466   5   277.0
470   5   277.0
474   5   277.0
478   5   277.0
3.70E+07
264   5   277.0
297   5   277.0
301   5   277.0
305   5   277.0
309   5   277.0
450   5   277.0
454   5   277.0
458   5   277.0
462   5   277.0
466   5   277.0
470   5   277.0
474   5   277.0
478   5   277.0
3.90E+07
264   5   287.0
297   5   287.0
301   5   287.0
305   5   287.0
309   5   287.0
450   5   287.0
454   5   287.0
458   5   287.0
462   5   287.0
466   5   287.0
470   5   287.0
474   5   287.0
478   5   287.0
4.20E+07
264   5   287.0
297   5   287.0
301   5   287.0
305   5   287.0
309   5   287.0
450   5   287.0
454   5   287.0
458   5   287.0
462   5   287.0
466   5   287.0
470   5   287.0
474   5   287.0
478   5   287.0
4.40E+07
264   5   299.5
297   5   299.5
301   5   299.5
305   5   299.5
309   5   299.5
450   5   299.5
454   5   299.5
458   5   299.5
462   5   299.5
466   5   299.5
470   5   299.5
474   5   299.5
478   5   299.5
5.20E+07
264   5   299.5
297   5   299.5
301   5   299.5
305   5   299.5
309   5   299.5
450   5   299.5
454   5   299.5
458   5   299.5
462   5   299.5
466   5   299.5
470   5   299.5
```

474	5	299.5
478	5	299.5
5.50E+07		
264	5	287.0
297	5	287.0
301	5	287.0
305	5	287.0
309	5	287.0
450	5	287.0
454	5	287.0
458	5	287.0
462	5	287.0
466	5	287.0
470	5	287.0
474	5	287.0
478	5	287.0
5.70E+07		
264	5	287.0
297	5	287.0
301	5	287.0
305	5	287.0
309	5	287.0
450	5	287.0
454	5	287.0
458	5	287.0
462	5	287.0
466	5	287.0
470	5	287.0
474	5	287.0
478	5	287.0
6.00E+07		
264	5	277.0
297	5	277.0
301	5	277.0
305	5	277.0
309	5	277.0
450	5	277.0
454	5	277.0
458	5	277.0
462	5	277.0
466	5	277.0
470	5	277.0
474	5	277.0
478	5	277.0
6.30E+07		
264	5	277.0
297	5	277.0
301	5	277.0
305	5	277.0
309	5	277.0
450	5	277.0
454	5	277.0
458	5	277.0
462	5	277.0
466	5	277.0
470	5	277.0
474	5	277.0
478	5	277.0

References

Adam, D., & Markiewicz, R. (2009). Energy from earth-coupled structures, foundations, tunnels and sewers. *Géotechnique*, *59*(3), 229–236.

Amis, T. (2010). Integrating Geothermal Loops into the Diaphragm Walls of the Knightsbridge Palace Hotel Project. *Proceeding of the 11th DFI / EFFC International Conference, London*, (July), 10.

Amis T., Loveridge F. (2014), "Energy piles and other thermal foundations for GSHP—developments in UK practice and research", REHVA J. 1.

Barla, G., Vai, L., 1999. Indagini geotecniche per la caratterizzazione del sottosuolodi Torino lungo il tracciato del passante ferroviario. *XX Convegno Nazionale diGeotecnica,* Parma, Italy.

Barla, G., Barla, M., 2005. Assessing design parameters for tunnelling in a cementedgranular soil by continuum and discontinuum modelling. In: In Proc. 11thIacmag Conference, Torino, Italy, pp. 475–484.

Barla & Barla (2012). Torino subsoil characterization by combining site investigations and numerical modelling. *Geomechanik und Tunnelbau 3* (Vol. 5), pp. 214–231.

Barla, M., & Perino, A. (2014). Geothermal Heat from the Turin Metro South Extension Tunnels, *In Proceedings of the Worl tunnel Congress 2014:Tunnels for a better life.* Iguaçu, Brazil.

Barla, M., Di Donna, A., & Perino, A. (2016). Application of energy tunnels to an urban environment. *Geothermics*, *61*, 104–113.

Barla, M., Di Donna, A., & Insana, A. (2017). Energy Tunnel Segmental Lining: an experimental Site in Turin Metro.

Barla, M., Di Donna, A., & Santi, A. (2018). Energy and mechanical aspects on the thermal activation of diaphragm walls for heating and cooling.

Renewable Energy.

Barla, M., & Di Donna, A. (2018). Energy Tunnels: concept and design aspects. *ScienceDirect*.

Barla, M., Donna, A. Di, & Insana, A. (2019). A novel real-scale experimental prototype of energy tunnel. *Tunnelling and Underground Space Technology*, *87*(August 2018), 1–14.

Batini, N., Rotta Loria, A.F., Conti, P., Testi, D., Grassi, W., Laloui, L. (2015). Energy and geotechnical behaviour of energy piles for different design solutions. *Elsevier*.

Bourne-Webb P.J., Bodas Freitas T.M., da Costa Goncalves R.A. (2015),. Retaining walls as heat exchangers: a numerical study, in *Geotechnical Engineering for Infrastructure and Development*, ICE Publishing, London, UK.

Bourne-Webb, P., Bodas Freitas, T., & da Costa Gonçalves, R. (2016). Thermal and mechanical aspects of the response of embedded retaining walls used as shallow geothermal heat exchangers. *Elsevier*, 130-141.

Bottino, G., Civita, M., (1986). Engineering geological features and mapping ofsubsurface in the metropolitan area of Turin, North Italy. In: *5th International IAEG Congress*, Buenos Aires, Argentina, pp. 1741–1753.

Brandl H. (1998). Energy piles and diaphragm walls for heat transfer form and into ground, in Proceedings of the *3rd International Symposium on Deep Foundations on Bored and Auger Piles*, Ghent, Belgium.

Brandl (2006). Energy foundations and other thermo active ground structures. *Géotechnique* **56**(2).

Cecinato, F., Loveridge, F.A., (2015). Influences on the thermal efficiency of energy piles. *Elsevier*.

Charlier, R. et al.2 nd International Workshop on the Finite Element Code LAGAMINE. (February), 2018.

Charlier R. Approche unifiée de quelques problèmes non linéaires de mécanique des milieux continus par la méthode des éléments finis: grandes déformations des métaux et des sols, contact unilatéral de solides, conduction thermique et écoulements en milieu poreux. Université de Liège, Faculté des sciences appliquées, 1987.

Collin F. Couplages thermo-hydro-mécaniques dans les sols et les roches tendres partiellement saturés. Université de Liège, Faculté des sciences appliquées, 2003.

Di Donna, A. Energy walls for an underground car park, *25th European Young Geotechnical Engineers Conference*, Sibiu, Romania, 2016.

Di Donna, A., & Laloui, L. (2014). Numerical analysis of the geotechnical behaviour of energy piles. *International journal for numerical and analytical methods in geomechanics*.

Di Donna, A., Cecinato, F., Loveridge, F., & Barla, M. (2016). Energy performance of diaphragm walls used as heat exchangers. *ice*.

Di Donna, A., Barla, M., & Amis, T. (2017). Energy Geostructures : Analysis from research and systems installed around the World, 1–11.

Frazius, J., & Pralle, N. (2011). turning segmental tunnels into sources of renewable energy. *Proc.ICE-Civil Eng.164(1),35-40*.

Gao J., Zhang X., Liu J., Li K., Yang J. (2008). Numerical and experimental assessment of thermal performance of vertical energy piles: an application, in *Appl Energy*.

ICConsulten. (2005). *Wirtschaftliche Optimierung von Tunnelthermie Absorberanlagen, Grundlagenuntersuchung und Planungsleitfaden.* Vienna, Austria.

Katzenbach, R., Bergmann, C., & Leppla, S. (2013). Safety assurance for challenging geotechnical civil engineering constructions in urban areas. *Open journal of civil engineering*.

Katzenbach R., Leppla S., Choudhury D. (2017). Foundation Systems for High-Rise Structures, CRC Press, USA.

Kovacevic, M., Bačić, M., & Arapov, I. (2013). Possibilities of underground engineering for the use of shallow geothermal energy. *Gradevinar*.

Knellwolf C., Peron H., Laloui L. (2011), Geotechnical analysis of heat exchanger piles, in *J Geotech Geoenviron Eng* (ASCE), 137(10).

Lancellotta, R. (2002). Analytical solution of passive earth pressure. *Geotechnique* Vol.52 Issue 8, pp. 617-619.

Markiewicz R., Adam D. (2006), "Extraction of geothermal energy from tunnels", *Millpress Science Publishers*/IOS Press, the Netherlands.

Nicholson D. P., Cheng Q., de Silva M., Winter A., Winterling R. (2014), The design of thermal tunnel energy segments for Crossril, UK. Proceedings of the Institution of Civil Engineers - Engineering Sustainability 167(3).

Suckling T. P., Smith P. E. H. (2002), "Environmentally friendly geothermal piles at Keble College, Oxford, UK".

Unterberger, W., Hofinger, H., Grünstäudl, T., Adam, D., & Markiewicz, R. (2005). Utilization of Tunnels as Sources of Ground Heat and Cooling - Practical Applications in Austria. *Tunnels & Tunnelling International*, 36–39.

Xia, C., Sun, M., Zhang, G., Xiao, S., & Zou, Y. (2012). Experimental study on geothermal heat exchangers buried in diaphragm walls. *Elsevier*, 50-55.

Zhang G., Xia C., Sun M., Zou Y., Xiao S. (2013), "A new model and analytical solution for heat conduction of tunnel lining ground heat exchangers", in Cold Regions Science and Technology 88.

Sitography

https://climate.nasa.gov/causes/

https://www.listverse.com

https://www.statista.com

https://www.wikimedia.com

https://www.isabelbarrosarchitects.ie

https://www.oilprice.com

https://www.tidewatermechanical.com

https://www.firstgeothermalenergy.com

https://www.gsi.ie

https://www.waterfurnace.com

https://www.buildingscience.com

https://www.omranista.com

https://www.quora.com

https://askjaenergy.com

http://tidewatermechanical.com

https://commons.wikimedia.org

http://www.firstgeothermalenergy.com

https://www.wbdg.org

http://tidewatermechanical.com

Acknowledgments

The goal of a master's degree is certainly one of the most awaited moments of my life. It was not easy to achieve this aim and certainly would not have been possible without the help of some people. Writing this thesis has had a strong impact on my personality.Therefore, I would like to use these last pages to thank all those who have supported and helped me during this journey.

First of all, for the following work, I would like to thank my supervisors, *Professor Marco Barla* and *Engineer Alice Di Donna*, who played a fundamental role in the drafting of the thesis. Despite the various difficulties encountered, both have always tried to find a suitable solution together, giving me the possibility of growth and autonomy. In addition, they allowed me to gain experience abroad, in France, where I was able to get involved knowing different realities and expanding my limits.

A special thanks goes to my parents, *Amedeo and Mariagrazia*, without whom I would not be the person I am today. Their support, not only economic but above all psychological, has been a beacon in the darkest moments of these years. They are and will always be my greatest example of how to face life, that is, always with positivity and lightness, because if there is commitment and determination, in the end, you get everything.

Deborah, a sister who plays more than just a role. You always knew how to motivate me and give me one more reason to try one last time. You always said what I needed to hear in order not to give up. You're one of the few people I really admire, because you're all I can't be and you're certainly the one I miss the most. But luckily, distance has only strengthened a solid bond.

I dedicate my degree to my grandmother *Rosa*, maybe she was the one who cared most about us all. She is the emblem of independence and willpower. I am happy to resemble her so much because with a single glance, without explanation, she knows what I feel and always knows how to distract me. Thank you for waiting for me.

I would also like to thank my uncles, *Daniela and Angelo*, who have always been present and interested in my university career; thank you for always bringing joy to Sunday lunches.

Last but not least, I would like to thank my friends.

My *Juliet*, with whom I have been a friend for 12 years, has always been present, even though our lives are so distant and different. It is also thanks to you that I have chosen to take this path. Our high school years are perhaps the most beautiful of my life.

Aurelio, one of the first people I met here in Turin, proved to be a trusted and understanding friend. You taught me many things, perhaps too many, including accepting different ideas and knowing how to communicate. In moments of despair you have always been present and you have been able to listen to me even when I was not speaking.

I thank my roommates, who were more of a family, *Stefano and Lilia*. The distance from home was acceptable thanks to you who made Bellini house, a safe place to spend these 3 years away from Sicily.

Amanda, Debora, Angela, Celeste, Marina, Ludovico, Tosku, Miriam, Niccolò impossible to describe how important it was to know you during these 3 years. To each of you I have said things about myself that I rarely share. The hours spent with you have always been one of lightheartedness and laughter, thanks for making my life lighter.

A last thanks goes to my friends of the gym *Alessandra, Valeria, Moc, Roni, Domenico, Ignazio* thanks to you my life was not only based on study, but also on sport and fun.

Thanks to all those who I have not mentioned, but who have left a mark on this path.

Ringraziamenti

Il traguardo di una laurea magistrale è di certo uno dei momenti più attesi della mia vita. Non è stato facile raggiungere questo obiettivo e di certo non vi sarei mai riuscita senza l'ausilio di alcune persone. Scrivere questa tesi ha avuto un forte impatto sulla mia personalità. Vorrei quindi sfruttare queste ultime pagine per ringraziare tutti coloro che mi hanno sostenuto e aiuato durante questo percorso.

In primis, per il seguente lavoro, vorrei ringraziare i miei relatori, il *professor Marco Barla* e *l'ingegner Alice Di Donna*, i quali hanno giocato un ruolo fondamentale per la stesura della tesi. Nonostante le varie difficoltà incontrate, entrambi hanno sempre cercato di trovare insieme una soluzione adeguata, dandomi la possibilità di crescita e autonomia. Inoltre, mi hanno permesso di fare una esperienza all'estero, in Francia, dove ho potuto mettermi in gioco conoscendo realtà diverse e allargando i miei limiti.

Un ringraziamento particolare va ai miei genitori, *Amedeo e Mariagrazia*, senza i quali non sarei la persona che sono oggi. Il loro sostegno, non solo economico ma soprattutto psicologico, è stato un faro nei momenti più bui di questi anni. Sono e saranno sempre il mio più grande esempio di come bisogna affrontare la vita, cioè sempre con positività e leggerezza, perché se c'è impegno e determinazione, alla fine, si ottiene tutto.

Deborah, una sorella che ricompre più di un semplice ruolo. Hai sempre saputo come motivarmi e darmi una ragione in più per provarci un'ultima volta. Hai sempre detto ciò di cui avevo bisogno di sentire per non mollare. Sei una delle poche persone che ammiro veramente, perché sei tutto quello che io non riesco ad essere e di sicuro sei quella che mi manca di più. Ma per fortuna, la distanza non ha fatto altro che rafforzare un legame già solido.

A mia nonna *Rosa* dedico la mia laurea, forse è stata quella che ci teneva più di tutti. Lei è l'emblema dell'indipendenza e della forza di volontà. Sono felice di assomigliarle così tanto perché con un solo sguardo, senza dare spiegazioni, sa quello che provo e sa sempre come distrarmi. Grazie per avermi aspettato.

Vorrei ringraziare anche i miei zii, *Daniela e Angelo*, che sono stati sempre presenti e interessati alla mia carriera universitaria; grazie per aver portato sempre allegria ai pranzi domenicali.

Per ultimi ma non meno importanti, è doveroso ringraziare i miei amici.

La mia *Giulietta*, con la quale sono amica da 12 anni, è sempre stata presente, nonostante le nostre vite siano così lontane e diverse. E' anche grazie a te se ho scelto di intraprendere questo percorso. I nostri gironi al liceo sono forse i più belli della mia vita.

Aurelio, una delle prime persone che ho consociuto qui a Torino, si è rivelato un amico fidato e comprensivo. Mi hai insegnato tante cose, forse troppe, tra cui accettare idee diverse e saper comunicare. Nei momenti di sconforto sei sempre stato presente e hai saputo ascoltarmi anche quando non parlavo.

Ringrazio i miei coinquilini, che sono stati più una famiglia, *Stefano e Lilia*. La lontanaza da casa è stata accettabile grazie a voi che avete reso casa Bellini, un posto sicuro dove poter trascorrere questi 3 anni da fuori sede.

Amanda, Debora, Angela, Celeste, Marina, Ludovico, Tosku, Miriam, Niccolò impossibile descrivere quanto sia stata importante conoscervi durante questi 3 anni. A ciascuno di voi ho detto cose di me che raramente condivido. Le ore trascorse con voi sono sempre state di spensieratezza e riso, grazie per aver alleggerito la mia vita.

Un ultimo ringraziamento va ai miei amici della palestra *Alessandra, Valeria, Moc, Roni, Domenico, Ignazio* grazie a voi la mia vita non è stata basata esclusivamente sullo studio, ma anche sullo sport e sul divertimento.

Un grazie a tutti coloro che non ho citato, ma che comunque hanno lasciato un segno durante questo percorso.